Shoreline Carbonate Structures in West Reflex Lake, Alberta-Saskatchewan

Jemma Harrison

A thesis submitted to the Faculty of Graduate Studies of

The University of Manitoba

in partial fulfilment of the requirements of the degree of

MASTER OF SCIENCE

Department of Geological Sciences

University of Manitoba

Winnipeg

Abstract

West Reflex Lake is a hypersaline lake in the Canadian Great Plains. The lake contains four types of shoreline carbonate structures: isolated pinnacles, bioherms (aggregates of pinnacles), laminated coatings, and beachrock. This study investigates the processes of formation of West Reflex Lake's shoreline carbonates. A variety of petrographic and geochemical techniques were used to characterize the texture, mineralogy, and chemistry of the carbonates. The shoreline carbonates formed as a result of biotic and abiotic precipitation at the site of saline springs that supply Ca^{2+} to the lake. Evidence for biologically-influenced precipitation includes strong epifluorescence, presence of micrite cements, and abundance of microbial filaments. Abiotically-precipitated cements formed due to groundwater inflow. The isolated pinnacles and bioherms formed as a result of groundwater percolating through a framework of microbial filaments, whereas the laminated coatings formed as a result of calcification of coherent microbial mats adhering to a substrate.

Summary

The Canadian Great Plains region contains many saline lakes that precipitate endogenic carbonates. However, studies of carbonate lacustrine microbialites from the region are scarce. West Reflex Lake is an alkaline, hypersaline lake on the Alberta-Saskatchewan border in the Canadian Great Plains. The lake water is Cl^--dominated, an unusual chemistry for Canadian Great Plains lakes. The lake appears to receive a large proportion of its solutes from saline, deep groundwater.

A decrease in water level over the past several decades has exposed carbonate microbialites along the shore of West Reflex Lake. The lake is located 22 km from Manito Lake, the only other lake in the region with microbialites that have been studied in detail. Despite the proximity of the lakes, their chemistries are very different. Thin section petrography, epifluorescence, cathodoluminescence, and scanning electron microscopy were used to describe the fabrics and textures in the West Reflex Lake microbialites and interpret the processes involved in their deposition.

The four types of shoreline carbonate structures that occur in West Reflex Lake are isolated pinnacles, bioherms (aggregates of pinnacles), laminated coatings, and beachrock. The shoreline carbonates are associated with sites of groundwater inflow. The isolated pinnacles and bioherms have a porous framework of clotted micrite and micrite-coated filaments. Fibrous and botryoidal aragonite and calcite cements are deposited on the other components. The laminated coatings are composed of alternating couplets of micrite and microspar with fenestral porosity. The beachrock is a lithic arenite cemented by microcrystalline aragonite.

The shoreline carbonates of West Reflex Lake developed in a closed-basin, saline lake with a high Mg/Ca ratio. Groundwater springs supplied Ca^{2+} to the lake. Extracellular polymeric

substances produced by microorganisms in the lake took up Ca^{2+} and controlled the biologically-influenced calcification of filaments. Biologically-induced calcification alternated with inorganic cement precipitation. The isolated pinnacles and bioherms formed as a result of groundwater percolating through the porous structures, whereas the laminated coatings formed as result of the development of cohesive microbial mats on the exterior surface.

Acknowledgements

First and foremost, I would like to thank my advisory committee, Drs. Fawn Last, William Last, Zou Zou Kuzyk and Nancy Chow. I sincerely appreciate all your support and encouragement. I couldn't have asked for a better group of people to help with my research and writing. Your positivity and enthusiasm for my project kept me going.

I would also like to thank the technical staff in the Department of Geological Sciences, in particular, Neil Ball, Mark Cooper, Misuk Yun, and Dr. Ravinder Sidhu. I appreciate all their help with the laboratory equipment. Thanks to the administrative staff, Brenda Miller, Pam Achtemichuk, and Steven Brown, who have also been very good to me.

Thanks are due to my family and friends who supported me throughout my project. I appreciate my parents and brothers for sending me anything they could find related to rocks. I would also like to thank my husband for humouring me during my MSc and in general. Thanks to my fellow grad students for moral support and the many coffee breaks.

This research would not have been possible without funding from my NSERC Canada Graduate Scholarship – Masters and from Dr. William Last's NSERC Strategic Grant SPG-SC Disappearing and Flooding Prairie Lakes: Solving an Aquatic Whodunnit and NSERC Discovery Grant Carbonate and Evaporite Sedimentology of Salt Lakes.

Table of Contents

List of Tables

List of Figures

1 Introduction

1.1 Prologue

The Canadian Great Plains region is bounded by the Precambrian Shield to the east and the Rocky Mountains to the west. It contains millions of shallow lakes that fill depressions in the flat to gently rolling topography (Last, 1984). Many of the lakes are topographically closed and saline (Last, 1984; Last *et al.*, 1994). The salinities and chemical compositions of the lakes are very diverse, and many lakes are saturated or supersaturated with respect to calcium carbonate minerals (Last and Last, 2012). Groundwater inflow dominates the hydrology of the closed lakes in the region (Last and Last, 2012). Sites where groundwater discharges into carbonate-saturated saline lake basins are suitable for the development of shoreline carbonate structures (Macdonald, 1982; Arp *et al*., 1999a; Rosen *et al.*, 2004; Last *et al*., 2010).

Reports of shoreline carbonate structures from the Canadian Great Plains are limited. Shoreline carbonates are present in West Reflex Lake, a permanent, hypersaline lake on the Alberta-Saskatchewan border. In many ways, West Reflex Lake is typical of the numerous small, shallow closed basin lakes in the Canadian Great Plains. However, its Na^+-Cl^--dominated chemistry is unusual for the region. During fieldwork at the lake in May of 2015, several types of shoreline carbonate structures were identified.

Carbonate deposits that form in association with microbial activity can be considered microbialites (Burne and Moore, 1987). The mineralogy, fabrics, and geochemistry of carbonate microbialites reflect the physical, chemical, and biological conditions of the lake (Talbot, 1990; Nelson *et al*., 2005). The first detailed report of lacustrine microbialites in the Canadian Great Plains is from Manito Lake, Saskatchewan, 22 km east of West Reflex Lake (Last *et al.*, 2010).

The proximity of the lakes and their differences in chemistry enable investigation of the processes controlling microbialite formation in the northern Great Plains.

1.2 Objectives

This project includes the first description of microbialites in West Reflex Lake and the second detailed investigation of lacustrine microbialites in the Canadian Great Plains. Many saline lakes in the Canadian Great Plains are saturated with respect to calcite, aragonite and/or dolomite (Last and Last, 2012). However, carbonate supersaturation may not be sufficient for carbonate mineral precipitation: microbial mediation may be required to initiate precipitation (Last and Last, 2012). The influences of biologically-influenced and abiotic precipitation in northern Great Plains lakes are not well-understood (Last and Last, 2012). Comparison of the shoreline carbonates of West Reflex Lake and Manito Lake will improve our understanding of the conditions required for microbialite formation in this region.

The objectives of this thesis are to 1) describe the mineralogy, texture, and structure of the shoreline carbonates in West Reflex Lake; 2) investigate the causes of the anomalous water chemistry of West Reflex Lake; 3) provide insight into the processes of formation of the shoreline carbonates; and 4) compare the shoreline carbonates to those in Manito Lake.

1.3 Previous work

1.3.1 West Reflex Lake

West Reflex Lake has been included in a number of surveys of lakes in the Canadian Great Plains. Rutherford (1970) compiled a water quality survey of Saskatchewan surface water that included West Reflex Lake. The lake's chemical and physical attributes were briefly mentioned in a series of publications on saline lakes in Saskatchewan by Hammer (1978) and

Hammer and Haynes (1978). Because West Reflex Lake is an important nesting site for the endangered piping plover, its physical characteristics have been listed in publications that deal with the nesting habitat of the birds (Wells and Cornish, 1999; Beyersbergen, 2009; Prescott *et al*., 2010). West Reflex Lake has also been included in surveys of benthic macroinvertebrates (Timms *et al.,* 1986), other benthic fauna (Hammer *et al*., 1990), diatoms (Blinn, 1993; Fritz *et al.,* 1993; Ryves, 1994), and vascular macrophytes (Hammer and Heseltine, 1988). However, no publications to date have focused on West Reflex Lake alone.

Water chemistry data for the lake are available from Rutherford (1970), Blinn (1993), Fritz *et al*. (1993), and Pham *et al*. (2009). Several studies have noted West Reflex Lake's high salinity and unusual, Na-Cl-dominated chemistry (Hammer, 1978; Timms *et al.,* 1986; Fritz *et al*., 1993; Ryves, 1994). A survey of saline wetlands and springs in eastern Alberta documented the saline springs and vegetation surrounding West Reflex Lake and noted the presence of "tufa deposits" associated with the springs (Wallis, 1991).

1.3.2 Lacustrine carbonates in the northern Great Plains

A review of the lacustrine carbonates in the Canadian portion of the northern Great Plains was compiled by Last and Last (2012). The review focused mainly on endogenic carbonate sediments in core because few studies of microbialite structures in the northern Great Plains exist. Stromatolitic tufa in Brush Lake, Montana was briefly described in a study of mass fluxes in an evaporative, groundwater-sourced lake (Donovan, 1994). Groundwater-associated carbonate tufa deposits associated with springs were reported in Muskiki Lake, Saskatchewan and Metiskow Lake, Alberta by Last (1989). Macdonald (1982), in a report on the marl resources of Alberta, listed locations where tufa had been reported, but did not distinguish between lacustrine and non-lacustrine tufa, and did not describe the structures in detail. Manito Lake is

the only Canadian Great Plains lake for which a detailed study of the lacustrine microbialites has been completed (Last *et al.*, 2010).

1.4 Setting

1.4.1 Location and physical properties

West Reflex Lake (locally known as Salt Lake) is situated on the Alberta-Saskatchewan border, 280 km west of the city of Saskatoon, SK (Fig. 1.1). The lake shore can be accessed from a gravel road east of Alberta Highway 17. The names "West Reflex Lake" and "East Reflex Lake" are used to differentiate the two adjacent basins officially known as Reflex Lakes (Fig. 1.2). Between the two Reflex Lakes is a small, closed basin called Gordon Lake. The land surrounding the lakes is used as rangeland (IBA Canada, 2010). To the east of the lakes are sand hills covered by grasses and aspen stands (IBA Canada, 2010).

Closed drainage systems cover much of southern Saskatchewan (Last and Last, 2012). Permanent saline lakes develop at the end of closed drainage systems where outflow from evaporation is balanced by inflow from precipitation, surface runoff, and groundwater (Williams, 2002). West Reflex Lake, like most of the lakes in the Canadian Great Plains, probably originated after Wisconsinian ice retreat left an irregular blanket of glacial drift over the region (Last and Ginn, 2005). Small, isolated lakes formed in depressions in the drift.

West Reflex Lake's present surface area is 4.0 km^2. The elevation of the lake's surface was 587 m asl in 2015. The area of the lake's watershed is 69.2 km^2 (Wells and Cornish, 1999). The maximum depth of the lake is 1.9 m (Pham *et al.*, 2009). The lake has decreased in size over the past several decades but monitoring shows that it has not evaporated completely between the 1980s and 2010 (Prescott *et al*., 2010).

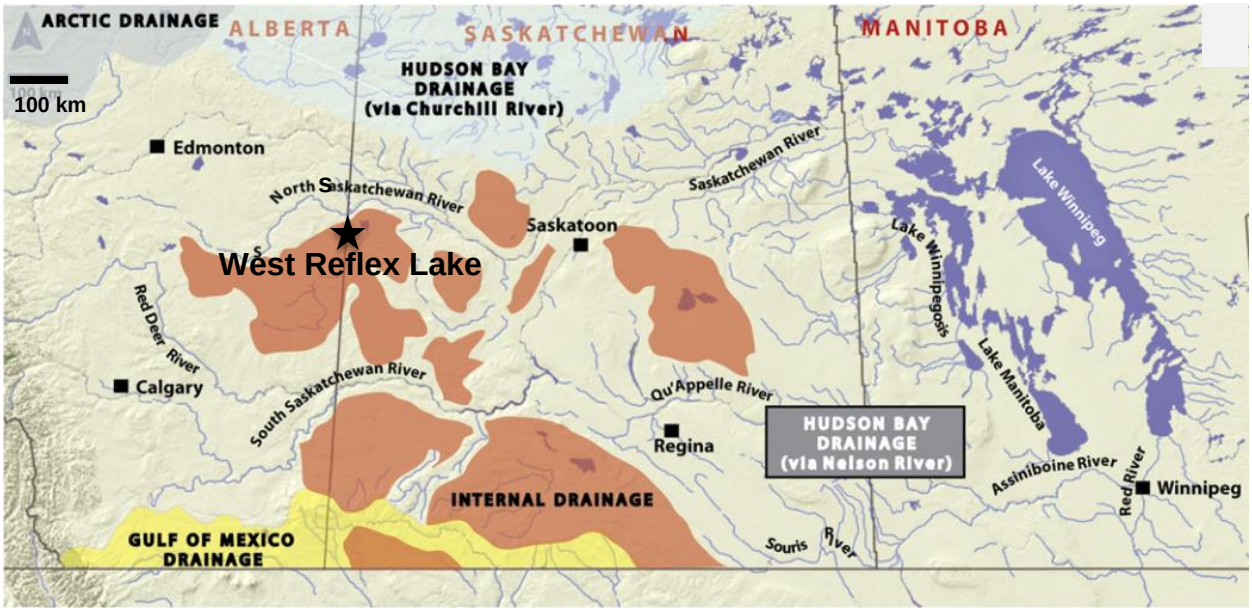

Figure 1.1: West Reflex Lake (star) is located in the Canadian Prairies in an area of internal drainage (orange). Modified from Last and Last (2012).

Figure 1.2: Location of West Reflex Lake relative to East Reflex and Gordon lakes. The white material on the north side of West Reflex Lake is an efflorescent salt crust. Modified from Google Earth (2016).

1.4.2 Climate and vegetation

The climate of the Canadian Great Plains is semi-arid to sub-humid (Last and Last, 2012). Evaporation exceeds precipitation by approximately 500 mm/year (Environment and Climate Change Canada, 2015). The West Reflex Lake area averaged 384 mm of precipitation annually between 1981 and 2010 (Environment and Climate Change Canada, 2015). Rain accounts for 75% of the annual precipitation; the other 25% falls as snow. The months with the highest precipitation are June and July, and the month with the least is February (Wells and Cornish, 1999). The area experiences a maximum daily average temperature in July of 17.5°C and a minimum daily average temperature in January of -14.4°C (Environment and Climate Change Canada, 2015).

West Reflex Lake is located in the aspen parkland ecozone. The area surrounding the basin is covered by grassland vegetation interspersed with aspen and balsam poplar woods (Wells and Cornish, 1999). The saline springs around the lake have diverse, salt-tolerant vegetation communities (Wallis, 1991). Immediately surrounding the shore of the lake, algae is the only vegetation present (Hammer *et al*., 1990).

1.4.3 Biology

Due to its high salinity, West Reflex Lake has very low biomass (<1.0 g/m^2) and low diversity of macroinvertebrates and macrophytes (Timms *et al.,* 1986; Hammer and Heseltine, 1988). The two species of benthic invertebrate identified in West Reflex Lake by Timms *et al.* (1986) were *Cricotopus,* a non-biting midge, and *Ephydra*, a brine fly. West Reflex Lake contains several types of diatoms: *Surirella ovata*, *Mastogloia smithii*, *Opephora cf. olsenii*, *Amphora veneta*, *Cocconeis placentula*, and *Fragilaria construens* (Ryves, 1994). Brine shrimp

were observed in the lake during sampling in May 2015. At that time, the lake water was clear and no vegetation was visible.

1.4.4 Geological setting

West Reflex Lake is situated in the Western Canada Sedimentary Basin. The oldest Phanerozoic units underlying the area are Paleozoic carbonates and evaporites that sit on the Precambrian basement (Wright *et al.,* 1994). The Upper Cretaceous bedrock units that overlie the Paleozoic rocks include, in ascending order, the Mannville Group, Colorado Group, Lea Park Formation, and the Judith River Formation (Fig. 1.3; Millard, 1990).

West Reflex Lake is located above a buried valley known as the Wainwright Valley or the Battleford Valley, which is incised into the Upper Cretaceous sedimentary rocks. The valley is filled by Quaternary glacial drift between 77 and 107 m thick (Carlson and Topp, 1971). The Quaternary glacial drift units that fill the Wainwright Valley are the Empress, Sutherland, and Saskatoon group sediments (Millard, 1990). The major bedrock aquifer in the area is the Judith River Formation and the major Quaternary aquifers are the Empress Group sediments, intertill sands and gravels, and Saskatoon Group surficial sediments. Deep-basin brines in the Paleozoic rocks flow eastward through the Western Canada Sedimentary basin, discharging in west-central Manitoba (Grasby, 2000). Glacial tills and bedrock clays act as aquitards. A north-south cross section between West Reflex and East Reflex lakes shows that the basin intersects Saskatoon Group till and sand, an unnamed intertill sand lens, and Sutherland Group till (Fig. 1.3).

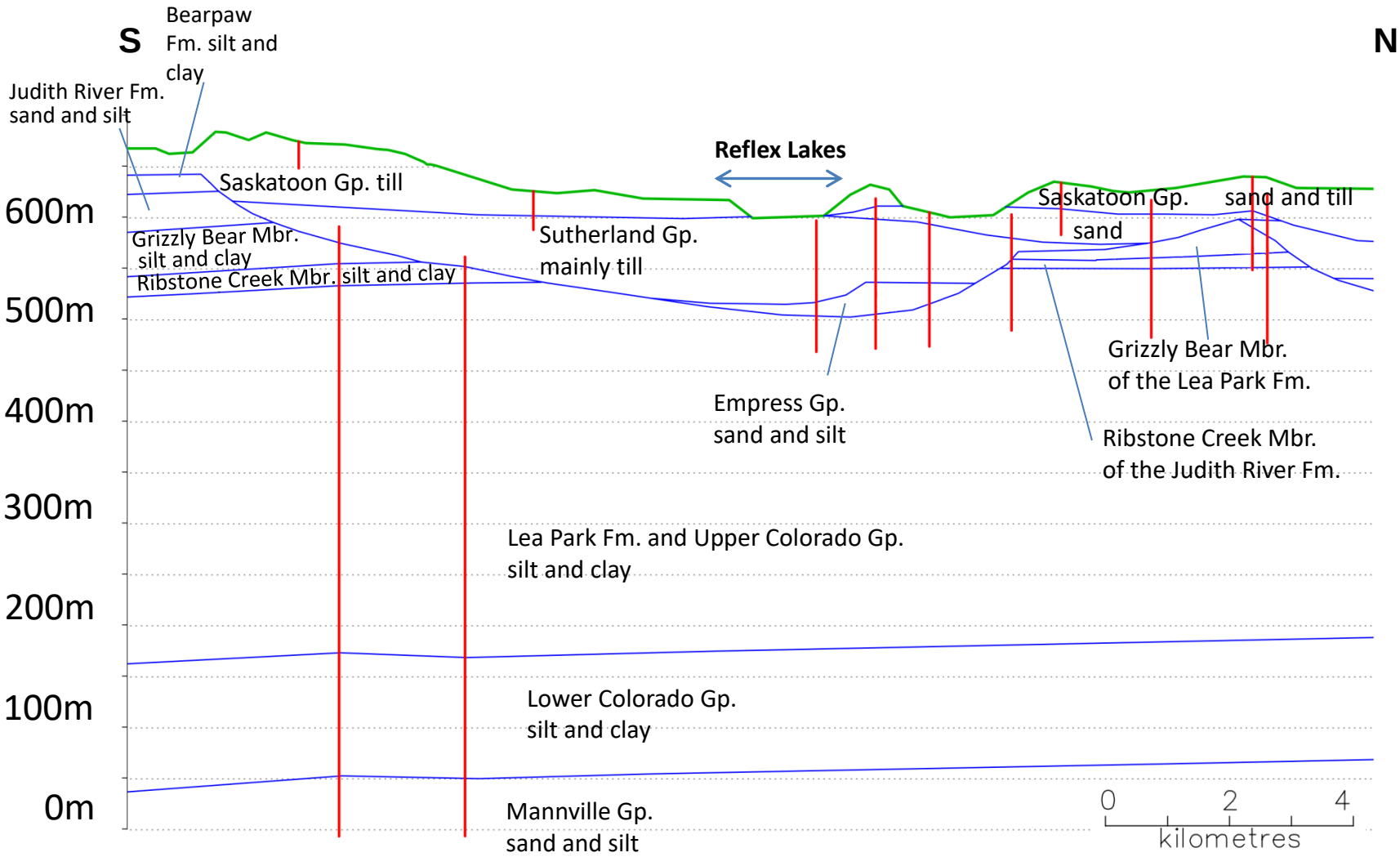

Figure 1.3: Cross section between West and East Reflex lakes showing Cretaceous bedrock units and Quaternary units underlying the lakes. Red lines are locations of wells. Modified from Millard (1990).

2 Methods

2.1 Sample collection

Eighteen shoreline carbonate samples and two beach surface sediment samples were collected from nearshore areas of West Reflex Lake, AB-SK in May of 2015. Shoreline carbonates could be distinguished from the surrounding sediment because of the carbonates' cream to orange colour and relief above the sediment surface. At each site around the lake where shoreline carbonates were present, at least one sample was collected. Samples were photographed *in situ,* their locations were recorded with a handheld GPS, and field notes describing the morphology were taken. The samples were collected with a rock hammer. The samples were chosen to reflect the variety of shoreline carbonate morphologies and locations surrounding West Reflex Lake. The samples were transported to Winnipeg in plastic sample bags and then air dried. Brief descriptions of the samples are included in Appendix A.

2.2 Water chemistry analysis

The temperature and pH of the lake water were measured using YSI probes during fieldwork in May 2015. A YSI ProODO instrument measured dissolved oxygen content and temperature and a YSI 63 instrument measured pH. Lake water samples for chemical analysis were collected at <30 cm depth. The samples were filtered and acidified in the field, then transported in a cooler to ALS Laboratories (Winnipeg). Dissolved oxygen, alkalinity, total Kjeldahl nitrogen, total phosphorus, and dissolved metals were analyzed by ALS Laboratories. Dissolved oxygen was determined using the Winkler method. Total alkalinity as $CaCO_3$ was determined by titration, and carbonate, bicarbonate and hydroxide alkalinity were determined by calculation. Total Kjeldahl nitrogen was determined using flow injection analysis. Total

phosphorous was determined by colourimetry after persulphate digestion of the sample. Dissolved metals were determined by inductively coupled plasma mass spectrometry. Chloride ion concentration was calculated by charge balance (W. Last, pers. comm., 2015). Chemical equilibrium modelling software (Visual MINTEQ) was used to calculate mineral supersaturation at 25°C, using the Davies equation for activity correction (Gustaffsson, 2010).

2.3 X-ray diffraction analysis

Powder x-ray diffraction (XRD) was used to determine bulk mineralogy. Subsamples of microbialites were collected using a hand held rotary tool and crushed with acetone in an agate mortar and pestle. Powder samples were pressed into the central well of a quartz slide to produce unoriented mounts. Mounts were analyzed using a Siemens (Bruker) D5000 Powder Diffractometer, employing Cu-Kα radiation. The samples were examined from 3° 2θ to 65° 2θ with a step size of 0.05° and a scan speed of 1 second per step. The data were processed using MDI Jade+ software. Semi-quantitative estimates of the proportions of minerals were obtained according to Last (2001).

2.4 Transmitted light microscopy

Nineteen polished thin sections were prepared by Calgary Rock and Materials Services. Thirteen tablets for thin sections were chosen as representative of the fabrics of microbialites, beachrock, and laminated crusts. A set of six tablets was also selected to illustrate the vertical changes in fabric from the bottom to top of a microbialite. Thin sections were described and photographed under plane and cross-polarized light using a Nikon Optiphot-POL polarizing microscope with a Nikon DS-L2 camera. Observations from transmitted light petrography were

used to choose locations for cathodoluminescence and epifluorescence microscopy and electron probe microanalysis.

2.5 Cathodoluminescence microscopy

Cathodoluminescence (CL) microscopy was used to examine 14 polished thin sections. A Relion Industries RELIOTRON cold-cathode instrument attached to a Nikon Optiphot microscope with a Nikon DS-Ri1 camera was operated with a beam current of 400 μA and an accelerating voltage of 7-10 kV. Photomicrographs were taken with a six second exposure. Cathodoluminescence was used to describe zonation and textures of carbonate cements. The colour of cathodoluminescence was used to examine spatial variation in mineralogy: calcite luminesces red-orange and aragonite luminesces yellowish-green (Götte and Richter, 2009).

2.6 Epifluorescence microscopy

Epifluorescence microscopy was completed on nineteen thin sections. A Nikon Optiphot-POL microscope with a Nikon Model HB-10101AF Hg lamp was used with an ultraviolet filter block (wavelength 365 nm). Epifluorescence microscopy was used to identify the presence of organic matter and zonation in cements. Strong epifluorescence in carbonates is an indication of residual organic matter (Dravis and Yurewicz, 1985). Red epifluorescence is due to the presence of chlorophyll (Power *et al.*, 2011).

2.7 Scanning electron microscopy

Subsamples from the microbialites were examined using scanning electron microscopy (SEM). The subsamples were air dried, mounted on aluminium pegs, and gold-coated. The subsamples were examined under high vacuum in an Inspect S50 SEM. The spot size was 35 μm

and the voltage was 10.00 kV. Secondary electron imaging was used to determine the size and morphology of grains and organic matter in the shoreline carbonates.

2.8 Electron probe micro-analysis

Electron probe micro-analysis (EPMA) was done on polished thin sections. The thin sections were carbon-coated and analyzed using a Cameca SX100. Quantitative analyses of cements and microbialite crusts were performed using a 10 µm beam, 15 keV voltage, and 20 nA current. The elements quantified were Mg, Ca, Mn, Fe, and Sr. The detection limit was less than 800 ppm for all elements.

2.9 Stable isotope analyses

Stable isotope analyses of carbon ($\delta^{13}C$) and oxygen ($\delta^{18}O$) were obtained using Gas Bench isotope-ratio mass spectrometry (GB-IRMS) at the University of Manitoba. Subsamples for analysis were selected and powdered in an agate mortar. The analyses were performed using a ThermoFinnigan GasBench II coupled to a ThermoFinnigan Delta V Plus Isotope-Ratio Mass-Spectrometer via a ThermoFinnigan ConFlo open-split interface. The data were calibrated using standards NBS-18 and NBS-19. The $\delta^{13}C$ and $\delta^{18}O$ values of carbonate are reported as per mil deviation relative to the Vienna Pee Dee Belemnite (VPBD) standard and have a precision of ±0.11‰.

2.10 Radiocarbon dating

Two samples were collected from microbialite WR-01 for accelerator mass spectrometry (AMS) radiocarbon dating. Plant material encrusted with carbonate was present in this

microbialite. The plant material and the surrounding carbonate were each sampled and sent to BETA Analytic, Inc for ^{14}C dating. The carbonate was pretreated with an acid etch and the plant material was pretreated with acid-alkali-acid washes. The radiocarbon ages were calibrated using INTCAL13 (Reimer *et al.*, 2013).

3 Modern hydrology and hydrochemistry

3.1 Hydrology

West Reflex Lake is a permanent, topographically closed lake. The lake has decreased in size over the past several decades: its present surface area is 4.0 km^2, whereas in 1946, its surface area was 5.8 km^2 (Fig. 3.1). The water level of the lake in May 2015 was 587 m asl. At higher water levels, West Reflex Lake connects to the adjacent basins East Reflex and Gordon lakes (Fig. 1.2). The divide between West Reflex Lake and East Reflex Lake has an elevation of 596 m asl. At a water level of 597 m asl, Gordon Lake would also join the two Reflex lakes.

West Reflex Lake's hydrologic budget is dominated by groundwater inflow and evaporative loss, like many other lakes in the Canadian Great Plains (Last and Last, 2012). Small, ephemeral creeks supply surface runoff to West Reflex Lake, but no permanent streams flow to or from the lake. Saline springs surround the lake (Wallis, 1991). The Artland, SK weather station, 7 km northeast of the lake, records an average annual precipitation of 384 mm (Environment and Climate Change Canada, 2015). Water leaves West Reflex Lake by evaporation at an average rate of >900 mm per year (Fisheries and Environment Canada, 1978). Groundwater inflow must offset the deficit between precipitation and evaporation in order to maintain West Reflex Lake as a permanent lake.

3.2 Groundwater

West Reflex Lake has "diverse and extensive" saline springs and seeps (Wallis, 1991). The springs are moderately saline and permanent, flowing even in extended droughts (Wallis, 1991). West Reflex Lake is situated on a buried valley known as the Wainwright Valley in

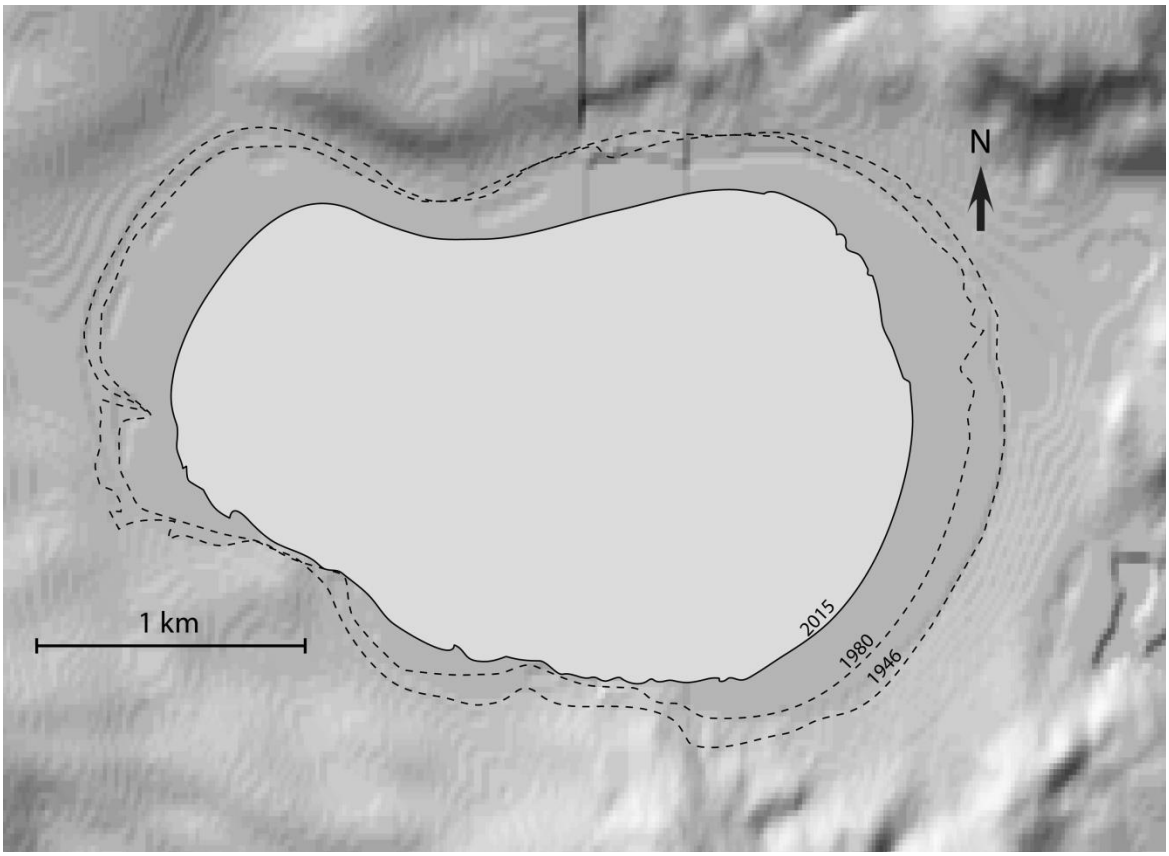

Figure 3.1: West Reflex Lake shoreline location on shaded relief image in 2015 (solid line), 1980 and 1946 (dashed lines).Traced from air photos (1946 location from National Air Photo Library, 1946 and 1980 location from Beyersbergen, 2009) and Google Earth (2016). Shaded relief image from Natural Resources Canada (2016).

Alberta and the Battleford Valley in Saskatchewan. Groundwater flow in the Canadian Great Plains is often channeled by buried valleys (Last and Ginn, 2005). The flow direction in the Battleford/Wainwright buried valley is from west to east, and a major discharge area occurs in the vicinity of West Reflex Lake (Hackbarth, 1975).

3.2.1 Groundwater chemistry

Input of groundwater from different sources is one of the major controls on lake water chemistry in the Great Plains (Last and Ginn, 2005). Groundwater in the region can be divided into shallow, Quaternary aquifers and deeper, bedrock aquifers. Chemistry differs between the Quaternary aquifers and the bedrock aquifers. Hackbarth (1975) found that the Quaternary aquifers in the Wainwright area tend to be dominated by Ca^{2+} or Mg^{2+} and $HCO_3^- + CO_3^{2-}$. The shallower (<46 m) Quaternary aquifers have more than 500 mg/L total dissolved solids (TDS), whereas the deeper (>46 m) Quaternary aquifers tend to have slightly less than 500 mg/L TDS. Bedrock aquifers tend to be dominated by $Na^+ + K^+$ and Cl^- or $HCO_3^- + CO_3^{2-}$, and they have a TDS greater than 1000 mg/L (Hackbarth, 1975).

Groundwater chemistry data are available from a few monitoring wells in the region of West Reflex Lake (Table 3.1). The chemistry of the wells corresponds with the observations of Hackbarth (1975) concerning variations in chemistry with depth and type of aquifer. The bedrock aquifers tend to have higher salinity than the Quaternary aquifers, ranging from 1594-2769 mg/L TDS. The bedrock aquifers are dominated by Na^+ and Cl^-. The Quaternary aquifers in Alberta are less saline (160-728 mg/L TDS) than the Quaternary aquifers in Saskatchewan (819-3274 mg/L TDS). Most of the Quaternary wells are dominated by Ca^{2+} or Mg^{2+} and $HCO_3^- + CO_3^{2-}$, but two (Wainwright #10 OBS 4 and Wainwright Farm 811E) are dominated by Na^+ and

HCO_3^- + CO_3^{2-}. The two Na-dominated wells are the only Quaternary wells with depths greater than 60 m.

Table 3.1: Groundwater chemistry from monitoring wells within 60 km of West Reflex Lake. Data for Alberta wells from Alberta Environment and Parks (2016) and data from Saskatchewan wells from W. Last, pers. comm. (2016).

	Station Name, Province	TDS (mg/L)	Cations (mg/L)				Anions (mg/L)		
			Ca^{2+}	Mg^{2+}	K^+	Na^+	HCO_3^-	SO_4^{2-}	Cl^-
Quaternary aquifers	Edgerton, AB	160	44	10	0.9	4	188	8	0.7
	Metiskow (South), AB	187	51	11	1.1	5	214	12	0.9
	Sunken Lake, AB	395	66	18	1.7	60	372	64	3
	Wainwright #10 OBS 4, AB	728	46	24	5.9	198	589	150	1
	Wainwright (East), AB	363	75	23	3.6	26	380	46	2
	Wainwright Farm 811E, AB	435	32.9	40.6	3.4	85.8	401	25	1.2
	GW 29-44-27, SK	1092	138	52	10.2	64	614	186	28
	GW 30-44-27, SK	3274	517	193	10.9	115	1253	905	281
	GW 36-44-27, SK	1321	184	85	6.6	42	595	310	99
	GW 21-44-28, SK	819	107	57	-	37	441	124	53
Bedrock aquifers	Metiskow 88-1, AB	1610	3	1	2.5	575	454	0.7	801
	GW 24-43-27, SK	1594	100	58	6.3	292	437	272	429
	GW 23-46-26, SK	2379	240	76	-	398	564	520	581
	GW 20-46-27, SK	2769	136	109	7.2	667	600	482	769

3.3 Lake water chemistry

West Reflex Lake is an alkaline, hypersaline lake, with pH 9.5 and 94.9 g/L TDS (Table 3.2). Water chemistry data is available in Appendix A. The salinity is dominated by Na^+ and Cl^-. Most lakes in the Canadian Great Plains are SO_4^{2-} or CO_3^{2-}-rich; West Reflex is one of only three Cl^--dominated natural lakes in Saskatchewan: the other two are lakes fed by salt springs in east-central Saskatchewan (Hammer, 1986). In 2004, West Reflex Lake's water had a heavy $\delta^{18}O$

value (-2.8‰ relative to VSMOW) compared to other closed basin lakes in Saskatchewan (Pham *et al.,* 2009).

Water chemistry data from 1967, 1982/85, 2004, and 2015 show that the salinity of the lake increased tenfold between the mid-1980s and mid-2000s (Table 3.2). The lake's surface area also decreased by approximately 30% during this time. The increase in salinity is probably due to evaporative concentration and coincides with Saskatchewan and Alberta's historic drought between 1999 and 2005 (Fang and Pomeroy, 2008). The concentrations of most of the major ions also increased by an order of magnitude, with the exception of Ca^{2+}. The decrease in Ca^{2+} between the 1980s and 2004 is probably related to calcium carbonate precipitation in the lake.

In general, the molar ratio of Mg/Ca tends to increase with increasing concentration of water due to the formation of calcium carbonate minerals with little or no Mg^{2+} (Valero-Garcés *et al.,* 1997). The Mg/Ca ratio of West Reflex Lake fluctuated as the lake level and water chemistry changed. The Mg/Ca ratio was 10 in 1967, 9 in 1982/85, 249 in 2004, and 48 in 2015. High Mg/Ca ratios (between about 10 and 100) favour the precipitation of aragonite over calcite (Deocampo, 2010).

Table 3.2: Water chemistry changes in West Reflex Lake between 1967 and 2015.

Measurement date	pH	TDS (g/L)	Alkalinity (ppm as $CaCO_3$)	Cations (mg/L)				Anions (mg/L)				
				Ca^{2+}	Mg^{2+}	Na^{+}	K^{+}	CO_3^{2-}	HCO_3^{-}	SO_4^{2-}	Cl^{-}	NO_3^{-}
June 23, 1967[1]	9.3	8.1	1660	10.4	65	2900	67	396	1220	480	3500	0.06
1982/1985[2]	9.2	8.08	-	9.3	52	2710	61	201	1096	596	3356	-
2004[3]	9.3	115.8	-	1	151	47400	273	-	5889	6788	64038	-
May 21, 2015	9.5	94.9	13200	4.09	120	35200	976	460	5000	8120	45000	43

[1]Rutherford, 1970
[2]Fritz *et al.,* 1993
[3]Pham *et al.,* 2009

3.3.1 Stable oxygen isotope chemistry

When measured in the summer of 2004, West Reflex Lake's water had the heaviest isotope value (-2.8‰ relative to VSMOW) of the 70 closed-basin lakes in Saskatchewan studied by Pham *et al.* (2009). This value is heavier than the sources of inflow to the lake. Bedrock groundwater near West Reflex Lake has isotope values between -23.0 and -15.8‰ VSMOW (Wallick, 1981; Kelley *et al.*, 1998). Local precipitation has similarly negative $\delta^{18}O$ values (weighted mean -17.0‰ VSMOW) (Rozanski *et al.*, 1993).

West Reflex Lake has a heavy $\delta^{18}O$ value compared to its source waters because it is a small, shallow, closed basin lake in semi-arid environment in which evaporation is the dominant process. Evaporation causes an increase in $\delta^{18}O$ as lighter isotopes are preferentially removed (Fig. 6.1; Leng and Marshall, 2004; Horton *et al.*, 2015). The degree of enrichment in $\delta^{18}O$ between West Reflex Lake's water and its source waters is consistent with other closed lakes in Alberta (Birks and Remenda, 1999) and Spain (Luzón *et al.*, 2009). Values of $\delta^{18}O$ in these lakes fluctuate seasonally and are up to 9.5‰ higher during the summer than the winter (Birks and Remenda, 1999; Luzón *et al.*, 2009). West Reflex Lake likely also shows similar seasonal variations in $\delta^{18}O$. The value of $\delta^{18}O$ in West Reflex Lake water in the summer, when evaporation is high, would be higher than the value in the winter, when evaporation is low and heavier oxygen isotopes fractionate into ice (Tranter, 2011).

3.3.2 Comparison to other lakes

The water chemistry of West Reflex Lake has anomalously high Cl^- and low SO_4^{2-} compared to other lakes in the region (Fig. 3.2). West Reflex Lake has similar proportions of

cations to Manito Lake and Tramping Lake: very little Ca^{2+}, and a small proportion of Mg^{2+} compared to Na^{+} and K^{+}. West Reflex Lake is much more similar to the bedrock groundwater

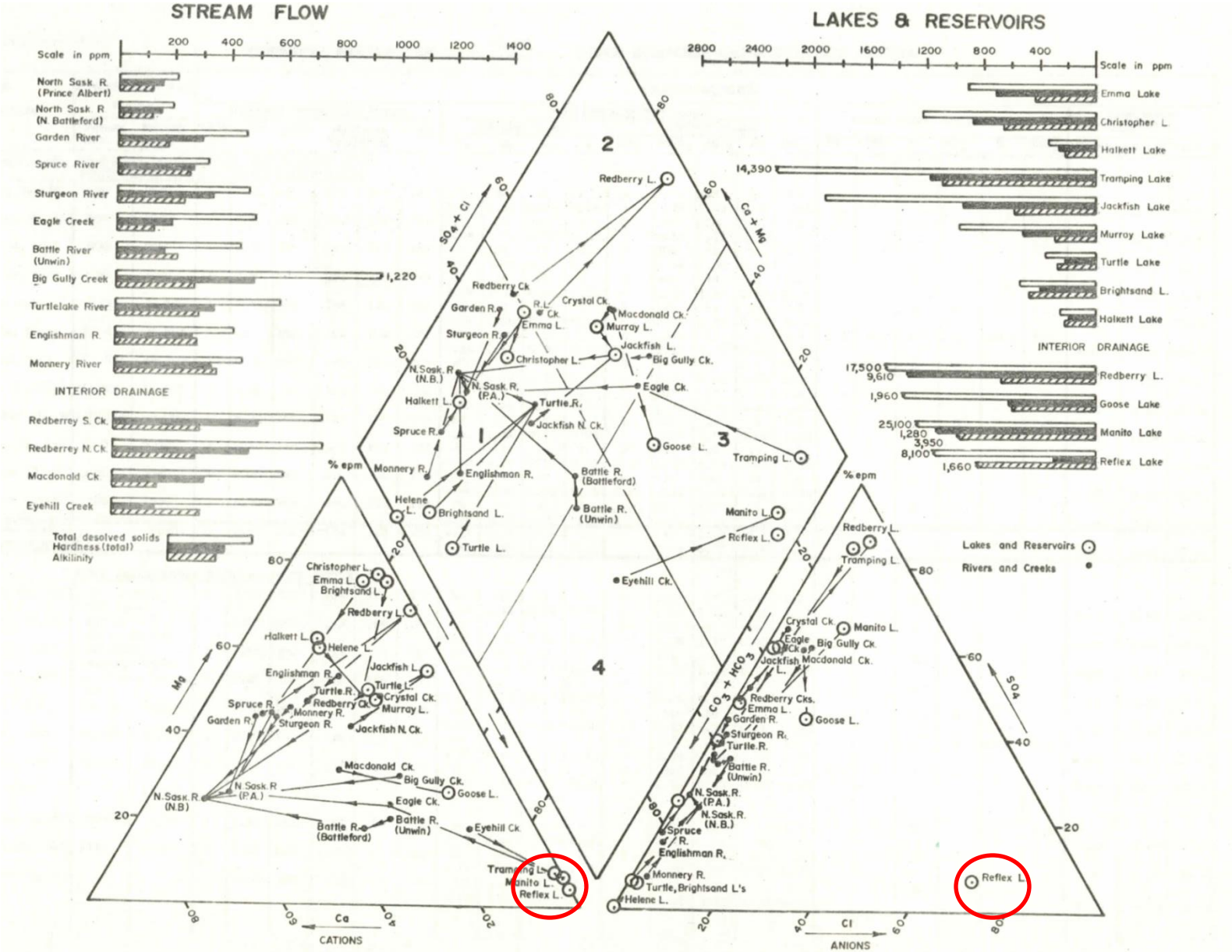

Figure 3.2: Piper diagram of water chemistry of lakes and rivers in the North Saskatchewan River basin, plotted in meq/L. In the anion triangle, West Reflex Lake (circled) has a distinctive chemistry. From Rutherford (1970).

than the Quaternary groundwater (Fig. 3.3). Based on comparison of the Piper diagrams showing the chemistry of groundwater from different depths (Fig. 3.3) with the diagram showing the chemistry of the other lakes in the region (Fig. 3.2), it is postulated that the other lakes receive most of their solutes from shallow groundwater, whereas West Reflex Lake receives solutes from deep groundwater. As the concentrations of solutes increased between 1967 and 2015, the relative proportions of Cl^- in West Reflex Lake water increased (Fig. 3.3). The increase in proportion of Cl^- could be a result of removal of other ions by the precipitation of evaporite minerals that are less soluble than chloride salts.

3.3.3 Mineral saturation and precipitation

At the time of sampling in 2015, West Reflex Lake was saturated with respect to huntite ($Mg_3Ca(CO_3)_4$), dolomite ($CaMg(CO_3)_2$), magnesite ($MgCO_3$), calcite ($CaCO_3$), aragonite ($CaCO_3$), and hydromagnesite ($Mg_5(CO_3)_4(OH)_2 \cdot 4H_2O$) (Fig. 3.4). Of these, magnesite, dolomite and huntite have a saturation index greater than 1 (10-fold supersaturation), which Arp *et al.,* (2001) consider to be prerequisite for carbonate precipitation. The saturation index of most minerals shown on Fig. 3.4 increased slightly between the 1980s and 2000s. Hydromagnesite was undersaturated in the 1960s and 1980s, saturated in 2004, and supersaturated by 2015.

The Jones triangle geochemical diagram (Fig. 3.5) can be used to show different scenarios of Ca- and Mg- carbonate precipitation. Calcite precipitation forces the composition to migrate directly away from the $HCO_3^- + CO_3^{2-}$ corner. Calcium is already depleted in the samples from West Reflex Lake, meaning the chemistry of the lake is conducive to early dolomite and Mg-carbonate precipitation (Deocampo, 2010; Last, 2013).

The Spencer triangle (Fig. 3.5) is a hydrochemical diagram used to illustrate the effects of calcium carbonate precipitation on a lake's water chemistry (Deocampo, 2010). When calcium

carbonate precipitates, the chemistry of the solution migrates directly away from the calcite point

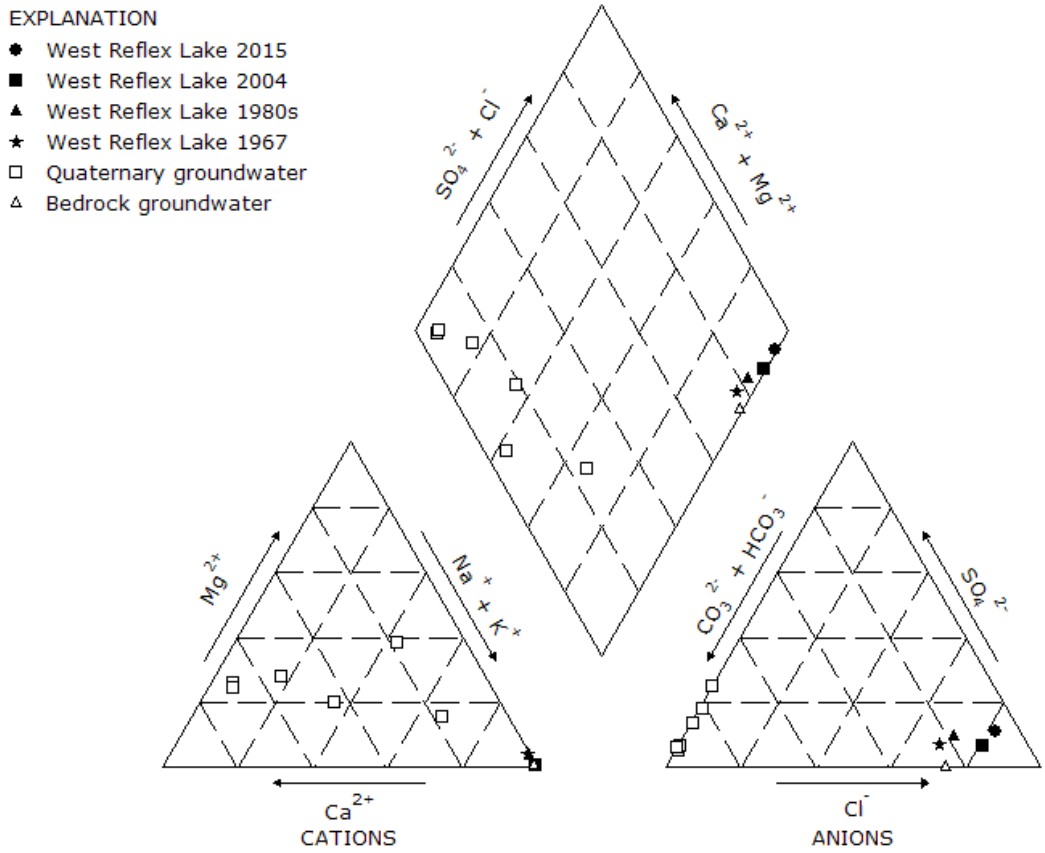

Figure 3.3: Piper diagram of the chemistry of West Reflex Lake water and Quaternary and bedrock groundwater. West Reflex Lake is more similar to the bedrock groundwater than the Quaternary groundwater. Data sources are provided in Tables 3.1 and 3.2.

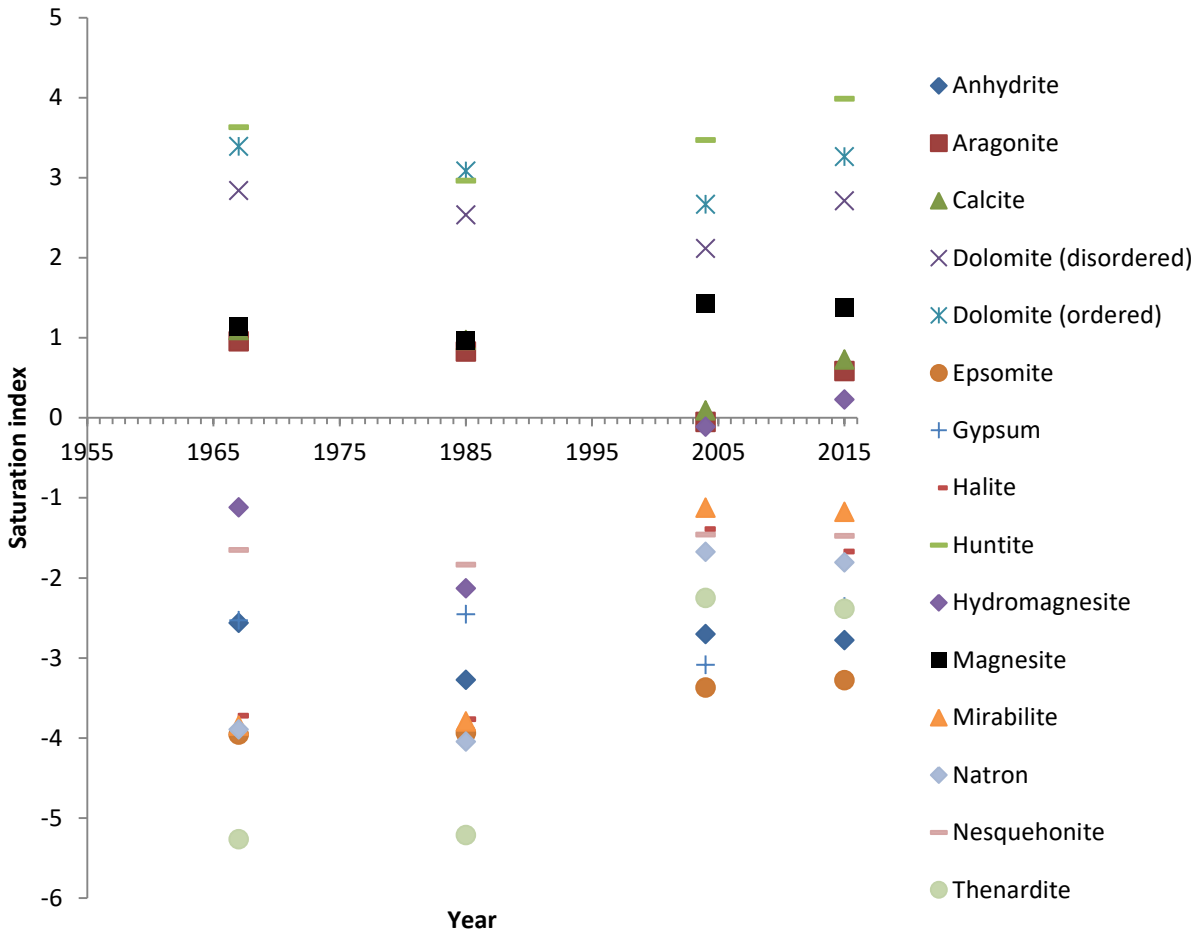

Figure 3.4: Saturation indices of selected minerals in West Reflex Lake. Data used for calculation of saturation indices are from sources in Table 3.2.

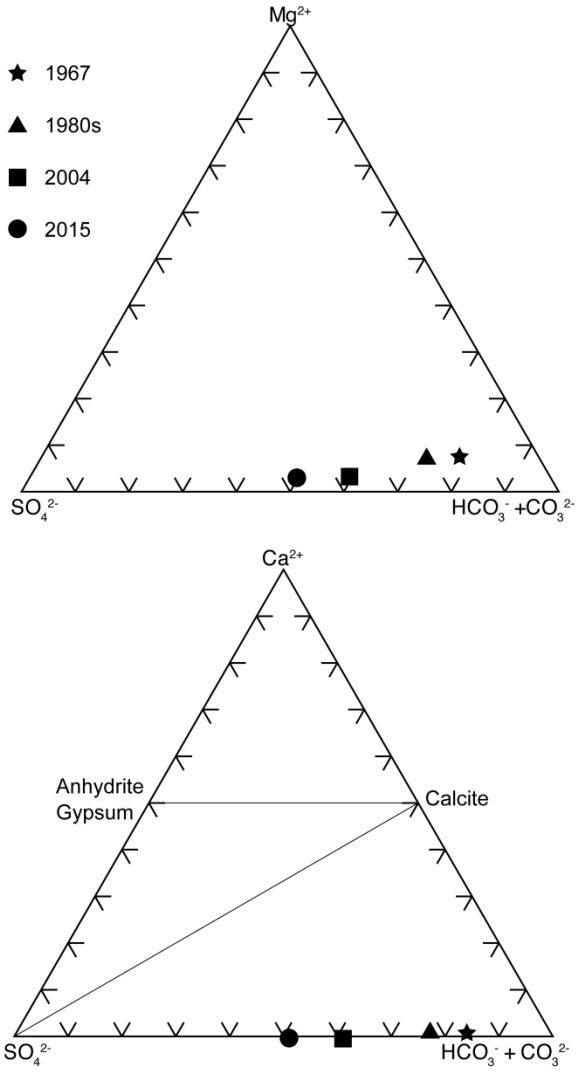

Figure 3.5: Jones (top) and Spencer (bottom) geochemical diagrams, showing changes in West Reflex Lake water through time. Data used for calculations are from sources in Table 3.2.

on the triangle. The West Reflex Lake water chemistry data do not show a trend consistent with calcite precipitation. Because West Reflex Lake's water has a very low proportion of Ca^{2+}, it is assumed that most of the Ca^{2+} taken up by $CaCO_3$ formation is contributed by groundwater. Therefore, the Spencer triangle does not adequately reflect $CaCO_3$ precipitation trends in West Reflex Lake.

3.3.4 Controls on lake water chemistry

The factors that control lake water chemistry are: 1) interaction between sediments and groundwater in the drainage basin; 2) quantity and composition of groundwater and surface water influx and efflux; and 3) physical, chemical, and biological processes operating in the water column itself (Last and Ginn, 2005). Quaternary deposits in the lake's drainage basin can interact with the water that flows through them. Water percolating through glacial till can exchange cations on clay minerals, dissolve feldspars and other soluble minerals, and precipitate a variety of minerals in the soils (Hendry *et al.*, 1986; Last, 2013). These processes will all affect the composition of the runoff that enters the lake.

Groundwater inflow is a major source of water and dissolved ions in West Reflex Lake. The shallow groundwater in Quaternary drift aquifers tends to be fresher, whereas the deeper groundwater in bedrock is more saline and often contains a larger proportion of Cl^-. Interaction between deep groundwater and the Paleozoic evaporites (predominantly in the Prairie Evaporite Formation) that underlie much of Saskatchewan and Alberta may be a source for the dissolved Na^+, Cl^-, and SO_4^{2-} (Grossman, 1968). During periods of drought, it is likely that the contribution of shallow groundwater to the lake will become smaller, since the response time is likely to be shorter in a shallow aquifer. However, the deep groundwater will not be affected by short term perturbations and will continue flowing into the lake. Thus, the solutes in the lake becomes more

concentrated both because of the decrease in the precipitation-evaporation ratio and because of the increase in the relative contribution of saline, bedrock groundwater.

The chemistry of West Reflex Lake probably varies seasonally. Unfortunately, seasonally resolved data are not available because water chemistry data from the lake were collected in the early summer. Springs floods decrease the salinity of the lake, and higher evaporation during the summer increases the salinity. The formation of ice on the surface of the lake in winter increases the salinity of the remaining liquid water (Canfield *et al.,* 1983). Mineral precipitation and dissolution as well as biological productivity can vary seasonally. Both these processes are influenced by, and can themselves influence, water chemistry.

4 Shoreline carbonate deposits

4.1 Introduction

4.1.1 Microbialite terminology

Microbialites are defined as "organosedimentary structures that have accreted as a result of a benthic microbial community trapping and binding detrital sediment and/or forming the locus of mineral precipitation" (Burne and Moore, 1987). Terminology used to describe microbialites suffers from a lack of standardization (Buick *et al.,* 1981; Dupraz and Strasser, 1999; Riding, 2000). For example, some structures labelled as "tufa pinnacles" may also be classified as microbialites (e.g. Scholl and Taft, 1964; Kempe *et al.,* 1991; Arp *et al*., 1998).Tufa is a porous rock deposited from ambient temperature springs (Macdonald, 1982; Flügel, 2010). Tufa can be deposited subaerially or subaqueously where springs enter alkaline lakes.

Burne and Moore (1987) proposed a classification scheme for microbialites based on their principal mode of accretion: those formed by trapping and binding are microbial boundstones, those formed by inorganic carbonate precipitation are microbial tufa, and those formed by biologically-influenced precipitation are microbial framestones. Most microbialites form by a combination of these end member processes. Trapping and binding of detrital sediment occur due to the filamentous nature of some cyanobacteria or the "sticky" extracellular polymeric substances (EPS) produced by microorganisms in microbial mats (Burne and Moore, 1987). Inorganic calcification occurs by processes such as degassing of CO_2 by turbulence, temperature increase, or freezing (Burne and Moore, 1987). Biologically-influenced calcification occurs in or on the sheaths of some cyanobacteria, partly as a result of the metabolic activity of the organism.

The features of microbialites can be described at the macro-, meso-, and micro-scales. Macroscopically, microbialites may occur as pinnacles or domes. These can form in metre-scale clusters called bioherms or biostromes (Cumings, 1932). The mesoscale fabric is commonly used to classify microbialites. Because the variety of fabrics in microbialites often defies classification by schemes such as Dunham's (1962) limestone classification, microbialite-specific classification schemes have been proposed by authors including Burne and Moore (1987) and Kennard and James (1986). In this paper, the classification used by Riding (2000) will be applied. Riding (2000) divided the fabric of microbialites into stromatolitic (laminated), thrombolitic (clotted), dendrolitic (branching), or leiolitic (aphanitic). Finally, the microstructure of microbialites includes cement and crystal morphology.

4.1.2 Shoreline carbonates in West Reflex Lake

West Reflex Lake contains four types of shoreline carbonate structures: isolated pinnacles, bioherms, laminated coatings, and beachrock (Fig. 4.1). The shoreline carbonates occur in discontinuous areas on the northern and southern shores of the lake. Multiple types of shoreline carbonate occur together, adjacent to or superposed on each other. Shoreline carbonates are larger and more abundant on the northern shore than on the southern shore. All carbonate structures are presently subaerially exposed; however, aerial photos show they would have been submerged in the 1940s (Fig. 3.1). The majority of the shoreline carbonates are located less than 50 m landward from the shore, but a few larger aggregates of pinnacles are up to 200 m from shore. Some of the shoreline carbonates are situated on or near springs. However, some springs are visible where no shoreline carbonates are observed. The outcrop and hand sample scale features and the microfabrics of each type of shoreline carbonate will be described.

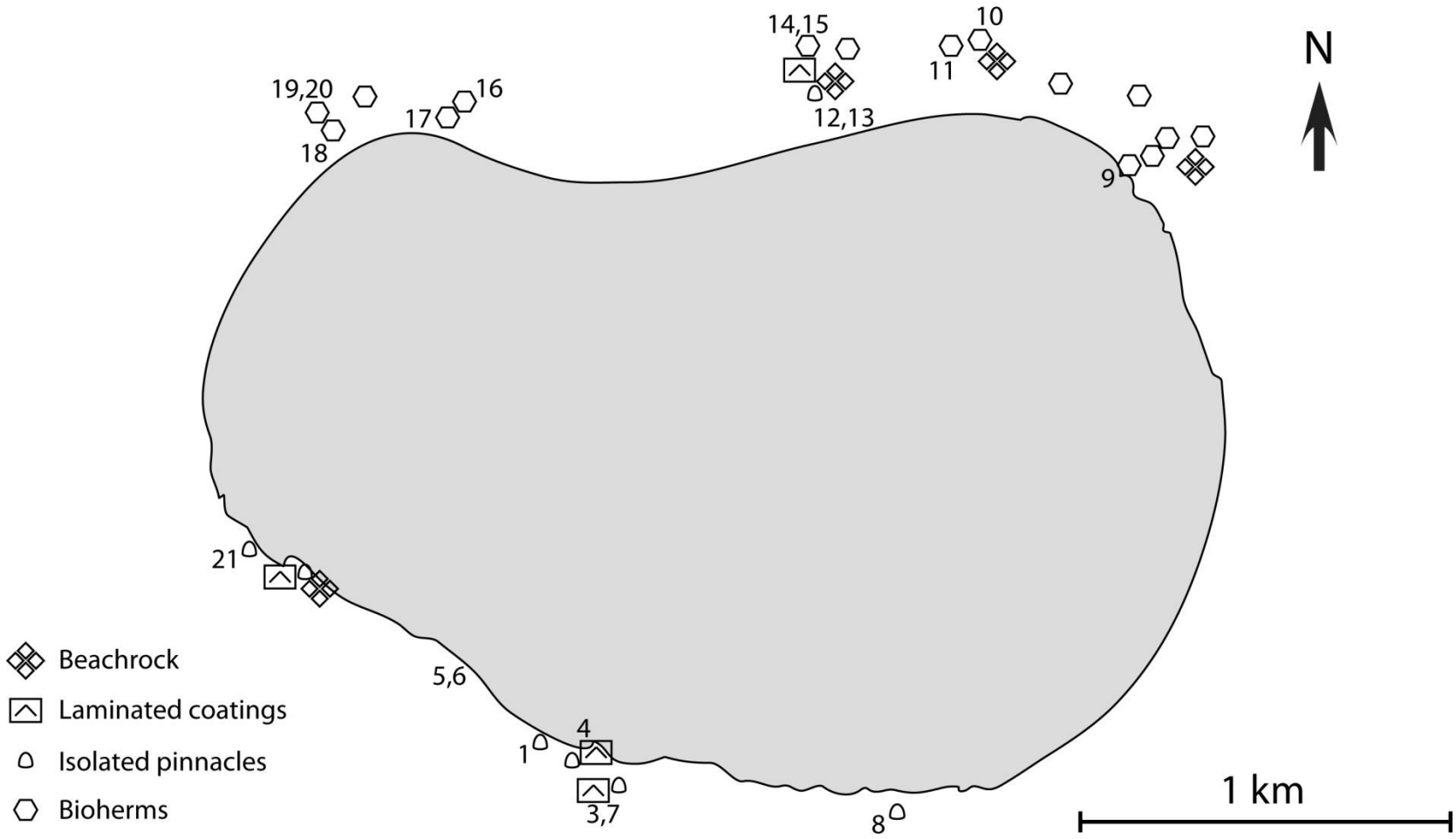

Figure 4.1: Occurrence of shoreline carbonates surrounding West Reflex Lake. Numbers refer to the locations of samples taken for this study (Appendix B). Sample IDs have the sample location number with the prefix WR.

4.2 Shoreline carbonate occurrence and macrostructure

4.2.1 Isolated pinnacles and bioherms

Isolated pinnacles and bioherms occur on the northern and southern shores of West Reflex Lake (Fig. 4.1). None were observed below the 2015 lake level. Bioherms are large aggregates of pinnacles. The northern shore of the lake is dominated by bioherms, and the southern shore is dominated by isolated pinnacles. Although the extent of induration varies from well-indurated to friable, bioherms tend to be more strongly indurated than isolated pinnacles. Both types of microbialite range from very pale orange (10 YR 8/2) to dark grey (N3).

Isolated pinnacles are common on the southern shore of West Reflex Lake. They are dome-shaped or columnar, 15-30 cm high and 8-20 cm wide (Fig. 4.2A, Fig. 4.3). The dome-shaped pinnacles tend to be preserved in growth position, whereas the columnar pinnacles are toppled onto their sides. The surfaces of the isolated pinnacles are rough and cauliflower-like or smooth and knobby. Rough textures make up most of the exterior surfaces and are formed by irregular aggregates of carbonate-coated filaments (Fig. 4.4A). The smooth texture is composed of cream-coloured, knobby carbonate and occurs mainly in depressions on the surfaces of the domes or columns (Fig. 4.4B).

Bioherms occur on the north side of the lake. They tend to be concentrated in clusters parallel to the shoreline or along ridges formed by beachrock. The bioherms are 30-80 cm in diameter. They are composed of numerous pinnacles on a base made up of ledges of carbonate-cemented sand (Fig. 4.2B). Several of the bioherms were toppled on their sides, likely due to erosion of sand away from the base. The exterior surfaces of the bioherms are rough and commonly contain molds of plant stems up to 1 cm in diameter. Rounded, bumpy to knobby

coatings are common on the exterior of the pinnacles making up the bioherms. Discontinuous, subhorizontal ledges of carbonate form much of the lower part of the bioherms.

The isolated pinnacles and bioherms are grouped together as thrombolites based on their internal fabric (Fig. 4.3). The thrombolitic fabric is composed of branching filaments that are oriented in growth position (subparallel, branching upward) or randomly. Interspersed with the filaments are patches of poorly indurated, rubbly carbonate. Molds of plant material (~1 mm diameter) are scattered through the thrombolites. Bands of reddish-brown and green staining are present a few millimetres inside the exterior crust of the microbialites. Convex upward growth surfaces, similar to the exterior crusts, are present in some thrombolites.

4.2.2 Laminated coatings

Laminated coatings are present on large bioherms, exposed edges of beachrock, and cobbles and boulders (Fig. 4.2C). The thickest, best developed laminated coatings are deposited on the largest bioherms, farthest from the lake's present shoreline. Cobbles and boulders with laminated coatings do not form a continuous band around the lake; rather, they are concentrated in areas with other types of shoreline carbonates. The coatings are 1-10 mm thick and yellowish grey (5 Y 8/1). They are only weakly attached to the substrates and are often partially eroded away. The exterior of the laminated coatings are smooth and shallowly pitted to knobby or bumpy. The meso-scale fabric of the laminated crusts is stromatolitic (Fig. 4.5). Crusts that are >4 mm thick have mm-scale lamination and fenestral porosity between laminae.

Figure 4.2: Field photographs of shoreline carbonates from West Reflex Lake. Field notebook (18 cm long) and pencil (14 cm long) for scale. A) Columnar isolated pinnacle (WR-14), toppled on its side. B) Bioherm (WR-19), toppled on its side. Carbonate-cemented ledges are visible, oriented vertically and parallel to the plane of the image, in the larger bioherms on the right. C) Laminated coating on boulders (WR-04) at the shoreline of the lake. The cream-coloured laminated coating is weathering away from the dark grey intrusive igneous boulders. D) Beachrock (WR-10), surrounded by grass near the lake's shore. Parts of the surface with higher relief are capped by laminated coatings that prevented erosion.

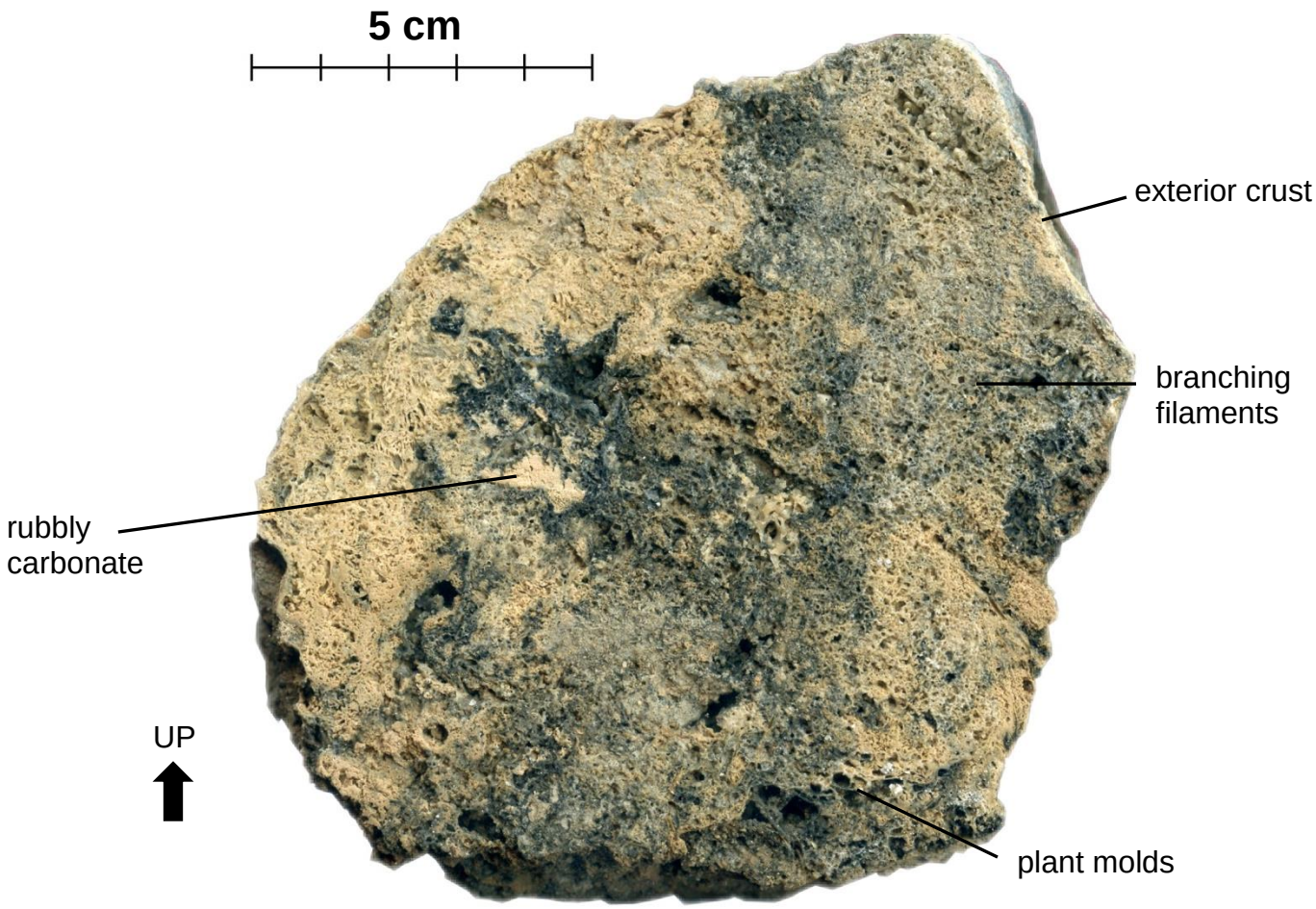

Figure 4.3: Internal texture of a dome-shaped isolated pinnacle (WR-01). Labels indicate locations of features described on page 29.

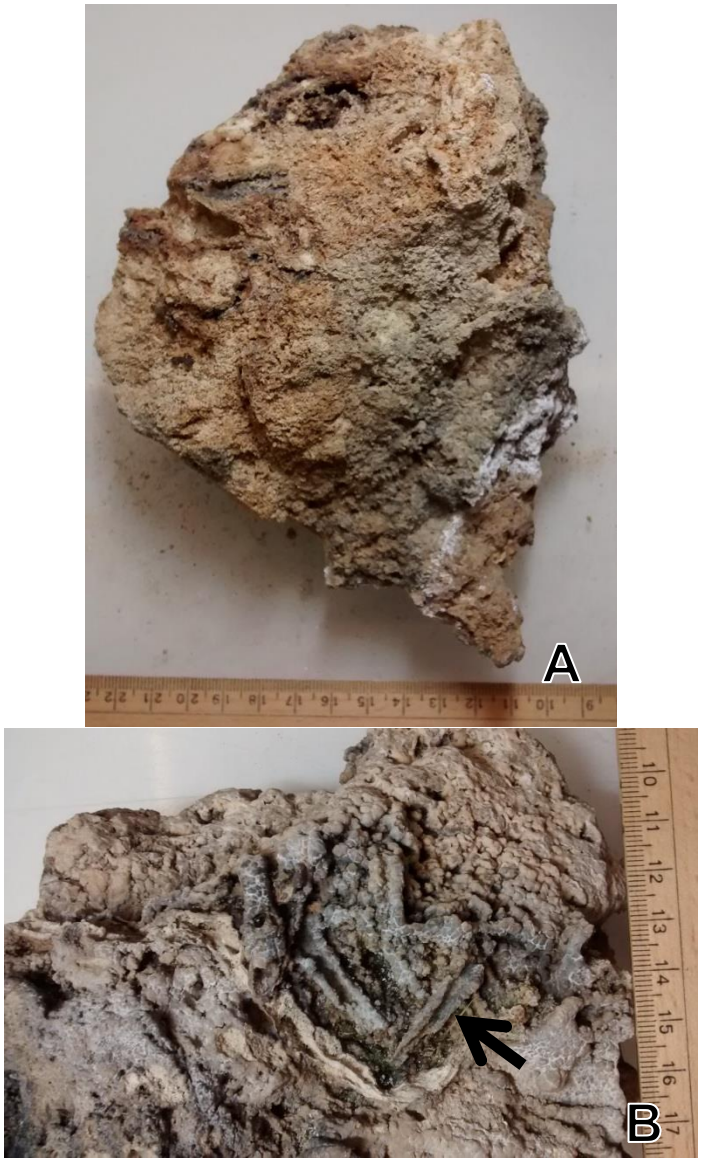

Figure 4.4: Rough (A) bottom surface and knobby (B) top surfaces on isolated pinnacle WR-03.The arrow in B indicates a mold of plant material in knobby carbonate. Scale bar in cm.

4.2.3 Beachrock

Beachrock underlies isolated pinnacles and bioherms. In places, the beachrock is encrusted with a laminated coating (Fig. 4.2D). In a sample from locality 13, beachrock has enveloped a small (~8 cm) isolated pinnacle (Fig. 4.6). The beachrock is well-indurated and dusky yellow (5 Y 6/4) to light olive grey (5 Y 5/2). The exterior of the beachrock is covered by a knobby laminated coating in places. The beachrock is laminated to bedded with layers 3 to 20 mm thick. The layers fine upward. Beds are often separated by mm-scale subhorizontal fenestral pores that have smooth, knobby carbonate coatings on their interior.

4.3 Microscale components

The microscale components of the shoreline carbonates of West Reflex Lake include irregular micrite, clotted micrite, pellets, filaments, non-filamentous microbial components, plant molds, evaporite pseudomorphs, carbonate rods, sand grains, and chert. The appearance, distribution, and relationships of these components will be described in the following section and are summarized in Appendix C. The components present in each type of shoreline carbonates are listed in Table 4.1.

4.3.1 Irregular micrite

Irregular micrite occurs in all types of shoreline carbonates. The micrite is dark grey and irregularly distributed in diffuse patches >100 μm (Fig. 4.7). Interparticle porosity varies from ~10 to 30%. The irregular micrite that occurs beneath fenestral pores in beachrock has the lowest porosity. In places, the micrite contains fine quartz and lithic sand grains.

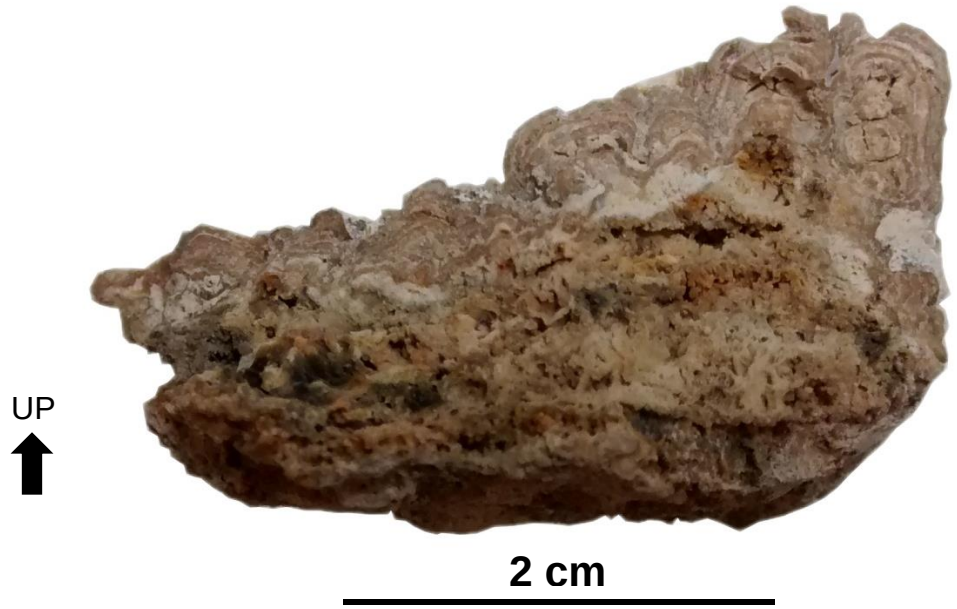

Figure 4.5: Cross-sectional view of laminated crust from the exterior of bioherms WR-14. The laminated crust adheres to underlying thrombolitic material.

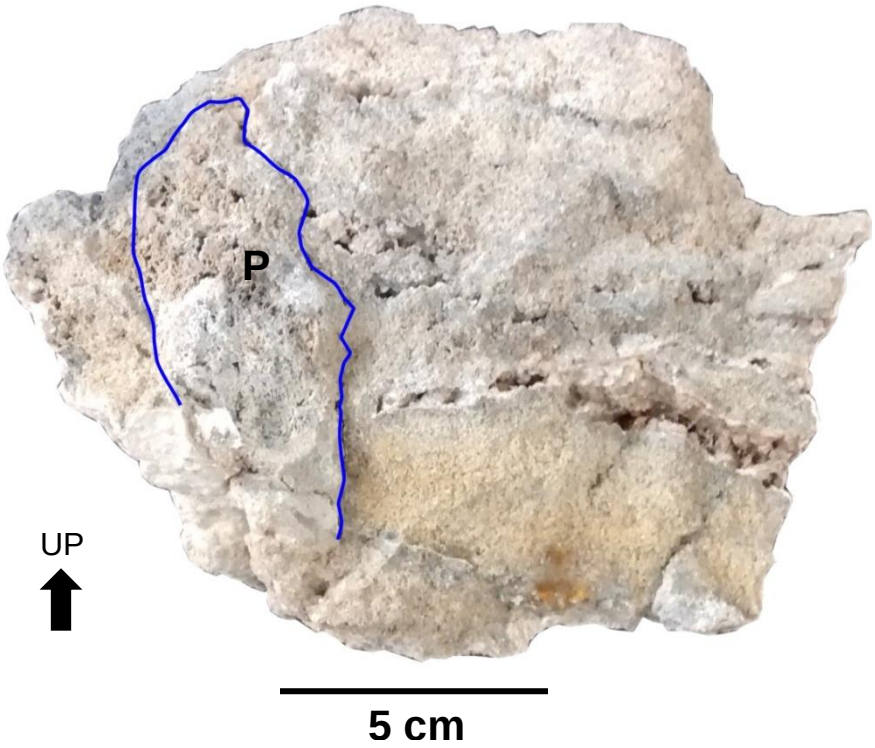

Figure 4.6: Cross-sectional view of beachrock sample WR-13 contains a small isolated pinnacle (P), outlined in purple.

Table 4.1: Summary of the components present in the shoreline carbonates of West Reflex Lake.

Component	Shoreline carbonate types			
	Isolated pinnacles	**Bioherms**	**Laminated coatings**	**Beachrock**
Irregular micrite	Common	Common	Rare	Rare
Clotted micrite	Common	Common	-	Rare
Pellets	Rare	Rare	-	Common
Micrite crust	Common	Common	-	-
Fine filaments	Common	Common	-	Rare
Coarse filaments	Common	Common	-	Rare
Non-filamentous microbial components	Common	Common	-	Common
Plant molds	Common	Common	Common	-
Evaporite pseudomorphs	Rare	Rare	-	-
Carbonate rods	Common	Common	-	-
Sand grains	Rare	Rare	Rare	Common
Chert	Rare	Rare	-	-

- not observed

4.3.2 Clotted micrite

Clotted micrite is the dominant component in the thrombolites and is present in smaller proportions in beachrock and laminated coatings. The micrite is dark grey and concentrated in clots 50-80 μm in size (Fig. 4.8). Clots are elongate and exhibit no lamination or zonation. The clots are clustered together in branching, shrub-like patterns, and locally contain molds of coarse filaments. The micrite clots are commonly interspersed with sand grains. Micrite clots also occur in moldic and fenestral pore space as geopetal fill.

4.3.3 Pellets

Brine shrimp fecal pellets are present in beachrock and thrombolites. In beachrock, pellets are interspersed with sand grains. They are uncommon in the thrombolites; where present, they are interspersed with clotted micrite and coarse filaments. Pellets are elongate, ~300 μm long, and have slightly squared-off ends (Fig. 4.9). They are composed of dark grey micrite with

no internal structure. Brine shrimp were observed in West Reflex Lake when sediment and water samples were collected. Brine shrimp congregate near springs entering saline lakes due to the slightly decreased salinity (Arp, 1995).

4.3.4 Micrite crust

Crusts of dense micrite drape over the exterior surface of thrombolites (Fig. 4.10). Micrite crusts range from 500 to 1000 μm thick. They are commonly thin, poorly developed, and weathered away from the substrate. The micrite smooths the irregular surface of the underlying porous material. The crust is massive or weakly laminated and coarsens outward to microspar. Rarely, filaments are entombed in the crust. The outermost surface of the micrite crusts fluoresces orange.

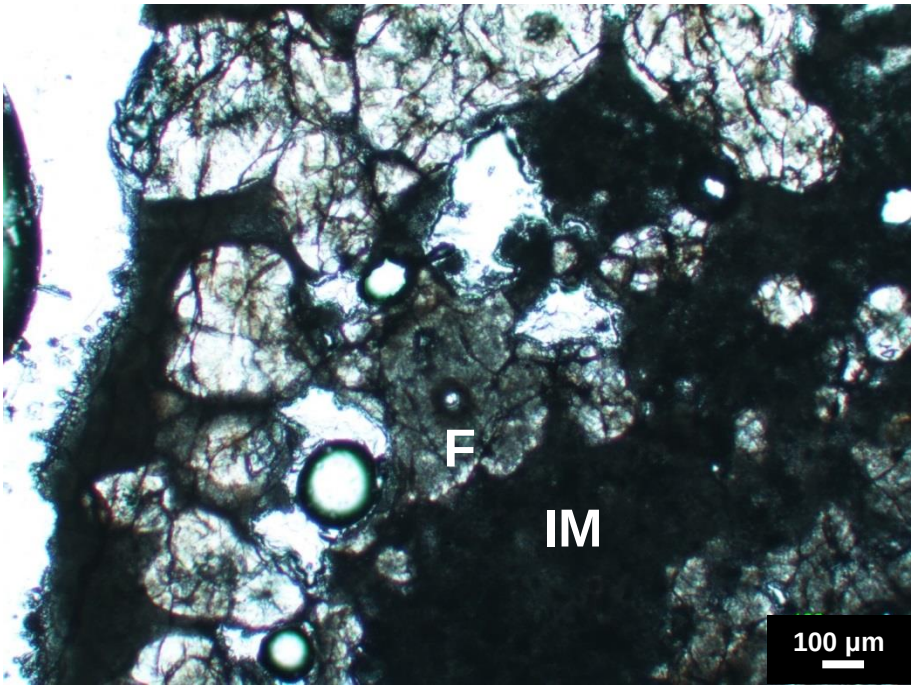

Figure 4.7: Thin section photomicrograph of irregular micrite (IM) between botryoidal cement-coated filaments (F) in a bioherm.

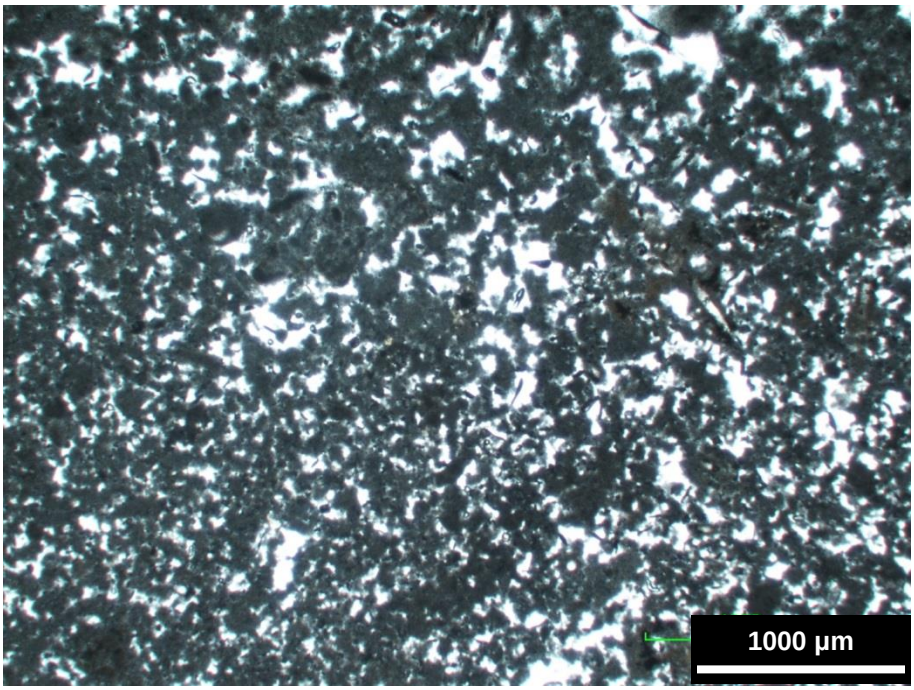

Figure 4.8: Thin section photomicrograph of clotted micrite (grey) from a bioherm. White areas are pore space.

4.3.5 Microbial filaments

Microbial filaments make up most of the volume of the isolated pinnacles, and a large proportion of the volume of bioherms. Two types of filaments can be distinguished by their diameter.

4.3.5.1 Fine filaments

Fine filaments are 0.5-8.0 µm in diameter. Because of their small diameter, they are best observed using a scanning electron microscope. The filaments are composed of organic matter and are round and smooth or flat and desiccated. Rarely, small carbonate bumps are observed on their surfaces (Fig. 4.11). The filaments occur predominantly as a network of flattened, branching filaments, draping over the exterior of other microscale components and cements (Fig. 4.12).

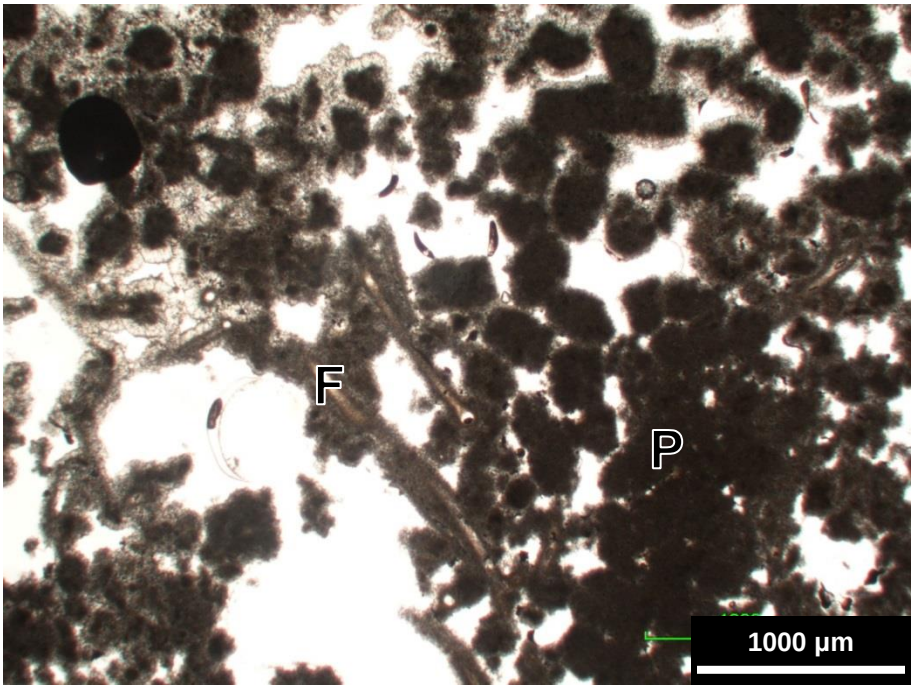

Figure 4.9: Plane-polarized light photomicrograph of pellets (P) next to micrite-coated coarse filament molds (F) in a thrombolite.

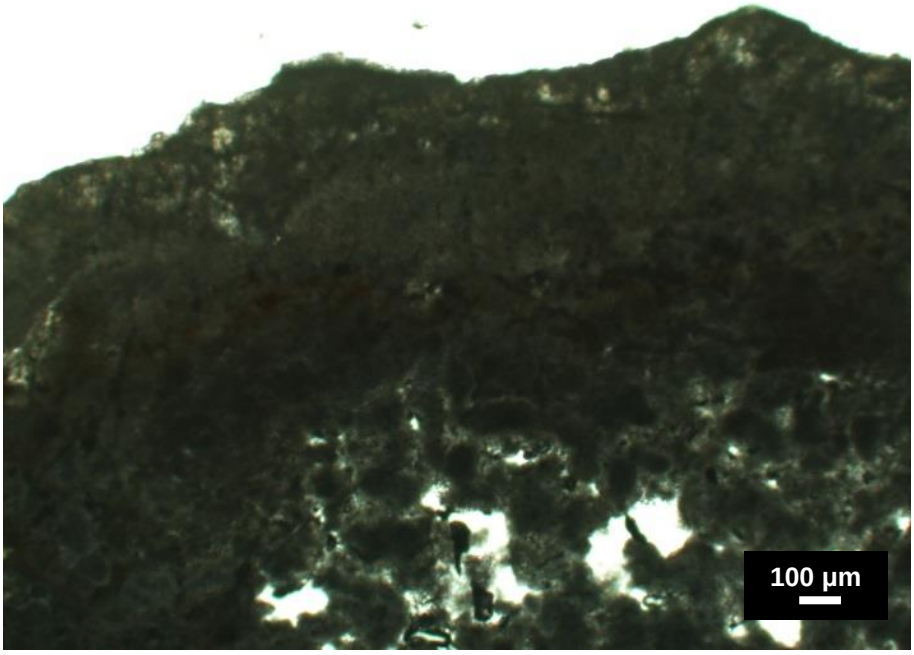

Figure 4.10: Plane-polarized photomicrograph of micrite crust over the exterior of an isolated pinnacle.

4.3.5.2 Coarse filaments

The coarse filaments are 200-3000 μm long and 15-40 μm in diameter. Coarse filaments are branching and have a smooth surface. They occur predominantly as molds in microcrystalline aragonite cement, but in places, the organic microbial filament is preserved (Figs. 4.13 and 4.14). A framework of carbonate cements surrounding the coarse filaments makes up the majority of the thrombolites. Filaments that have a similar diameter but have scalloped edges are present in isolated pinnacle sample WR-21 (Fig. 4.15). In the scalloped filaments, organic material is preserved, surrounded by botryoidal calcite and isopachous fibrous aragonite cements.

4.3.6 Non-filamentous microbial components

Other features attributed to microbial activity in the shoreline carbonates in West Reflex Lake include cell molds, preserved cells, and desiccated biofilm. Cells and molds were identified based on their similarity to microbial cell molds in microbialites identified by Braithwaite *et al.* (1989). Molds of two adjacent cells 35 μm in diameter were observed in micrite (Fig. 4.16). Preserved cells 7-9 μm in diameter were observed in a pore of a bioherm sample (Fig. 4.17). A sub-micron scale desiccated biofilm is present on the surfaces of some filaments and beachrock cement (Fig. 4.18). The biofilm has a wrinkled, spiky appearance and coats the exterior of other components. Desiccated biofilms from Death Valley microbialites (Douglas *et al*., 2008) are similar in appearance.

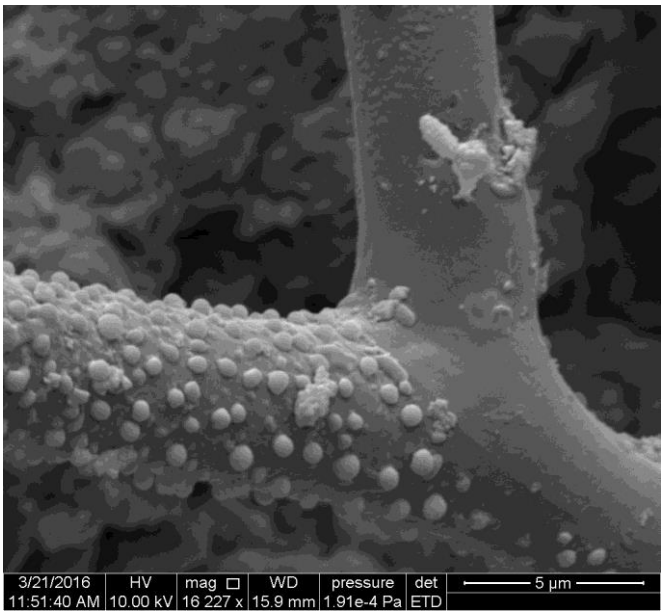

Figure 4.11: SEM photomicrograph of a fine filament from a bioherm. Carbonate bumps are visible on the left branch of the filament.

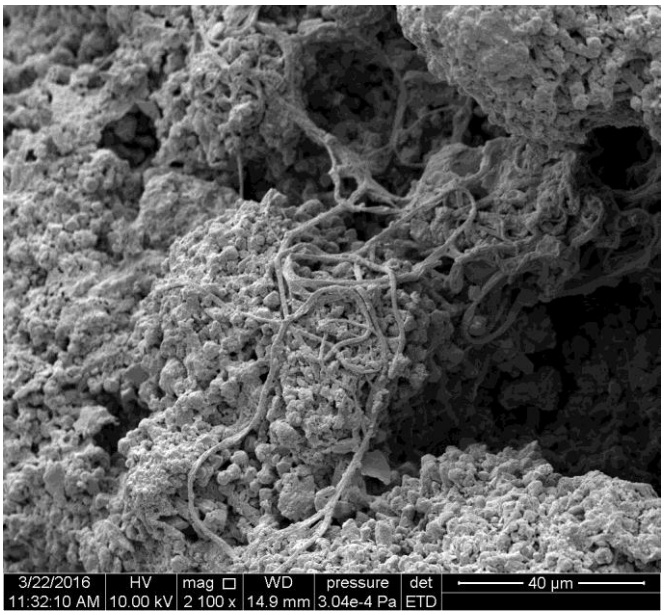

Figure 4.12: SEM photomicrograph of a network of desiccated, fine filaments in a bioherm.

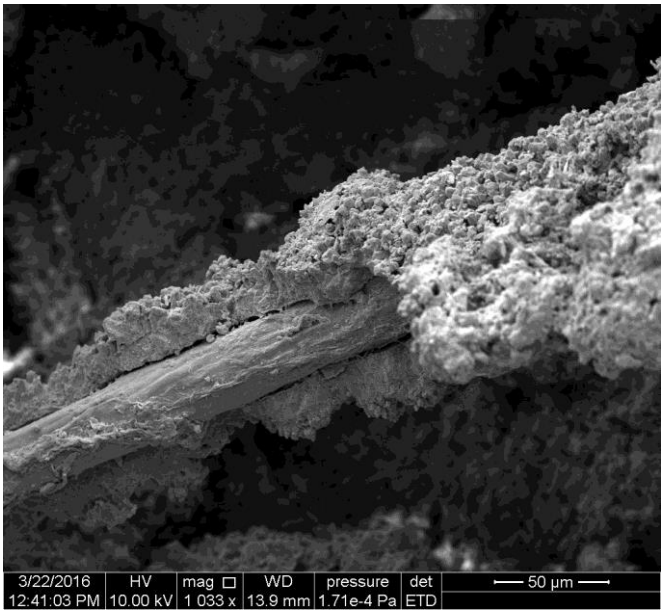

Figure 4.13: SEM photomicrograph of a coarse microbial filament encrusted with calcite. The sample is from an isolated pinnacle.

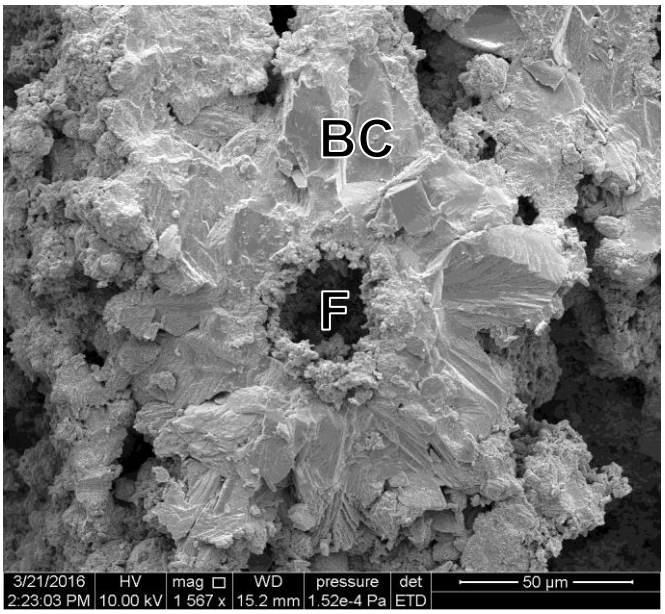

Figure 4.14: SEM photomicrograph of a mold of a coarse filament (F) in botryoidal calcite (BC) from a bioherm. Micrite is present in interior of the mold.

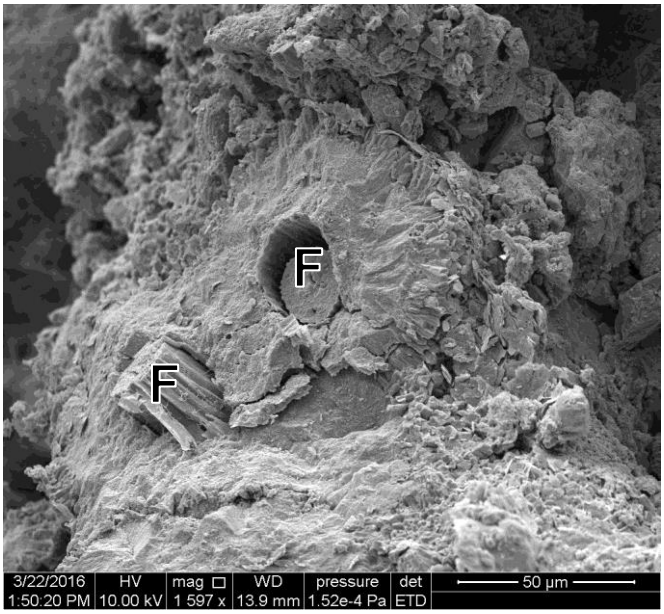

Figure 4.15: SEM photomicrograph of scalloped filaments (F) in an isolated pinnacle. Organic matter is preserved in the centre of the filament.

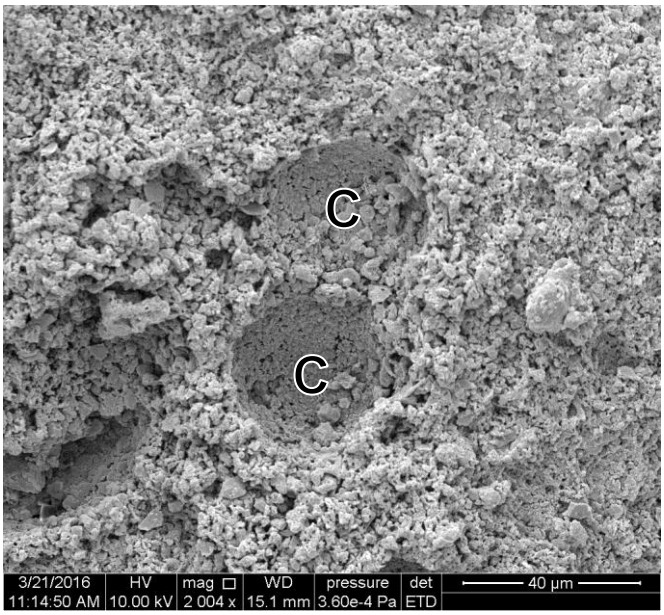

Figure 4.16: SEM photomicrograph of micrite containing molds of two cells (C) in a beachrock.

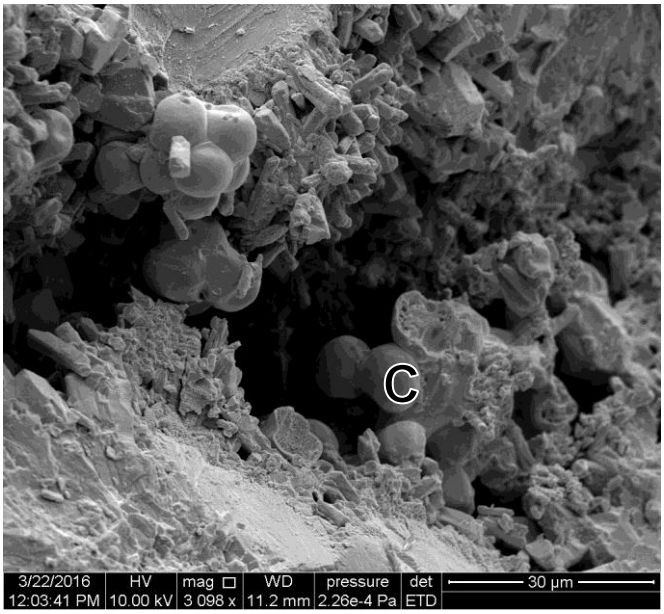

Figure 4.17: SEM photomicrograph of preserved cells in a fenestral pore within a bioherm.

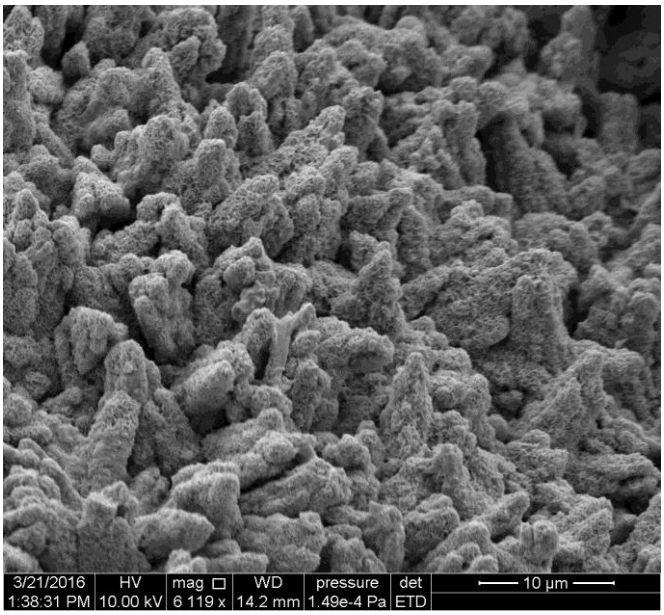

Figure 4.18: SEM photomicrograph of sub-µm wrinkled texture (desiccated biofilm) on the surface of bladed cement in beachrock.

4.3.7 Plant molds

Cylindrical molds of plant material are scattered throughout many thrombolites and on the upper surface of some beachrock (Figs. 4.4B, 4.19). The plant molds are between 200 and 5000 μm in size and coated by microcrystalline aragonite cement. Some large molds in the thrombolites are filled by cements or geopetal clotted micrite.

4.3.8 Evaporite pseudomorphs

Lath-shaped structures with microcrystalline aragonite walls, up to 2 mm long and 400 μm wide, occur in bioherms (Fig. 4.20). They have a lozenge-shaped cross section and occur in parallel clusters or intersect each other at right angles (Fig. 4.21). The walls of the pseudomorphs are composed of micrite to microspar or carbonate rods, and the hollow centres contain micrite or clear, equant calcite crystals that are 50-300 μm in size. Pseudomorphs from modern marine stromatolites that similar in morphology to the pseudomorphs in West Reflex Lake's microbialites were interpreted by Von der Borch *et al.* (1977) to have formed by replacement of the exterior of gypsum crystals by aragonite.

4.3.9 Carbonate rods

Carbonate rods are present in pinnacles and bioherms. They are 7-29 μm in length, 4-15 μm in diameter and are widest at the midsection (Fig. 4.22). The average length to width ratio is 1.7. Carbonate rods are composed of bladed crystals 2.0-4.0 μm long and 0.9-2.0 μm in diameter, with the c-axes oriented parallel to the long dimension of the rod. Coalesced carbonate rods form planar surfaces or spiky balls in the thrombolites (Fig. 4.23). They make up the walls of evaporite pseudomorphs.

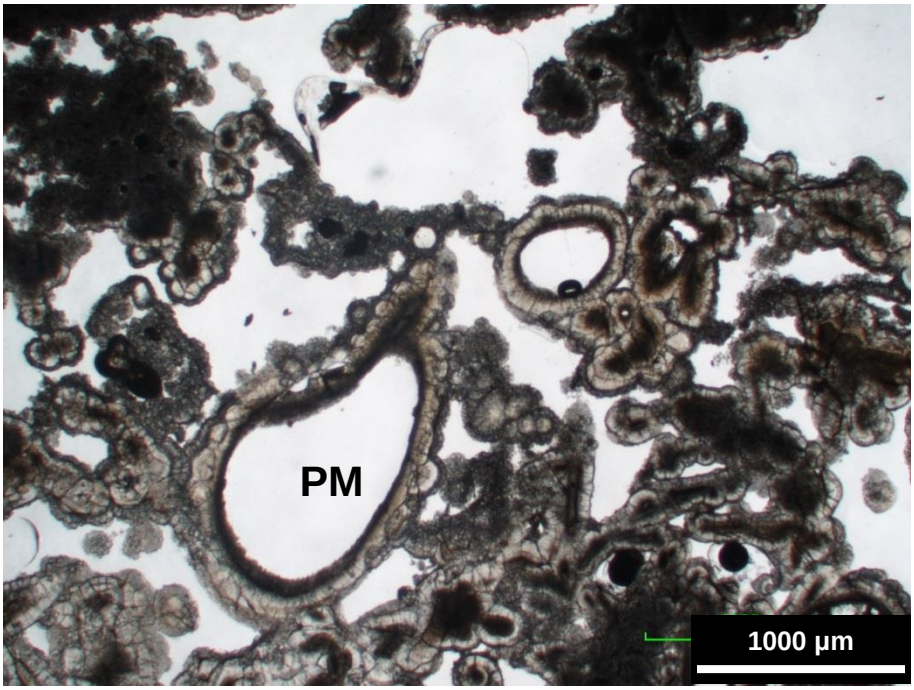

Figure 4.19: Plane-polarized light photomicrograph of plant molds (PM) in a thrombolite. The molds are coated with botryoidal cements.

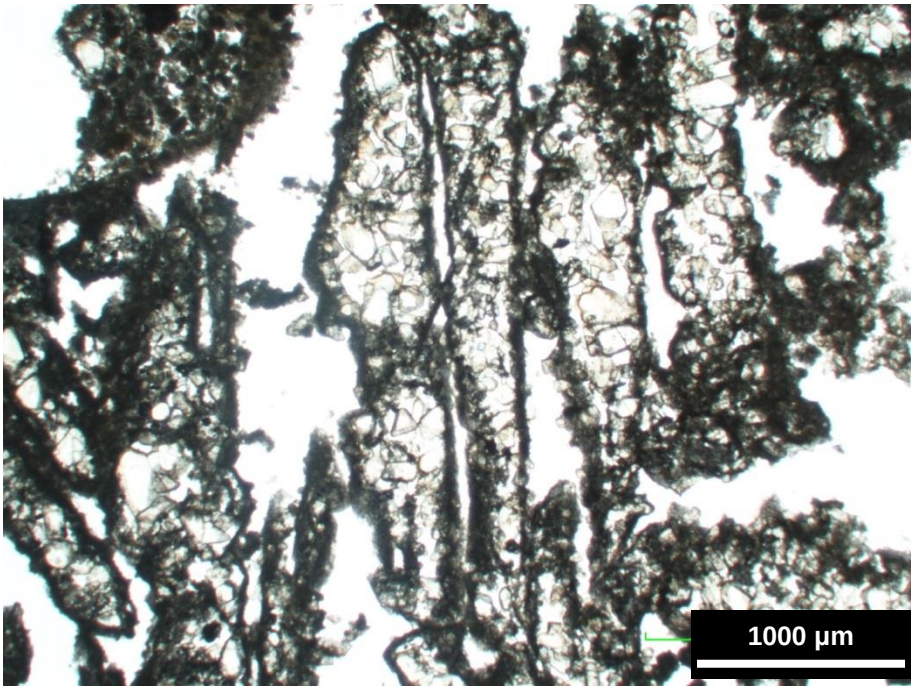

Figure 4.20: Thin section photomicrograph of evaporite pseudomorphs in a thrombolite. Each pseudomorph contains equant calcite crystals.

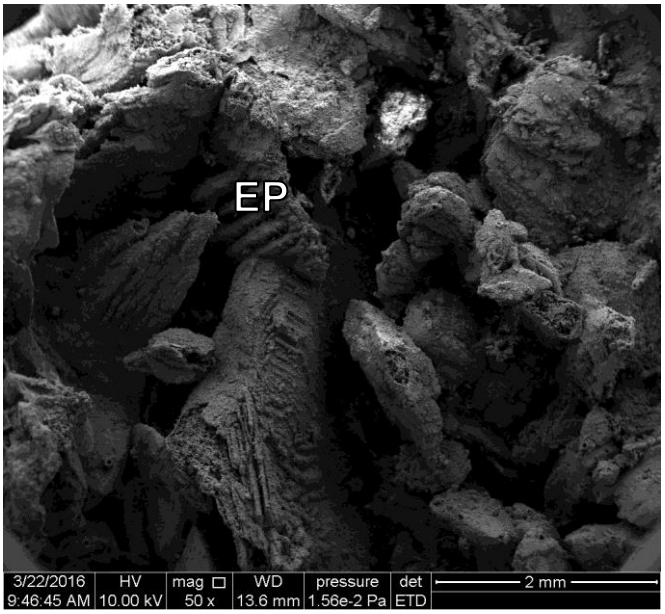

Figure 4.21: SEM photomicrograph of intersecting evaporite pseudomorphs (EP) in a bioherm.

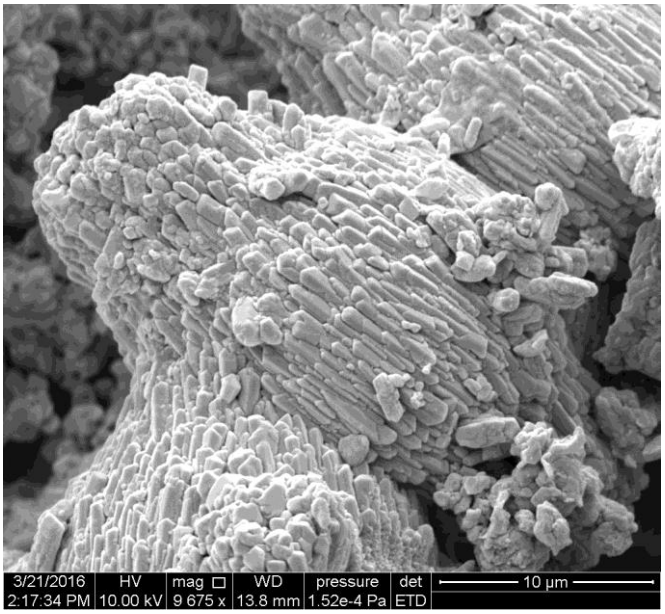

Figure 4.22: SEM photomicrograph of a single carbonate rod, aligned parallel to neighbouring rods. Each carbonate rod is composed of smaller bladed crystals. The photomicrograph is from a bioherm.

4.3.10 Sand grains

Sand grains are incorporated into the thrombolites, beachrock, and laminated coatings and are similar in composition and texture to the beach sediment. Sand grains are the dominant component in the beachrock, which can be classified as a lithic arenite. The sand grains are fine sand to medium sand size, subrounded to rounded, and well-sorted. They are 40-60% quartz, 20-40% lithic fragments, and 10-20% feldspar. Sand grains occur in a matrix of irregular micrite or cemented by microcrystalline aragonite. Peloids occur between sand grains in places.

4.3.11 Chert

Chert was observed in the top portion of bioherms WR-08 and the exterior of isolated pinnacle WR-01. It is a very minor component of the total volume of the thrombolites. Chert is not coated with other cements. The chert is composed of equant microquartz grains and contains small, angular, black inclusions. The chert replaces evaporite pseudomorphs or patches of irregular micrite (Figs. 4.24 and 4.25).

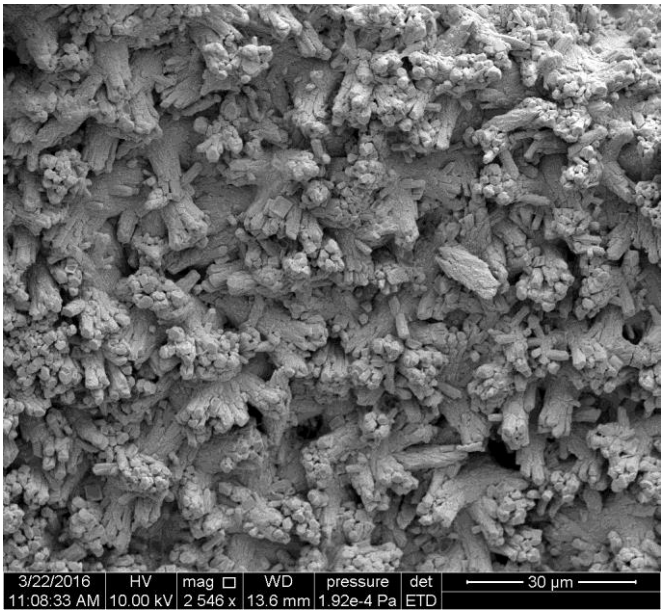

Figure 4.23: SEM photomicrograph of a surface made up of carbonate rods in a bioherm. The rods intersect each other at various angles.

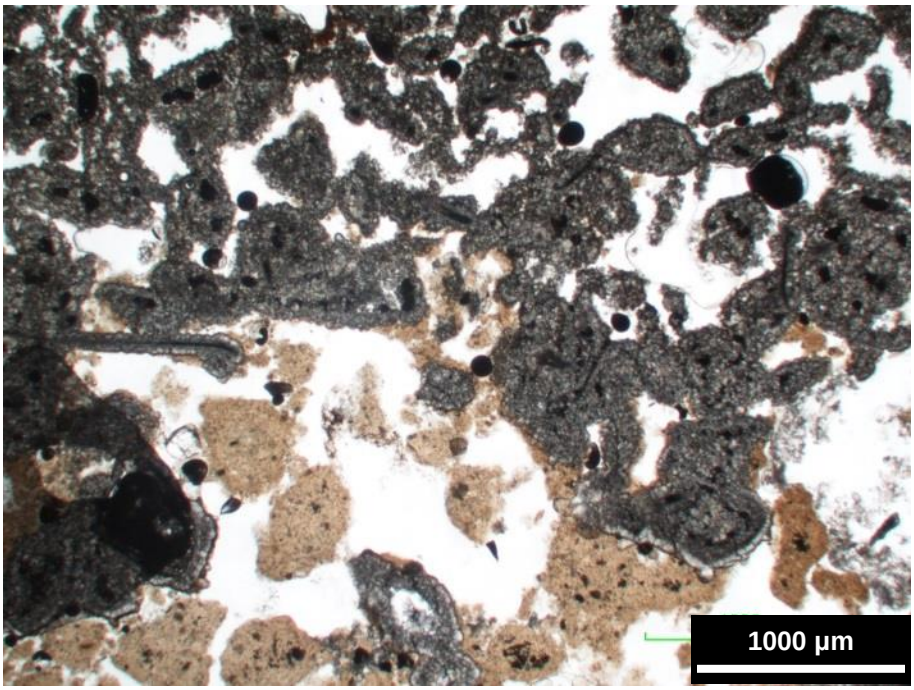

Figure 4.24: Plane-polarized light photomicrograph of chert (light brown) replacing evaporite pseudomorphs (grey) in an isolated pinnacle.

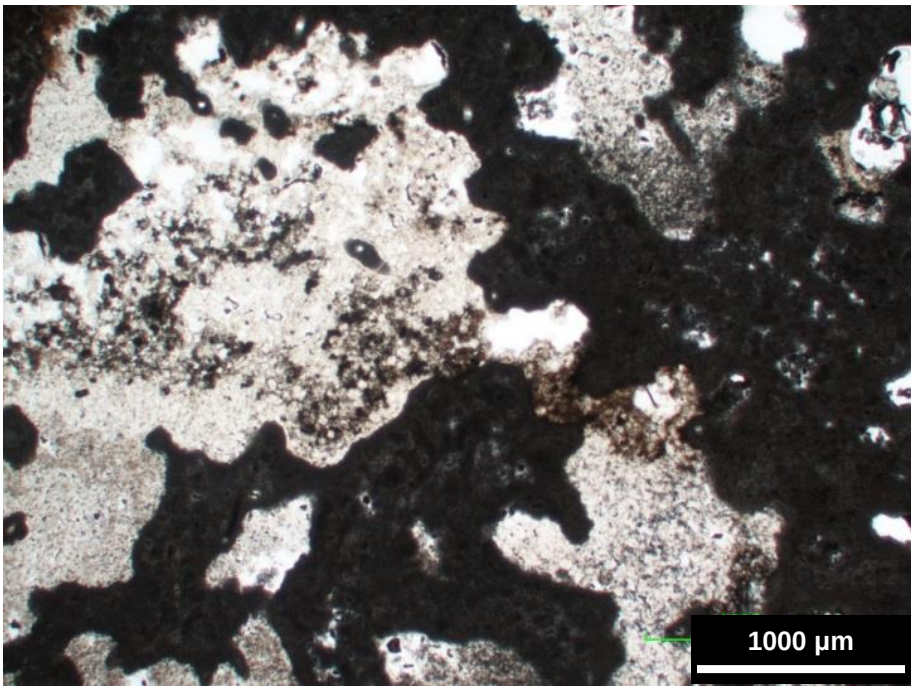

Figure 4.25: Plane-polarized light photomicrograph of chert (light) and micrite (dark) in an incipient bioherm. The micrite appears to have been replaced by chert.

4.4 Cements

Nine types of cement were identified in the shoreline carbonates of West Reflex Lake. The cements are described in the following sections.

4.4.1 Microcrystalline aragonite cement

Microcrystalline aragonite cement occurs in all shoreline carbonate types. It coats coarse filaments, plant material, and sand grains. Several generations of microcrystalline cement are interlaminated with other cements in many areas. Microcrystalline cement has a bumpy, irregular surface and variable thickness. Microcrystalline cement often contains black clots that are probably remnant organic matter. The cement exhibits bright blue to light brown fluorescence and patchy dull green luminescence with specks of bright red (Fig. 4.26). The cement locally appears weakly banded in cathodoluminescence.

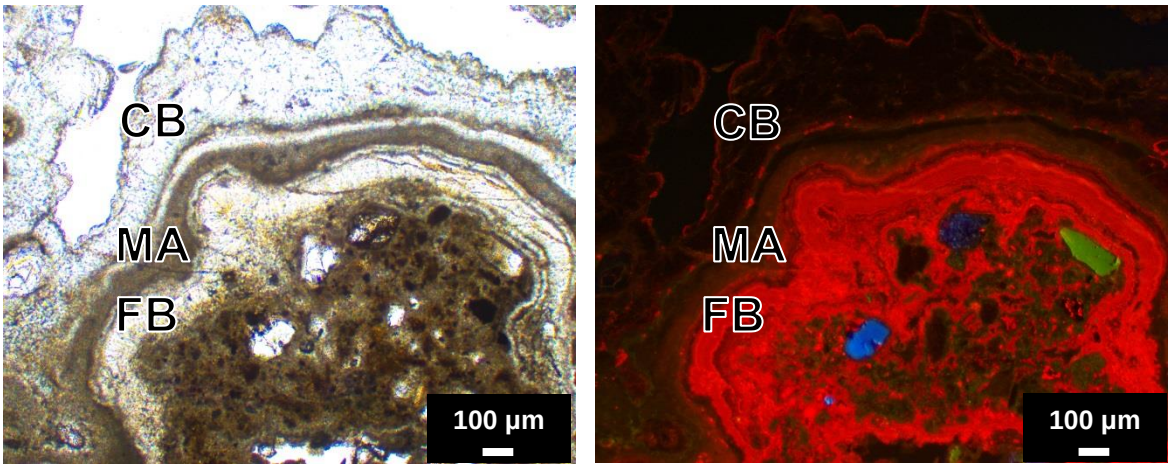

Figure 4.26: Plane polarized light (left) and cathodoluminescence (right) images of several generations of cement in a beachrock. Cements developed on a substrate of irregular micrite and fine sand. From oldest to youngest, the cements are finely laminated botryoidal calcite cement (FB), microcrystalline aragonite cement (MA), and colourless botryoidal calcite cement (CB).

4.4.2 Colourless botryoidal calcite cement

Colourless botryoidal calcite cement occurs mainly in large pores in beachrock, but are also present in thrombolites. It coats irregular micrite, clotted micrite, coarse filaments, microcrystalline aragonite cement, and coarsely laminated botryoidal cement. It underlies dogtooth calcite cement, finely laminated botryoidal cement and microcrystalline aragonite cement. This cement rarely contains filament molds. The cement is composed of clusters of small (<100 μm diameter) botryoids, forming a bumpy coating on the substrate (Fig. 4.27). The cement has dull blue fluorescence and dull red luminescence, typically with a thin bright red band at the exterior surface (Fig. 4.28).

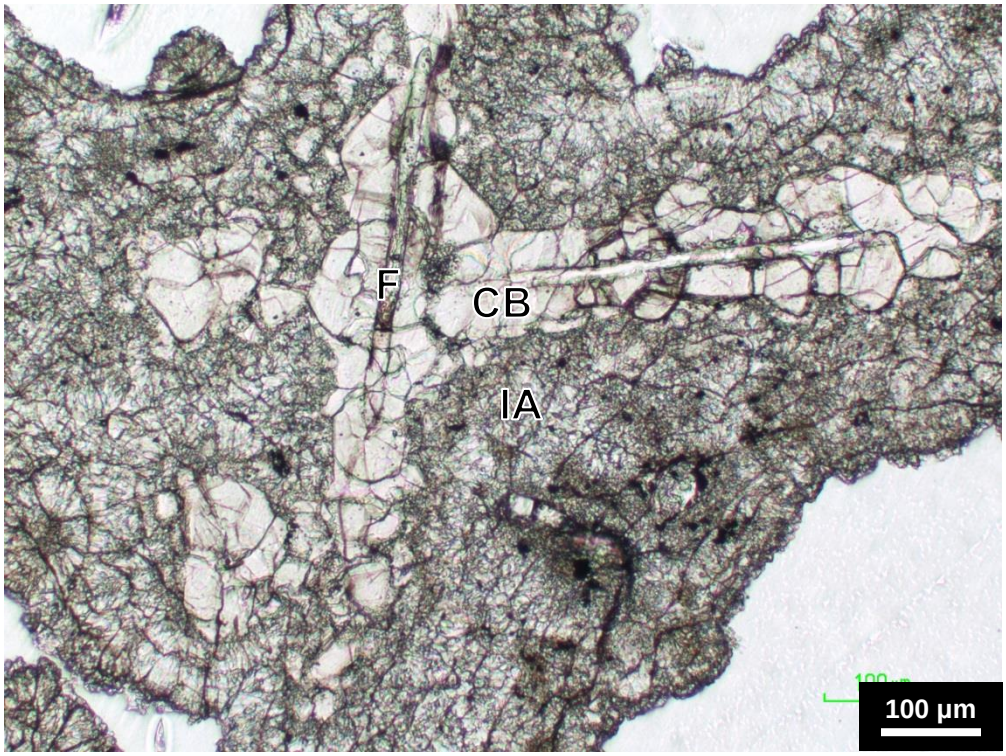

Figure 4.27: Plane polarized light photomicrograph of colourless botryoidal calcite cement (CB) coating coarse filaments (F) in a beachrock. The colourless botryoidal cement is overlain by irregular aragonite cement (IA).

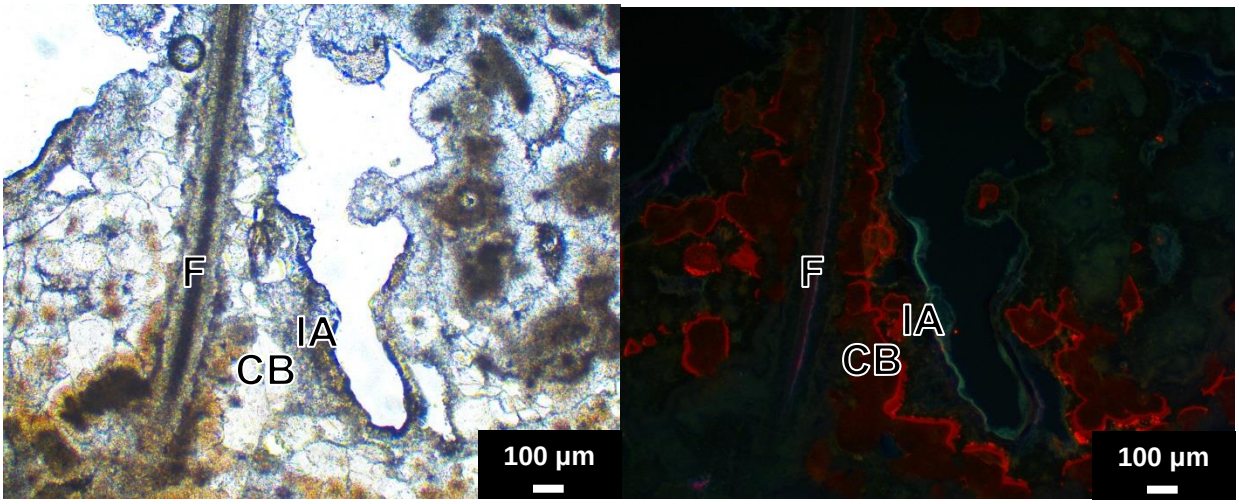

Figure 4.28: Plane-polarized light (left) and cathodoluminescence (right) images of colourless botryoidal calcite cement (CB) and irregular aragonite (IA) in an incipient bioherm. Micrite coated filaments (F) are the substrate.

4.4.3 Dogtooth calcite cement

Dogtooth calcite cement occurs throughout the shoreline carbonates, but is thickest in large pores. It precipitates on the surfaces of clotted micrite, coarse filaments, or other cements, often as the last cement deposited. Multiple generations of this cement are commonly separated by layers of microcrystalline aragonite cement. Dogtooth calcite crystals are scattered over the surface of the underlying cement. Crystals are colourless and have slightly stepped sides (Fig. 4.29). Crystal length to width ratio is about 1.6, and the length of the crystals varies from ~25 um to ~170 um. The cement exhibits dull blue fluorescence. The cement luminesces bright to dull red, and in places, the crystals are zoned. The zones are serrated, parallel to the edges of the crystals (Fig. 4.30).

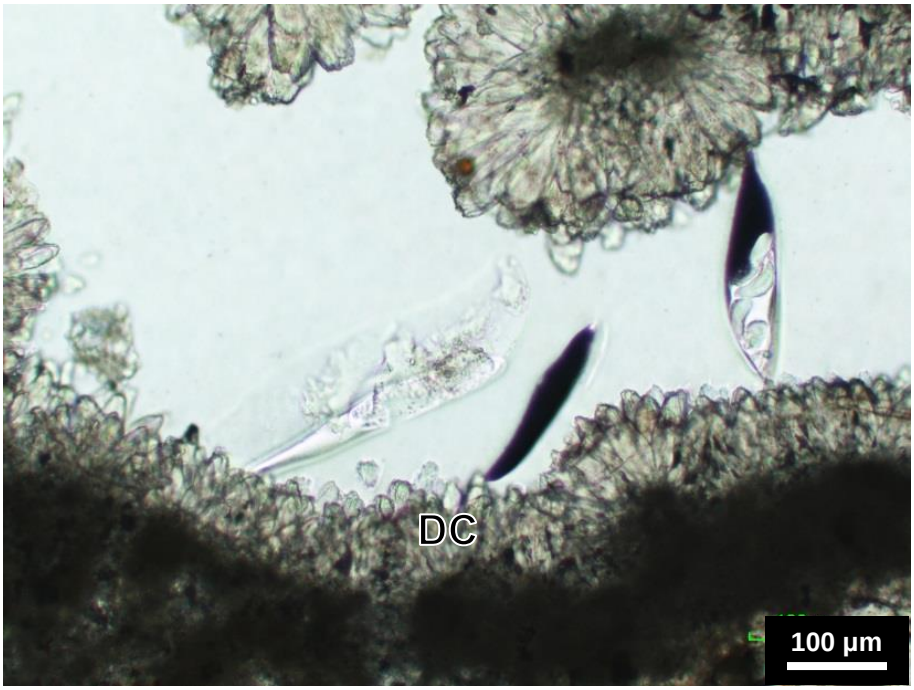

Figure 4.29: Plane-polarized light photomicrograph of dogtooth calcite cement (DC) on clotted micrite in a bioherm.

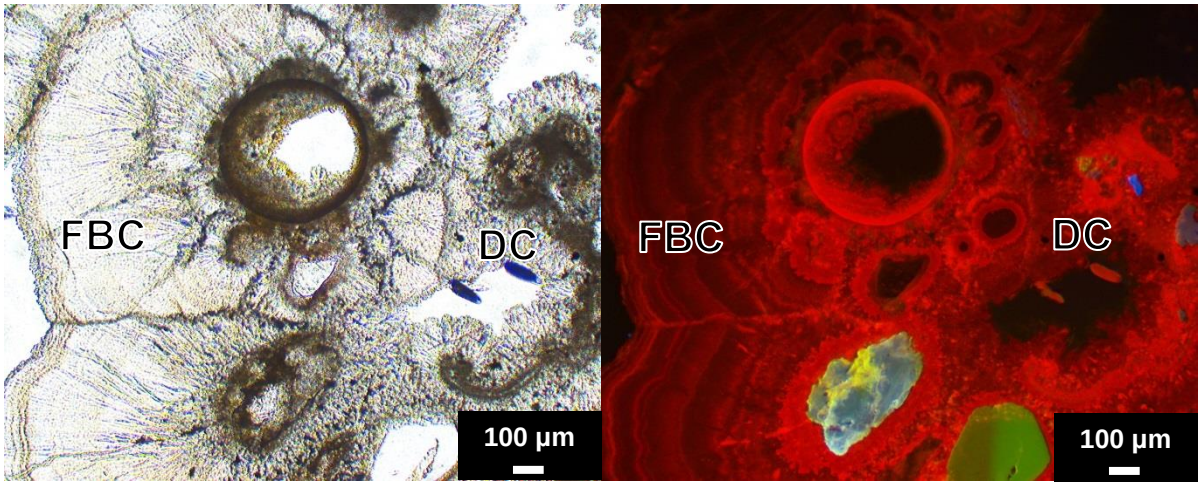

Figure 4.30: Plane-polarized light (left) and cathodoluminescence image (right) of dogtooth calcite (DC) in a bioherm. Finely laminated botryoidal calcite cement (FBC) is an overgrowth on the dogtooth calcite.

4.4.4 Pendent calcite cement

Pendent calcite cement is uncommon in the shoreline carbonates. It is present on the roofs of some large, fenestral pores in beachrock and thrombolites. It consists of alternating, scalloped laminae of colourless, bladed calcite and red-brown, equant calcite (Fig. 4.31). Bladed calcite crystals are <100 μm long and equant crystals are < 20 μm. Pendent cement tends to be overlain by colourless botryoidal calcite cement. The pendent cement has a dull blue fluorescence and a dull to bright red luminescence.

4.4.5 Coarsely laminated botryoidal aragonite cement

Coarsely laminated botryoidal aragonite cement occurs in thrombolites. It surrounds clotted micrite and micrite-coated filaments. The cement is approximately 200 μm thick (rarely up to 400 μm thick) and is composed of alternating colourless and brown botryoidal aragonite laminae (Fig. 4.32). Each lamina is approximately 40 μm thick. Laminae are thickest and best defined near large fenestral pores. Brown laminae fluoresce bright blue, and colourless laminae fluoresce dull blue. The cement luminesces dull green with patches of bright red (Fig. 4.32).

4.4.6 Isopachous radial fibrous aragonite cement

Isopachous radial fibrous aragonite cement is present in thrombolites and beachrock. Fibrous aragonite surrounds clotted micrite, peloids, evaporite pseudomorphs and coarse filaments (Fig. 4.33). The cement is 80-110 μm thick and finely laminated in places. The inner zone of the cement is darker and less well organized. The outer zone of the cement is colourless and has a sweeping extinction. The exterior surface is smooth. Fibrous aragonite cement is locally overlain by finely laminated botryoidal cement. The cement exhibits dull blue fluorescence and dull green luminescence, with patches of bright red. In places, cathodoluminescence reveals weak lamination that is serrated due to crystal terminations.

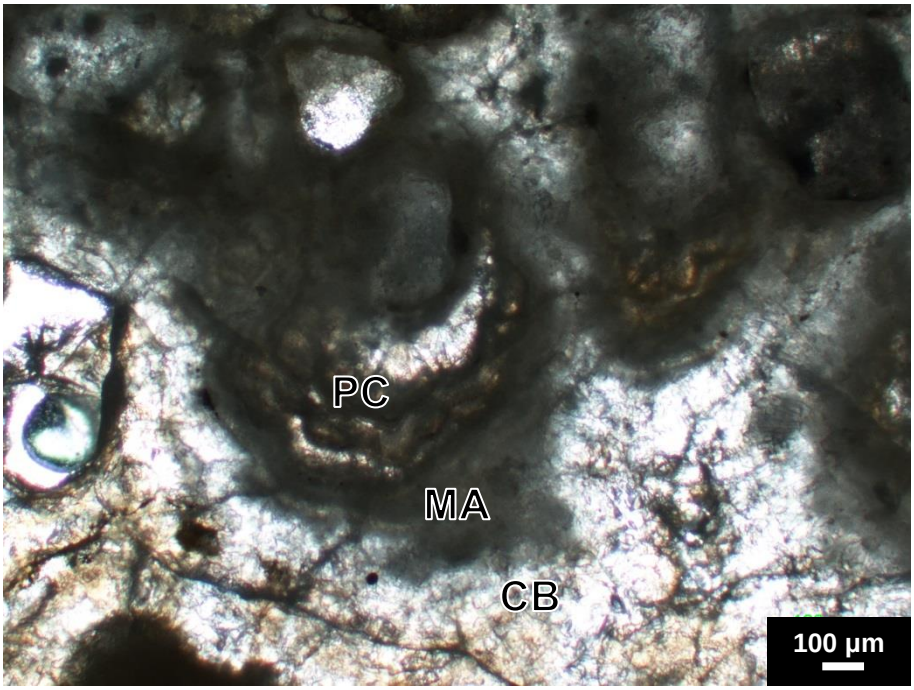

Figure 4.31: Plane-polarized light photomicrograph of pendent calcite cements (PC) at the roof of a large fenestral pore in beachrock. Microcrystalline aragonite cement (MA) and colourless botryoidal calcite cement (CB) are deposited on the pendent cement.

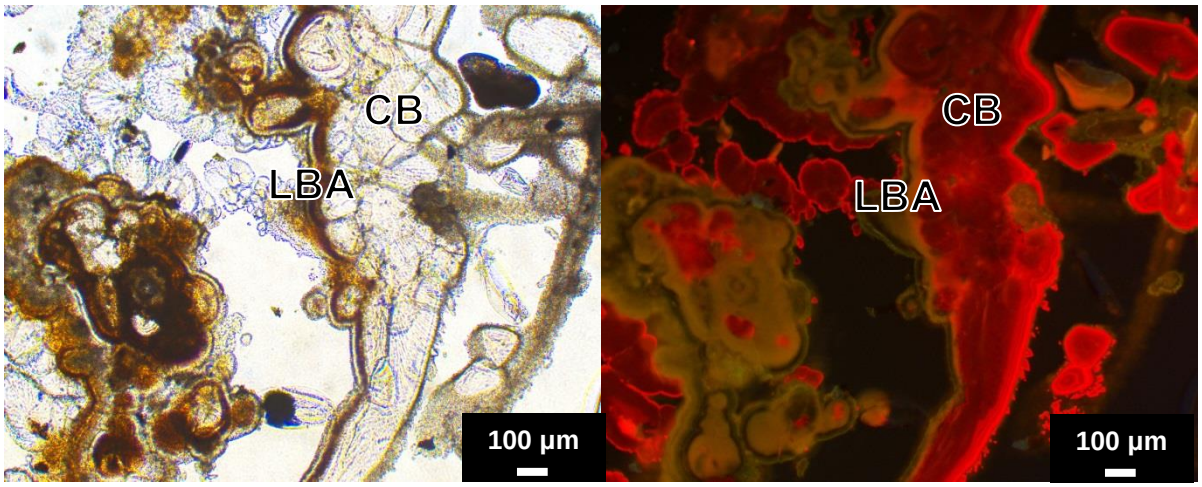

Figure 4.32: Plane polarized light (left) and cathodoluminescence image of coarsely laminated botryoidal aragonite cement (LBA) and colourless botryoidal calcite cement (CB) in a bioherm.

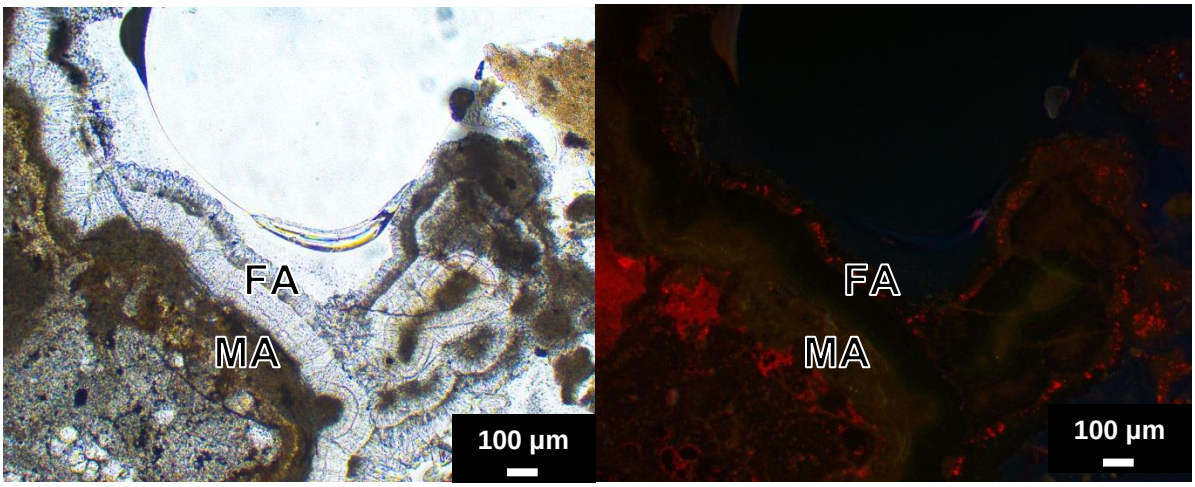

Figure 4.33: Plane-polarized light (left) and cathodoluminescence (right) images of isopachous radial fibrous aragonite cement (FA) in an incipient bioherm. Fibrous aragonite overlies microcrystalline aragonite cement (MA) on an irregular micrite to microspar substrate.

4.4.7 Reddish-brown botryoidal aragonite cement

Reddish-brown botryoidal aragonite cement occurs in isolated pinnacles and bioherms. It is present on clotted micrite, coarse filaments, plant molds, micrite-coated filaments and colourless botryoidal calcite cement. In places, colourless, botryoidal calcite cement also overlies this cement. The cement is up to 350 µm thick. The botryoids grade between reddish-brown and colourless and are locally finely laminated (Fig. 4.34). The colourless portion of the cement fluoresces dull blue, whereas the reddish-brown portion fluoresces lighter blue. In cathodoluminescence, the cement is dull green to non-luminescent.

4.4.8 Irregular aragonite cement

Irregular aragonite cement was observed in one beachrock sample and one bioherm sample. It commonly occurs around colourless botryoidal calcite cement (Fig. 4.31). The thickness varies from 100 to 300 µm. Crystals are 10-30 µm diameter, colourless and equant. In places, crystals arranged into radial fans are present near the exterior of the coarse irregular

cement. The cement exhibits dull blue to brown fluorescence. It luminesces bright to dull green and in places is finely laminated (Fig. 4.28).

4.4.9 Finely laminated botryoidal calcite cement

Finely laminated botryoidal calcite cement is thickest in large pores in beachrock and thrombolites. It has precipitated on plant molds, microcrystalline cement, clotted micrite, and micrite-coated filaments. Rarely, this cement is coated by fibrous aragonite cement. The botryoids are up to 400 μm thick. Laminations are fine and continuous (Fig. 4.35). The cement fluoresces dull blue with fine laminations of brighter blue. It luminesces dull red with smooth concentric bands of bright red (Fig. 4.35).

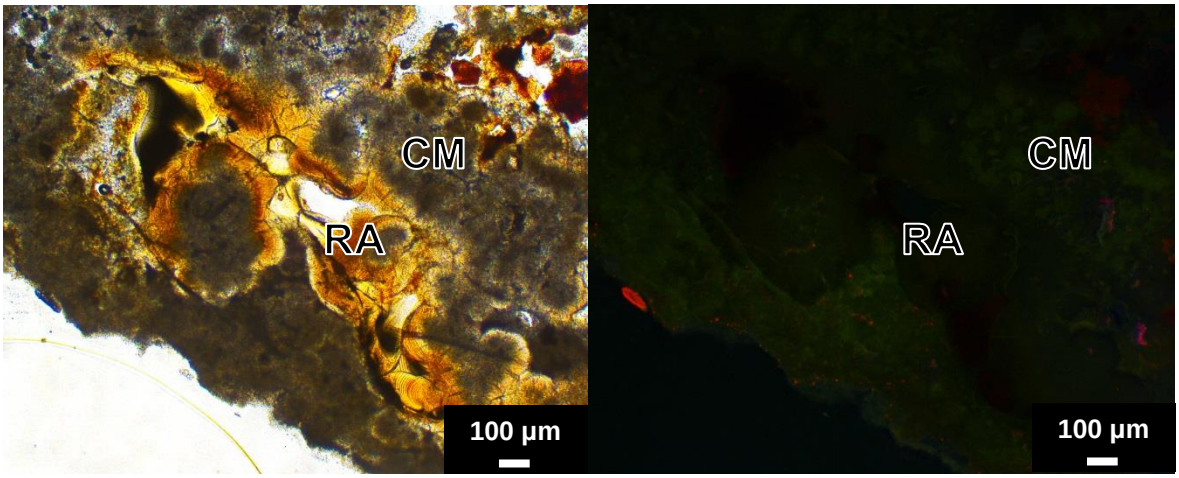

Figure 4.34: Plane-polarized light (left) and cathodoluminescence (right) images of reddish-brown aragonite cement (RA) on a clotted micrite (CM) substrate in a bioherm.

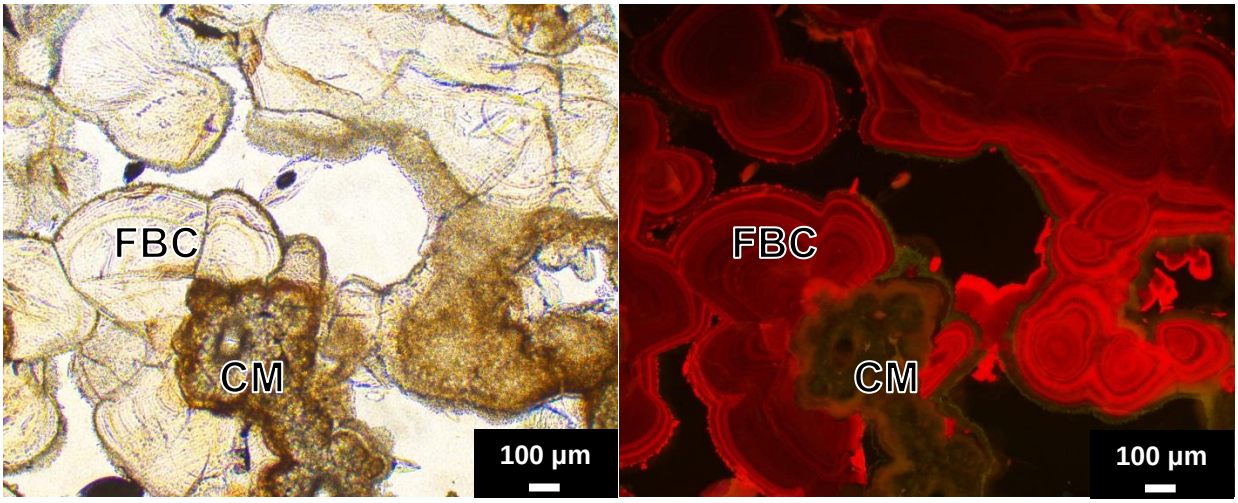

Figure 4.35: Plane-polarized light (left) and cathodoluminescence (right) images of finely laminated botryoidal calcite cement (FBC) on clotted micrite (CM) in a bioherm.

4.5 Paragenesis

The components in the West Reflex Lake shoreline carbonates can be divided into three phases of formation (Table 4.2). Components in the first phase of formation precipitate directly on microbial filaments. Components in the second phase of formation are only observed to precipitate on top of pre-existing cements. Components in the third phase of formation are the last to form in the shoreline carbonates.

Phase 1 components are clotted micrite, microcrystalline aragonite cement, colourless botryoidal calcite cement, and dogtooth calcite cement. They precipitated throughout the growth of the shoreline carbonates. They coat microbial filaments and other cements. Phase 1 cements do not exhibit meniscus or pendent features, so they are interpreted have formed in the phreatic zone. Micrite in microbialites is often biologically-influenced (Neumeier, 1999; Della Porta, 2015). The bright epifluorescence and irregular shape and thicknesses of the clotted micrite and microcrystalline aragonite are other indications that these components are microbial precipitates.

Table 4.2: Paragenesis of carbonate cements and associated components in West Reflex Lake shoreline carbonates.

Phase	Component	Early	Late
1	Clotted micrite	———————————	
	Microcrystalline aragonite cement	———————————	
	Colourless botryoidal calcite cement	———————————	
	Dogtooth calcite cement	———————————	
2	Pendent calcite cement	———	
	Coarsely laminated botryoidal aragonite cement	———	
	Isopachous fibrous aragonite cement	———	
	Reddish-brown botryoidal aragonite cement	———	
	Irregular aragonite cement	———	
	Finely laminated botryoidal calcite cement	———	
3	Chert		———
	Micrite crust		———

The large, well-formed crystals and lack of epifluorescence are evidence that colourless botryoidal aragonite cement and the dogtooth calcite cement precipitated abiotically. Phase 1 cements precipitated on organic matter to form a lithified framework on which other cements developed.

Phase 2 cements precipitated on the framework formed by phase 1 cements and did not precipitate directly on microbial filaments. The micritic cements of phase 1 are commonly overgrown by several generations of botryoidal aragonite and calcite cements, reflecting a fluctuation between the dominance of biotic and abiotic carbonate precipitation. The majority of the phase 2 cements, with the exception of pendent calcite cement, are interpreted to be phreatic based on their isopachous nature. The only vadose cement is the pendent cement, which is uncommon in the shoreline carbonates. The increased thickness of coarsely laminated botryoidal aragonite cement in the large pores is interpreted to be related to groundwater flowing preferentially through these pores. Groundwater flow supplies Ca^{2+} to the lake and increases carbonate saturation, inducing abiotic carbonate precipitation. Epifluorescence reveals that

reddish-brown botryoidal cements and coarsely laminated botryoidal cements incorporate some organic matter but are predominantly abiotic. In phase 2 precipitation, the shoreline carbonates may be rarely exposed (pendent cements), with alternation of biotic and abiotic precipitation.

Phase 3 components are the last to form in the shoreline carbonates. Chert coats clotted micrite, evaporite pseudomorphs, and irregular micrite, but is never coated with any other cements. For chert to form in an alkaline lake, where silica solubility is high, the lake may either become concentrated by evaporation or the pH must decrease to lower silica solubility (Hay, 1968). Micrite crusts drape over the exterior of thrombolites and smooth the irregular surface of clotted micrite, coarse filament molds, or evaporite pseudomorphs.

4.6 Summary of shoreline carbonate microfabrics

A wide variety of microfabrics are present in each type of shoreline carbonate from West Reflex Lake (Table 4.1). A generalization of the microfabrics of each type of shoreline carbonate is presented in the following section.

4.6.1 Thrombolites

The microfabrics of the bioherms and isolated pinnacles in West Reflex Lake are similar and will be discussed together. The thrombolites have 20-40% framework porosity and are composed dominantly of clotted micrite and micrite-coated coarse filaments. The micrite clots are easily weathered and often occur as a geopetal fill in large voids. Plant molds are scattered throughout the microbialite and evaporite pseudomorphs are concentrated in patches. Some larger pores have a smooth, knobby appearance due to botryoidal cements lining pore walls. The exterior of most thrombolites is coated in a 200-300 μm thick crust of micrite. Regardless of texture, the exterior of the thrombolites fluoresces dull orange (Fig. 4.36).

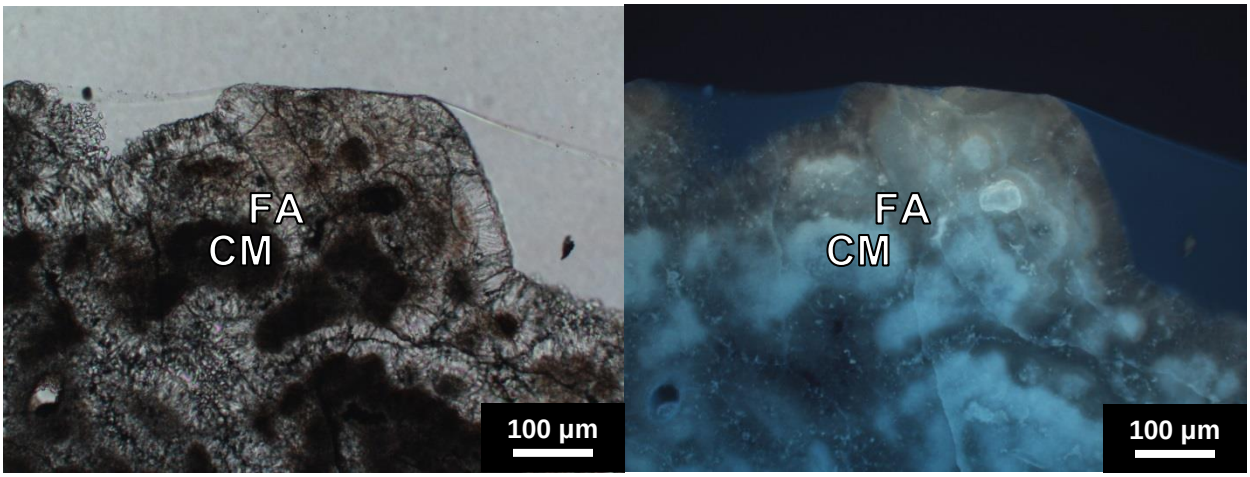

Figure 4.36: Plane-polarized light (left) and epifluorescence (right) images of the exterior surface of an isolated pinnacle. Isopachous fibrous aragonite cement surrounds clotted micrite. The cement appears uniform in PPL but fluoresces orange only at the exterior surface of the pinnacle.

4.6.2 Laminated coatings

The laminated coatings on bioherms and cobbles are made up of alternating layers of micrite and microspar. Thickness ranges from 1 to 10 mm. The coatings commonly have a "bumpy" appearance formed by small domes. Porosity is fenestral (~20-40%) and common at the apex of domes. Some laminae are truncated and overlain by subsequent layers of aragonite, indicating that deposition was marked by alternating periods of erosion and accretion.

Sample WR-15, a 2-10 mm thick laminated coating on the exterior of a bioherm, contained the most complete sequence of laminated crust development observed in the collected samples (Fig. 4.37). The laminations are described in detail in Appendix D. The laminated coating in WR-15 was deposited on a thrombolitic substrate. The majority of the coating is composed of couplets of thin, grey-brown micritic aragonite laminae topped by thicker laminae of coarser, beige aragonite and calcite microspar (Fig. 4.37). Above the couplets are finely laminated micritic layers. Large, lenticular voids with spiky edges that cut across laminae are

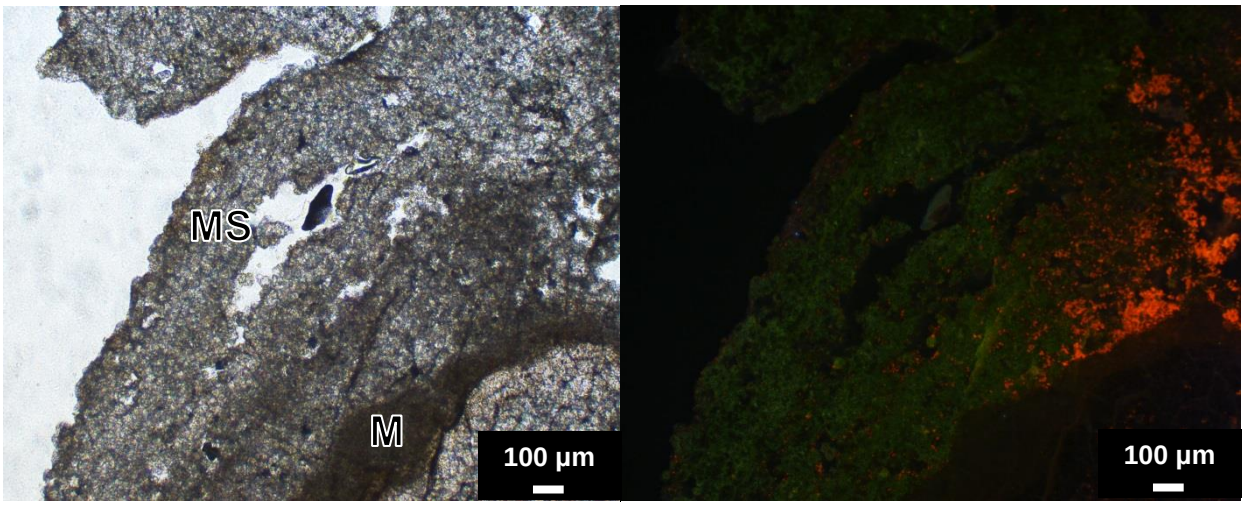

Figure 4.37: Plane-polarized light (left) and cathodoluminescence (right) images of a micrite (M) and microspar (MS) couplet in the laminated coating on sample WR-15, from a bioherm. Calcite microspar (luminescing orange) is present in the middle left of the microspar lamina; aragonite microspar is present (luminescing green) elsewhere in the microspar lamina.

present in the microspar layers, at the tops of domes. Some of these pores are filled with sand grains or clotted micrite. Blocky, equant carbonate cements are rarely present in lenticular voids.

The laminated coatings on cobbles surrounding the shoreline are 1 to 5 mm thick and not as well laminated as the coatings on the bioherms. The coatings also alternate between micrite and aragonite, but the thicknesses of the laminae are irregular, and some laminae are absent on parts of the cobble. Many laminae contain fine sand grains. It appears that layers of carbonate were deposited and then partially eroded before the deposition of the succeeding layer. The porosity of the laminated crust surrounding the cobbles is low.

4.6.3 Beachrock

The beachrock in West Reflex Lake is a thin-bedded to laminated lithic arenite. The sand grains that compose much of the beachrock are sub-rounded to rounded, well-sorted, and predominantly medium sand size. The beachrock contains medium sand grains (95%), clotted micrite (5%), and peloids (<1%). The sand grains are cemented by isopachous (35-70 µm thick)

microcrystalline aragonite, overgrown by dogtooth calcite crystals. Typically, finely laminated botryoidal calcite cements are thickest at the top of fenestral pores, and the bottom of fenestral pores is lined with clotted micrite. The rock has 5-20% interparticle porosity and up to 25% fenestral porosity where pores are up to several cm in length and 1-3 mm in aperture.

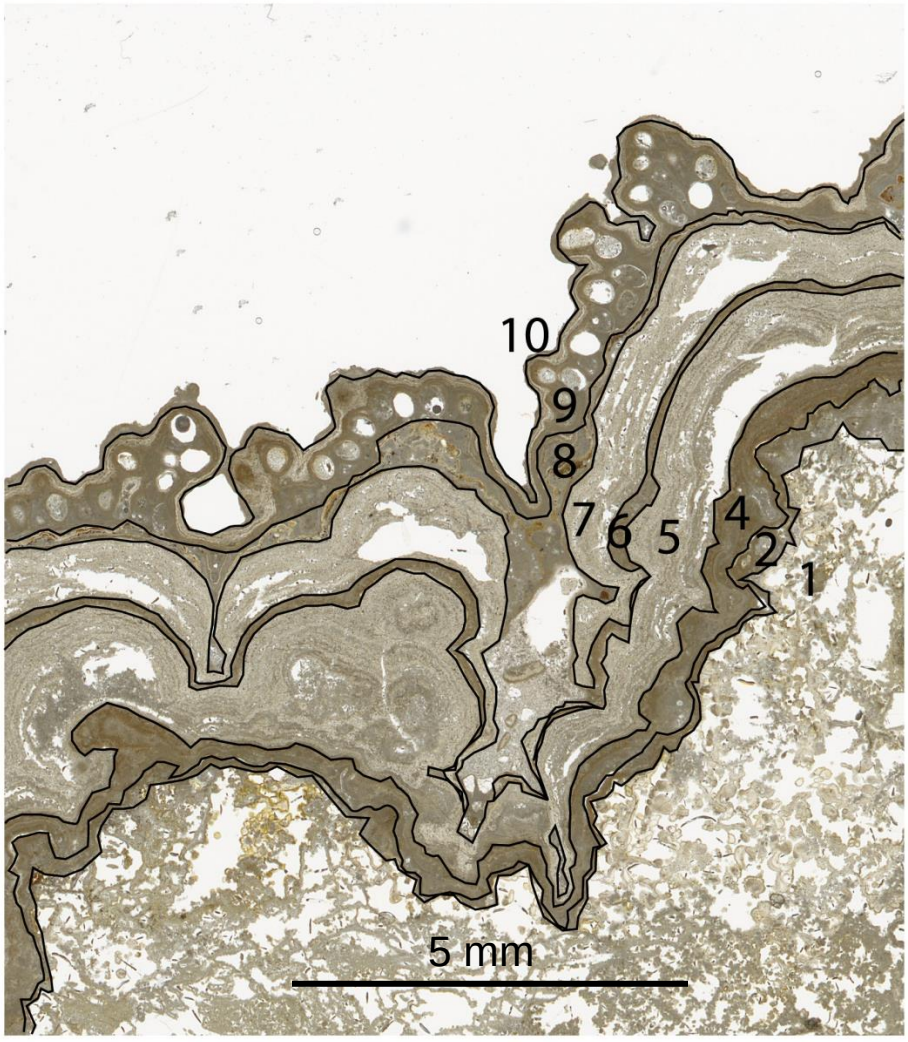

Figure 4.38: Scanned image of thin section through laminated coating on sample WR-15. Numbered layers are (1) porous thrombolitic substrate, (2) micrite, (4) microspar, (5) microspar, (6) micrite, (7) microspar, (8) finely laminated micrite, (9) micrite containing molds, (10) massive micrite. Layer 3 (porous thrombolitic material) is not present at this part of the crust.

5 Microbialite mineralogy and geochemistry

5.1 Mineralogy

Bulk mineralogy of the shoreline carbonates of West Reflex Lake was determined using XRD. Semi-quantitative estimates of the proportions of minerals are listed in Appendix E and summarized in Table 5.1. The isolated microbialites and bioherms are composed primarily of aragonite. The bioherms contain more calcite than the isolated thrombolites. Minor amounts of dolomite and protodolomite are present in both. The bulk mineralogy of the beachrock is dominated by quartz but beachrock also contains high-Mg calcite and aragonite. The laminated coatings are composed of aragonite with minor amounts of protodolomite and quartz. The white efflorescent crust on the beach sand surrounding West Reflex Lake is composed of halite, thenardite, and trona.

Table 5.1: Mean mineral proportions in West Reflex Lake shoreline carbonates.

Shoreline carbonate type	Quartz (%)	Plagioclase (%)	Calcite (%)	HMC* (%)	Proto-dolomite (%)	Dolomite (%)	Aragonite (%)	Halite (%)
Bioherm	6.22	0.31	10.84	3.82	2.63	0.06	74.23	1.765
Isolated thrombolite	8.02	0	1.54	6.21	3.19	1.23	79.81	0
Laminated coating	7.61	0	0.96	0	8.63	0	82.81	0
Beachrock	75.67	0	0	9.43	0	5	9.9	0

*HMC – high-Mg calcite

5.2 Geochemistry

Electron probe microanalysis (EPMA) was used to identify variation in geochemistry from the interior to exterior of botryoidal cements and the laminated crust. Microprobe data are available in Appendix F. The trace element composition of the botryoidal cements does not vary significantly from the interior to exterior. The number of samples of each cement was too low to meaningfully compare the geochemistry between cements. In the laminated crust, the micritic laminae have low mean Mg/Ca ratios (<0.01). The basal microspar layer has a very high mean Mg/Ca ratio, approximately 0.15, whereas the top microspar layer has an Mg/Ca ratio of 0.005. Variations in Sr/Ca in the laminated crust are plotted in Fig. 5.1. The ratios increase within laminations. The ratios tend to be lower in the microspar layers than the micrite layers.

Backscattered electron (BSE) images produced during EPMA were used to identify changes in geochemistry with changes in mineralogy. Protodolomite was identified by its lower intensity (brightness) relative to aragonite and calcite. Aragonite and calcite were distinguished by comparison of BSE images to cathodoluminescence images. Protodolomite has much higher Mg/Ca and lower Sr/Ca than aragonite and calcite (Table 5.2). Aragonite has slightly higher mean Mg/Ca and Sr/Ca than calcite. The range of mol% $CaCO_3$ in protodolomite determined using electron microprobe (56.5-65.6%) corresponds to the range determined by XRD (55.3-65.5%). The significance of Mg/Ca and Sr/Ca values will be examined in the discussion.

Table 5.2: Variation in mean Mg/Ca and Sr/Ca ratios from EPMA with mineralogy in West Reflex Lake shoreline carbonates.

Mineral	**Mean Mg/Ca**	**Mean Sr/Ca**
Calcite	0.022	0.0029
Aragonite	0.029	0.0034
Protodolomite	0.60	0.00081

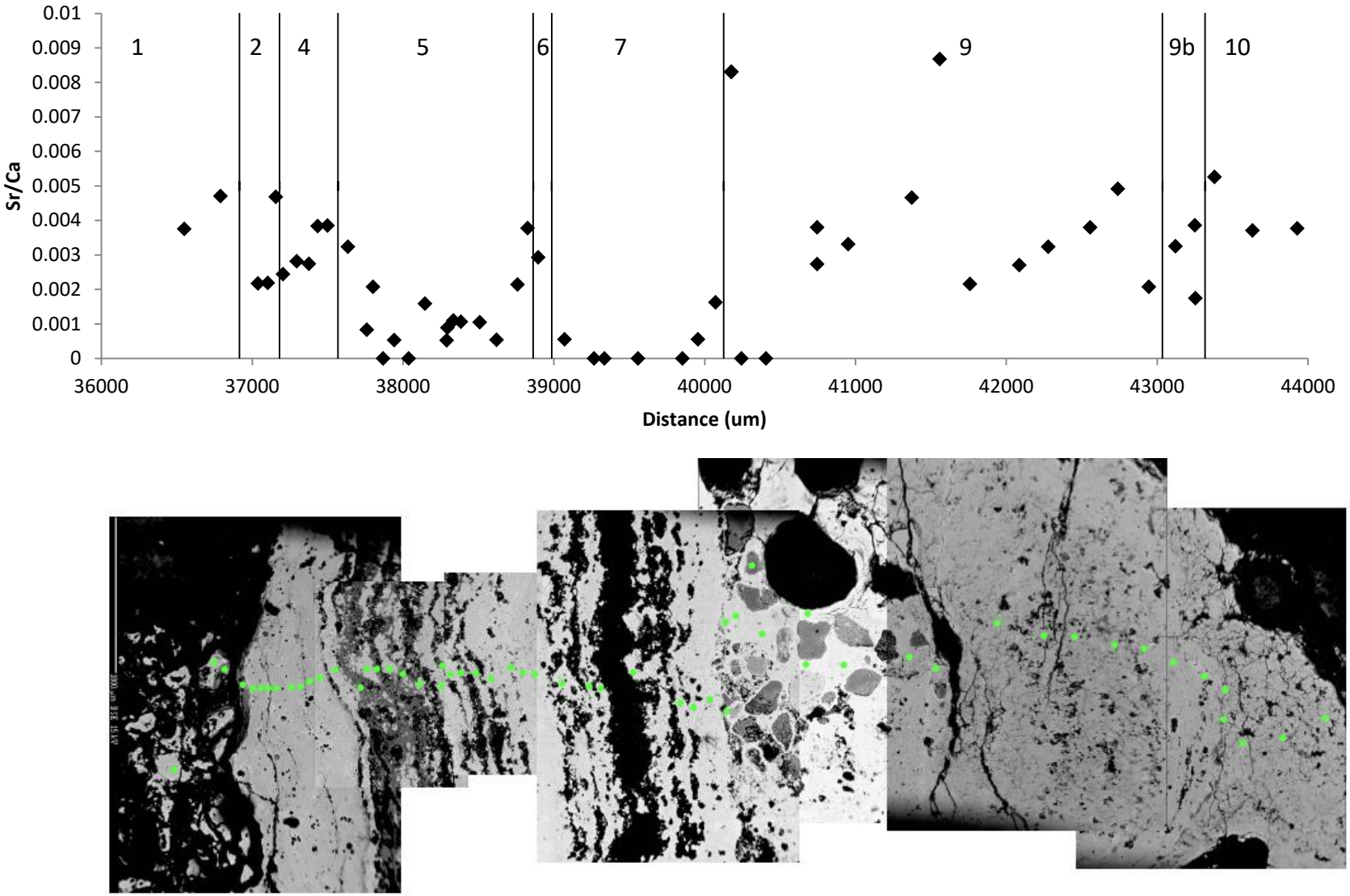

Figure 5.1: Variation in Sr/Ca ratio from bottom (left) to top (right) of laminated crust on WR-15. Green dots indicate sample spot locations. Vertical lines divide laminations. Labels correspond to Fig. 4.38 and Appendix E.

5.3 Stable isotopes

The $\delta^{13}C$ and $\delta^{18}O$ values of West Reflex Lake's shoreline carbonates are presented in Fig. 5.2 and Appendix G. The $\delta^{13}C$ and $\delta^{18}O$ covary ($r = 0.71$; significant at $\alpha = 0.001$). The $\delta^{13}C$ values range from -0.1 to 4.7‰ and the $\delta^{18}O$ values range from -11.6 to -5.8.‰. Differences between the stable isotope values of the isolated pinnacles, bioherms, laminated coatings and beachrock were not statistically significant ($p = 0.466$).

Samples for stable oxygen isotope analysis were taken from laminae within thrombolites to examine changes as the thrombolites developed. Because of the lack of age control between individual structures, changes in $\delta^{18}O$ can only be examined within individual thrombolites. The values of both $\delta^{13}C$ and $\delta^{18}O$ tend to increase from the interior to the exterior of isolated pinnacles. The laminated crusts are more enriched in $\delta^{18}O$ than the thrombolitic material that they enclose.

5.4 Radiocarbon dating

To determine if a reservoir effect exists in West Reüex Lake, a sample of terrestrial plant material encrusted with aragonite was dated. If the reservoir effect is negligible, the plant material and the surrounding aragonite should have consistent radiocarbon ages. The conventional radiocarbon age of the aragonite is 4400 ± 30 yBP. The 2 σ calibrated result is 5045 to 4856 cal BP. The terrestrial plant material had a result of 102.6 ± 0.3 pMC (percent modern carbon). This indicates that the plant had an age post 0 BP, i.e. it was living in the past 60 years. The difference in radiocarbon age between the plant material and the surrounding carbonate is due to a reservoir effect in West Reflex Lake.

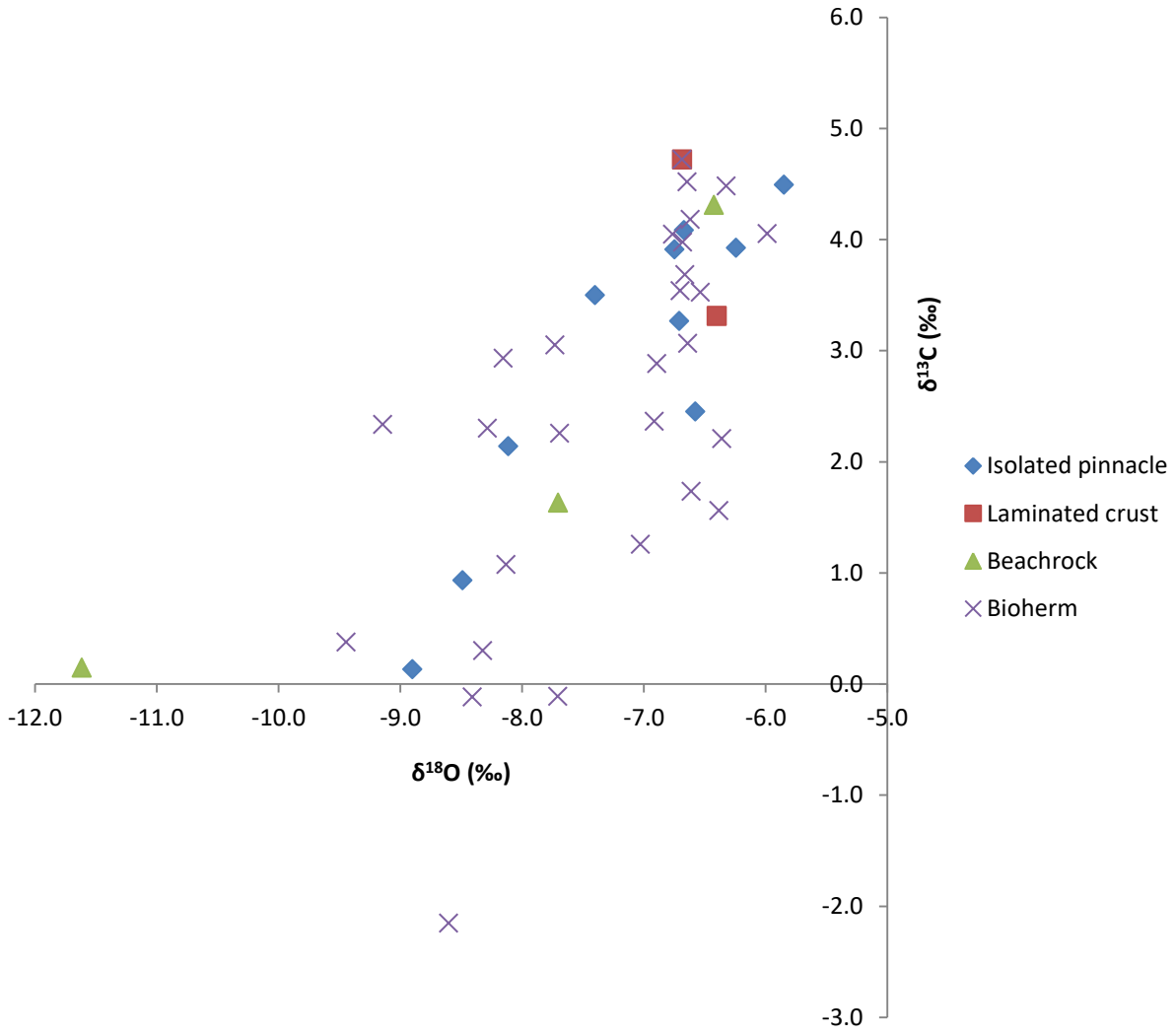

Figure 5.2: Stable carbon and oxygen isotopes of shoreline carbonates from West Reflex Lake.

6 Discussion

6.1 Stable carbon and oxygen isotopes

Stable carbon and oxygen isotope ratios in lacustrine carbonates can be used to make paleoenvironmental interpretations. Stable oxygen isotope values of lacustrine carbonates are affected by the $\delta^{18}O$ composition and temperature of the water in which they formed (Talbot and Kelts, 1990). Oxygen isotopic fractionation is temperature dependent: an increase in water temperature decreases the $\delta^{18}O$ of the precipitating carbonates. Changes in $\delta^{13}C$ reflect changes in the dissolved inorganic carbon (DIC) pool in the lake by processes including uptake of ^{12}C by primary producers, release of DIC produced during respiration, inflow of groundwater, and exchange with atmospheric CO_2 (Valero-Garcés *et al.,* 1997; Horton *et al.,* 2015).

In lacustrine carbonates, covariance between $\delta^{13}C$ and $\delta^{18}O$ with $r \geq 0.70$ is typical of closed hydrologic conditions (Talbot, 1990; Talbot and Kelts, 1990; Benson *et al.,* 1996). The strong covariance in carbon and oxygen isotope values in this study (Fig. 5.2) is interpreted to result from the basin remaining closed during the time the shoreline carbonates have been forming (cf. Li and Ku, 1997). Covariance occurs in closed basin lakes because evaporation in a closed basin increases $\delta^{18}O$ and high biological productivity and longer residence times increase $\delta^{13}C$ (Talbot and Kelts, 1990). Caution must be used when interpreting isotopic covariance as an indication of closed basin conditions since processes such as recrystallization or non-equilibrium precipitation can affect stable isotope values (Yuan *et al.,* 2006). However, these processes do not appear to be operating in West Reflex Lake: evidence of carbonate recrystallization was not observed, and calculated values of $\delta^{18}O$ based on lake water $\delta^{18}O$ and temperature agree with the range of values in the shoreline carbonates.

In general, lacustrine carbonates that precipitated when lake level was high tend to plot toward the more negative end of the covariant trend and vice versa (Talbot, 1990). The small, isolated pinnacles in West Reflex Lake are closer to shore and may have been deposited at lower lake level than the large bioherms, which are situated farther from shore. Despite the difference in proximity to shore and by inference lake level, the difference between $\delta^{18}O$ and $\delta^{13}C$ values of small, isolated pinnacles and large bioherms is not statistically significant ($p = 0.466$). This similarity could be a result of the conditions necessary for carbonate formation or sampling bias. Microbialite formation may only have occurred within a restricted range of lake level and corresponding $\delta^{18}O$ and $\delta^{13}C$ values. Sampling bias could affect the isotope values because samples were taken from the exterior of large pinnacles for practical reasons. The carbonate on the exterior of the large pinnacles likely formed contemporaneously with the small, isolated microbialites.

6.1.2 Stable oxygen isotopes in shoreline carbonates

The shoreline carbonates of West Reflex Lake have $\delta^{18}O$ values (-11.6 to -5.8.‰) that are similar to those from nearby Manito Lake (Last, 2013). The water $\delta^{18}O$ (-3.3‰) composition of Manito Lake agrees with that in West Reflex Lake (-2.8‰). Last (2013) noted that the $\delta^{18}O$ values of carbonates from northern Great Plains lakes are depleted relative to other Holocene lacustrine carbonates from around the world. The depleted values might result from a combination of input of relatively depleted groundwater and precipitation in the northern Great Plains and differences in the precipitation/evaporation ratios around the world.

The $\delta^{18}O$ values of the West Reflex Lake thrombolites increase from the interior to the exterior. Laminated crusts precipitated on thrombolites also have higher values than the material they enclose. These results imply that lake level was decreasing as the thrombolites precipitated.

It is postulated that lake level is the main control on $\delta^{18}O$ values of the carbonates (Fig. 6.1A) and that laminated crusts are the last type of shoreline carbonate to form before the microbialites are exposed and precipitation ceases.

6.1.3 Stable carbon isotopes in shoreline carbonates

West Reflex Lake's shoreline carbonates exhibit $\delta^{13}C$ values ranging from -0.1‰ to 4.7‰. These values are higher than the $\delta^{13}C_{DIC}$ values from the sources of inflow to the lake (-14‰ to -12‰) (Wassenaar *et al.,* 1991). The high values are due to a combination of equilibration with the atmosphere and selective uptake of ^{12}C by photosynthesis (Fig. 6.1B). High $\delta^{13}C$ (upwards of 0‰) can occur in closed lakes where $\delta^{13}C$ of total dissolved organic carbon (TDIC) tends toward equilibration with atmospheric CO_2 (Leng and Marshall, 2004). Additionally, a lake's $\delta^{13}C_{TDIC}$ increases when productivity in the lake is enhanced, as plants preferentially take up ^{12}C. Therefore, carbonate minerals associated with phototrophs may be enriched in ^{13}C relative to abiotically precipitated minerals (Power *et al.,* 2011).

6.2 Radiocarbon dating

Dating of terrestrial plant material and the surrounding carbonate suggests that the carbonates of West Reflex Lake have a reservoir effect of almost 5000 years. This is consistent with the idea that West Reflex Lake receives a large proportion of its water from groundwater, especially bedrock groundwater (Fig. 6.1B). Reservoir effects are common in alkaline lakes that contain old carbon dissolved from the bedrock (MacDonald *et al.,* 1991; Gischler *et al.,* 2008). Reservoir effects on the order of several thousand years have been reported in a few freshwater

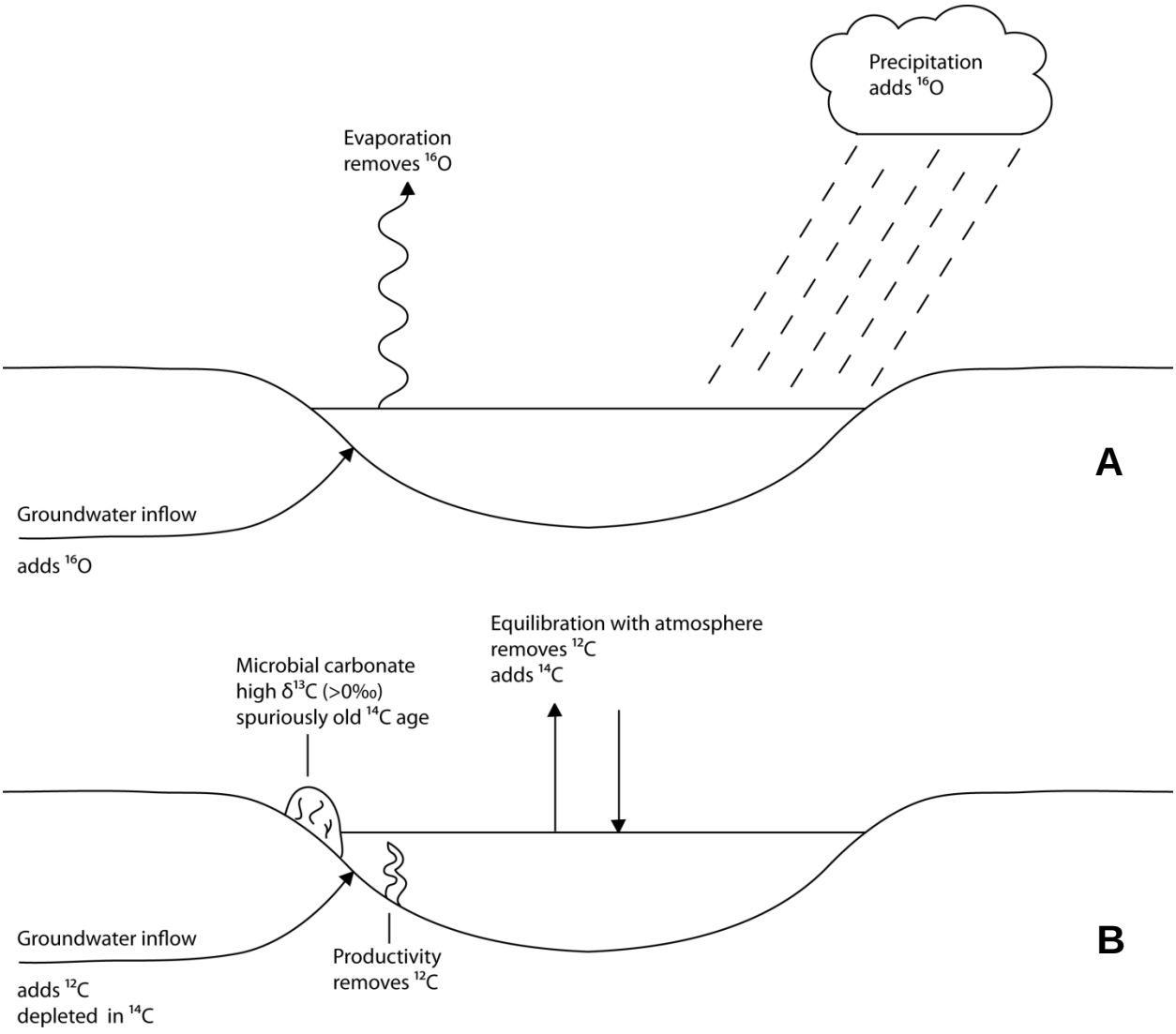

Figure 6.1: Schematic diagrams showing factors influencing (A) $\delta^{18}O$ values and (B) $\delta^{13}C$ values and ^{14}C age in West Reflex Lake.

and saline lakes (Grosjean *et al.*, 1995; Gischler *et al.*, 2008). Endogenic carbonate precipitated in lakes with a reservoir effect will be deficient in ^{14}C and will have spuriously old ^{14}C ages.

It is interpreted that the ^{14}C age of the terrestrial plant matter encased in the microbialite is the true age of the carbonate. The microbialite that was sampled for ^{14}C dating was small, unweathered, and was situated near a flowing spring. It is plausible that the microbialite precipitated in the last 60 or so years. A more detailed chronology of the West Reflex Lake microbialites would require the collection of many more ^{14}C dates and is beyond the scope of this M.Sc. project. Additional complexity exists because the deficiency in ^{14}C (hard water effect) may vary over time (MacDonald *et al.*, 1991).

6.3 Geochemistry

The Sr/Ca ratio of autochthonous lacustrine carbonates reflects changes in mineralogy and water chemistry (Valero-Garcés *et al.*, 1997). Aragonite has higher Sr/Ca ratios than calcite because the aragonite crystal lattice can accommodate more Sr than calcite. Because of this, the relative abundance of each mineral affects the Sr/Ca ratio (Fritz *et al.*, 1994; Valero-Garcés *et al.*, 1997). The Sr/Ca ratio of lake water is affected by changes in relative inputs of groundwater.

In the laminated crust, the Sr/Ca ratios tend to increase within each layer and steeply drop off between layers. Changes in the Sr/Ca ratio reflect changes in salinity: as salinity increases, aragonite is more likely to form. The ratios of Sr/Ca are higher in micrite than microspar layers, indicating that micrite layers contains more aragonite and may have formed when the lake was more saline. The increase in Sr/Ca within layers could reflect a seasonal cycle in mineralogy with aragonite increasingly likely to precipitate as evaporation proceeds through the summer and the salinity of the lake increases.

6.4 Origins of anomalous water chemistry

West Reflex Lake has anomalously high Cl^- and low SO_4^{2-} concentrations compared to other lakes in the region (Fig. 3.3). Groundwater is widely considered to be the source of solutes in closed-basin Great Plains lakes (Donovan and Rose, 1994). Deep groundwater is Cl-rich and SO_4-poor compared to shallow or intermediate groundwater (Donovan and Rose, 1994). The similarity of West Reflex Lake's chemistry to that of deep groundwater is evidence for the contribution of deep groundwater to the lake (Fig. 3.4). Hackbarth (1975) noted that upward groundwater flow and discharge take place in the Battle Valley near West Reflex Lake.

Considering that Cl^--rich, SO_4^{2-}-poor, deep groundwater occurs widely in the northern Great Plains, it is puzzling that most other lakes in the region have very different chemistry from West Reflex Lake and do not reflect deep groundwater influence. The unusual chemistry of West Reflex Lake may be due to a combination of its location in a buried glacial valley, a floor of relatively impermeable glacial till, and fracture systems allowing the upward flow of solutes from the Middle Devonian Prairie Evaporite. West Reflex Lake is located on the Battleford/Wainwright buried valley. Buried bedrock valleys appear to control the distribution of saline lakes in the northern Great Plains (Grossman, 1968; Last and Schweyen, 1983; Last, 1992). A base of till may be required to prevent the escape of water carrying solutes (Witkind, 1952). West Reflex Lake is situated in Saskatoon and Sutherland Group till (Fig. 3.2). Grossman (1968) noted that evaporation in such a lake would concentrate all salts and lead to high concentrations of Cl^-, which is observed in very few northern Great Plains lakes. Local fracture systems may allow flow of saline groundwater up from the Prairie Evaporite through thousands of metres of overlying sedimentary rocks (Grossman, 1968).

6.5 Epifluorescence

Strong epifluorescence in carbonates indicates the presence of residual organic matter (Dravis and Yurewicz, 1985; Reitner *et al.,* 1995; Russo *et al.,* 2006; Spadafora *et al.,* 2010). The colour of fluorescence can also be used to make interpretations: aragonite fluoresces blue and chlorophyll fluoresces red (Power *et al.,* 2011). In the shoreline carbonates of West Reflex Lake, clotted and irregular micrite fluoresce strongly blue, whereas botryoidal cements fluoresce weakly, if at all. The micrite precipitated in the presence of organic matter, and the botryoidal cements precipitated with less biological influence. The interior of preserved microbial filaments fluoresces red due to the presence of preserved chlorophyll.

The exterior crusts of the microbialites fluoresce orange. The orange fluorescence varies in intensity between samples and is absent in places. The fluorescence is not affected by variations in texture and is restricted to the exterior surface of the microbialite. This suggests that the orange fluorescence is the result of a process occurring on the exposed surfaces of the stromatolites rather than a chemical variation between components. One possible process is penetration of the carbonate by endolithic microorganisms. Photosynthetic endolithic microorganisms can penetrate carbonate and form a pigmented layer a few mm below the surface (Horath *et al.,* 2006). Pigmented layers just below the microbialite surface were observed in West Reflex Lake microbialites. The pigments may be the cause of fluorescence in the exterior crusts. Some micritic laminae within the microbialites also exhibit orange fluorescence. The fluorescence illustrates that the structures were subaerially exposed for enough time for an endolithic microbial community to develop before becoming resubmerged and encrusted with carbonate.

6.6 Controls on carbonate precipitation

Four end member primary processes are involved in microbialite deposition: trapping and binding of sediment, skeletal calcification, biologically-influenced calcification, and inorganic calcification (Burne and Moore, 1987). Trapping and binding of detrital sediment by microorganisms plays only a minor role in the formation of West Reflex Lake's thrombolites. With the exception of brine shrimp pellets, which can make up a large proportion of the fabric locally, few grains are incorporated into the porous framework of the thrombolites. The laminated crusts contain a few detrital sand grains in a matrix of microcrystalline aragonite. Skeletal calcification is absent in the West Reflex Lake carbonates, as a result of the high salinity and extremes in environmental conditions. Inorganic calcification occurs predominantly as secondary cements in the microbialites. Rarely, inorganically precipitated crystals are present on the surface of filamentous microorganisms, but this is not the process that makes up the bulk of the microbialite framework.

Biologically influenced calcification appears to be the dominant process in the formation of West Reflex Lake's microbialites. In biologically influenced calcification, the organisms do not control the habit of the mineral precipitate (Dove *et al.,* 2003; Dupraz *et al.,* 2009). Biologically influenced precipitates are typically heterogeneous (Dove *et al.,* 2003). Thus, by process of elimination of three of the primary processes, and supported by the heterogeneity of the observed precipitates, it is interpreted that the precipitates in West Reflex Lake are biologically influenced.

In continental water bodies, carbonate precipitation is influenced by water chemistry, carbonate supersaturation, skeletal biota, vegetation, algae, and microorganisms (Della Porta, 2015). Approximately ten-times supersaturation is necessary to precipitate calcium carbonate in

microbial mats (Arp *et al.,* 1999a). Several physiological processes of microorganisms can produce alkalinity and increase supersaturation. The processes include photosynthesis, sulfate reduction, nitrate reduction and ammonification (Arp *et al.,* 1999a). In a supersaturated, highly alkaline lake like West Reflex Lake, photosynthesis is likely not a major control on carbonate precipitation (cf. Arp *et al.,* 1999a, Arp *et al,* 1999b).

One of the major influences that microorganisms exert on carbonate precipitation is the production of extracellular polymeric substances (EPS). These substances are polymers produced by microorganisms that help them adhere to substrates and form microbial mats (Arp *et al.,* 1999a). The EPS chelates metal ions including calcium and magnesium (Arp *et al.,* 1999a). The supply of Ca^{2+} to the water must exceed the ability of the EPS to bind it in order for $CaCO_3$ precipitation to occur. In Ca^{2+}-poor alkaline lakes that are supplied by comparatively Ca^{2+}-rich springs, such as West Reflex Lake, calcification of biofilms is controlled by the supply of Ca^{2+} at spring sites (cf. Arp *et al.,* 1999b).

Extracellular polymeric substances may also act as a template for carbonate precipitation. Microcrystalline and microsparitic aragonite nucleate within the biofilm (Arp *et al.,* 1999a; Dupraz *et al.,* 2009). Biofilms are heterogeneous and can vary in their ability to bind Ca^{2+} (Dupraz *et al.,* 2009). The biofilm itself may limit the size crystals can grow to microsparite (Arp *et al.,* 1999b).

The breakdown of EPS by heterotrophic bacteria also releases Ca^{2+} (Arp *et al.,* 1999a; Dupraz *et al.,* 2009). Sulfate-reducing bacteria in microbial mats can promote the precipitation of carbonate by increasing pH due to sulfate reduction simultaneously with the release of Ca^{2+} (Braissant *et al.,* 2007; Dupraz *et al.,* 2009). Where water saturated with $CaCO_3$ is in direct contact with carbonate crystals that are not coated by EPS, precipitation occurs abiotically and is

not inhibited (Arp *et al.,* 1999a). In alkaline, evaporative conditions, EPS binding capacity can be overcome and carbonate precipitation can proceed, producing well-developed crystals lacking EPS (Dupraz *et al.,* 2009).

6.7 Formation of different shoreline carbonate types

West Reflex Lake contains thrombolites, laminated coatings, and beachrock. Physical, chemical, and biological conditions in the lake must vary to produce these different types of shoreline carbonates (cf. Power *et al*., 2011). The precise origin of the different fabrics is not fully understood (cf. Ferris *et al.,* 1997). This section will attempt to interpret some of the factors influencing the formation of the different shoreline carbonates.

6.7.1 Thrombolites

Thrombolites occur as bioherms and isolated pinnacles in discontinuous belts around West Reflex Lake. Bioherms are larger, older, and composed of isolated pinnacles that have coalesced. Bioherms and isolated pinnacles have similar fabrics and probably precipitated by the same processes. The large bioherms with laminated coatings on their exteriors are interpreted to have formed earliest, at a time when lake level was higher. Isolated pinnacles have been forming within the last 60 years.

The locations of thrombolite development are constrained by the availability of nutrients and light for microbial communities to grow and the availability of Ca^{2+} for calcification (cf. Power *et al.,* 2011). The microbial communities forming thrombolites were laterally discontinuous compared to those that form laminated coatings (cf. Kennard and James, 1986). Filamentous microorganisms are preserved as molds in the thrombolites, and the micrite in the thrombolites appears to be biologically-influenced. Because the micrite coats filaments, plant

molds, and sand grains indiscriminately, it is interpreted that the filamentous microorganisms were not controlling the precipitation of aragonite. Precipitation on a variety of substrates could be a result of microbial EPS coating the substrates (Dupraz *et al.,* 2009).

The thrombolites of West Reflex Lake contain gypsum crystal pseudomorphs. The lake water is presently undersaturated with respect to gypsum. In order for gypsum to precipitate in the lake, the chemistry of the lake must have been different than it is at present. For example, saturation of gypsum may have increased if the lake was more saline due to evaporative concentration. The precipitation of carbonate at the expense of gypsum may be related to the action of sulfate-reducing bacteria (Friedman, 1972; Von der Borch *et al*., 1977; Petrash *et al*., 2010; Wright and Kirkham, 2011). When the lake water became undersaturated with respect to gypsum, gypsum dissolved, leaving hollow rinds of aragonite. The absence of microbial EPS in the voids left by gypsum dissolution allowed for the development of well-formed, inorganic calcite crystals (Fig. 4.20; cf. Arp *et al.,* 1998).

A variety of cements precipitated on the microbial framework of the thrombolites. Colourless botryoidal calcite and dogtooth calcite cements formed early in the development of the thrombolites and coat microbial filaments. These cements are interpreted as abiotic precipitates due to their clarity and lack of epifluorescence. The cements are composed of low-Mg calcite, whereas the biologically-influenced micritic precipitates are composed of aragonite. Aragonite precipitates from water that has a high Mg/Ca ratio (Deocampo, 2010). Low-Mg calcite precipitated from water with a lower Mg/Ca ratio. West Reflex Lake's water has a high Mg/Ca ratio (48), but the groundwater that flows into the lake has much lower Mg/Ca (<1). The low-Mg calcite cements precipitated where groundwater inflow dominated the chemistry of the solution.

In the West Reflex Lake thrombolites, the cements that precipitated after the phase 1 cements are coarsely laminated botryoidal aragonite cement, reddish-brown botryoidal aragonite cement, isopachous fibrous aragonite cement, irregular aragonite cement, and finely laminated botryoidal calcite cement. The two botryoidal aragonite cements both contain red-brown material that fluoresces. The red-brown material is interpreted to be organic matter incorporated into the crystal. Abiotic and biotic precipitation processes may have been both been operating when these cements were deposited. The majority of the cements are composed of aragonite, indicating that the Mg/Ca ratio of the solution was high. Finely laminated botryoidal calcite is commonly the last cement to form during this phase, indicating that Mg/Ca ratios were lower (groundwater influence was stronger).

The last components to have formed in the thrombolites are chert and the micrite crust. Chert replaces carbonate when the lake becomes concentrated by evaporation (Hay, 1968). The micrite crusts that drape over the surface of the thrombolites are similar in appearance to the micritic bands in the laminated coatings. The micrite crusts may have formed by carbonate precipitation in a cohesive microbial mat. The crust may then have been subaerially exposed, meaning that no further laminae were able to form.

6.7.2 Laminated coatings

West Reflex Lake's laminated coatings are composed of alternating light and dark coloured bands. The bands are thickest at the apex of domes, which suggests a biogenic origin, since physico-chemical precipitation should form bands of uniform thickness (cf. Planavsky and Grey, 2007). Millimeter-scale light and dark coloured laminae are present in a variety of continental carbonates, including microbialites, oncoids, speleothems, and travertines (Braithwaite *et al.,* 1989; Guo and Riding, 1992; Sami and James, 1994; Riding, 2008). In West

Reflex Lake, the light and dark bands are finely laminated, microspar laminae with fenestral fabric, and denser, more organic-rich micritic laminae, respectively. The development of these couplets has been attributed to alternation of cement precipitation and microbial mat growth (cf. Sami and James, 1994; Riding, 2008). The variation is likely to be seasonal (cf. Riding, 2008).

The light, microspar laminae in the laminated coatings contain large lenticular voids. The lenticular voids probably result from shrinkage during desiccation of the microbial mats (Arp *et al.,* 1998). The desiccation voids in the microspar laminae indicate that the laminated coatings were occasionally exposed during deposition. Exposure of the laminated coatings is most likely to happen during the late summer, when evaporation is high and precipitation is low. Therefore, the microspar laminae are interpreted to have formed during the summer.

Laminated coatings formed on a variety of substrates including cobbles, beachrock, and thrombolites. Laminated coatings develop from laterally continuous calcified biofilms that can bridge gaps in the topography of the substrate (cf. Power *et al.*, 2011). The draping of laminae onto the exterior surface of thrombolites indicates the presence of a coherent microbial mat (cf. Von der Borch *et al.,* 1977), since physicochemical precipitation would completely line the voids. The coatings are thinner and more friable on the cobbles and thicker on the bioherms and beachrock. Thicker biofilms in areas of Ca^{2+} influx (springs) formed more porous crusts, while thinner biofilms situated far from Ca^{2+} sources formed thin, irregular, dense crusts (cf. Arp *et al.*, 1999b). The thickness of the laminae may also relate to lake level. The thickest coatings are on the thrombolites farthest from the present shore, which developed during higher lake level and lower salinity. Lower salinity led to greater biological productivity and an increase in the thickness of the microbial mats which produced the laminated coatings (G. Goldsborough, pers. comm., 2017). A laminated coating is not present on the thrombolite that was radiocarbon dated

for this study. This indicates that conditions (e.g. salinity, water depth) were not favourable for stromatolite formation in West Reflex Lake within the last 60 years.

6.7.3 Beachrock

Beachrock in West Reflex Lake occurs sporadically around the lake's shore. The limited extent of the beachrock suggests that the processes involved in beachrock formation vary spatially and temporally. Beachrock formation occurs at the shoreline, near sites of groundwater inflow and development of other shoreline carbonates. Due to seasonal variations, the water level is occasionally lower than the surface of the sediment, forming pendent cements.

Beachrock cementation can occur as a result of physicochemical precipitation or microbial activity (Webb *et al.*, 1999; Hillgärtner *et al.*, 2001). Microbial activity plays an important role in sediment stabilization and the development of microcrystalline aragonite cement in beachrock (Neumeier, 1999; Hillgärtner *et al.*, 2001). Clots up to 50 μm in diameter are another indicator of microbial activity (Hillgartner *et al.*, 2001). Physio-chemical precipitation (prismatic cement) is superposed on the micritic cement after conditions are no longer favourable for the growth of microorganisms (Neumeier, 1999). The micritic cements in West Reflex Lake shoreline carbonates are often found with several generations of botryoidal cements developed on top, reflecting a fluctuation between the dominance of biotic and abiotic carbonate precipitation. The fluctuation may be seasonal: abiotic precipitation is able to occur as long as carbonate supersaturation is sufficient, whereas biotic precipitation may occur mainly in the summer, when microorganisms are able to grow in the lake.

Fenestral porosity in the beachrock is lined with several generations of botryoidal cements which are for the most part restricted to the fenestral pores. The fenestral porosity is interpreted to have formed when the top few mm of sand were bound together by the EPS of a

microbial community. Photosynthesis in the microbial community produced oxygen bubbles that lifted the microbial mat and trapped sediment away from the underlying sand. Micrite cements formed around the sand grains, lithifying them and preserving the fenestral pore underneath (cf. Neumeier, 1999). Cements such as coarsely laminated botryoidal cement are thickest in the fenestral pores, leading to the interpretation that Ca^{2+}-rich groundwater preferentially flowed along these open pathways, allowing physico-chemical precipitation to occur within the fenestral pores.

6.8 Comparison with Manito Lake

Manito Lake is a closed-basin, hypersaline lake located 22 km east of West Reflex Lake. Due to their proximity, the two lakes have similar climate and geological setting. However, the chemistry of the lakes differs. Differences in the chemistries of the lakes affect mineralogy and radiocarbon age, but the morphologies of the shoreline carbonates appear to be similar in the two lakes.

Table 6.1: Comparison of physical and chemical properties of Manito and West Reflex Lakes.

Parameter	**West Reflex Lake, AB-SK**	**Manito Lake, SK (Last, 2013)**
Location	52°39'N 110°00'W	52°54'N 109°43'W
Surface elevation (m asl)	587	583
Area (km^2)	4	65
Maximum depth (m)	1.9	22
pH	9.5	9.9
TDS (ppt)	94.9	40-50
Cation sequence	Na>K>Mg>Ca	Na>Mg>K>Ca
Anion sequence	$Cl>SO_4>HCO_3>CO_3$	$SO_4>HCO_3>Cl>CO_3$
Mg/Ca	48	50-60

Manito Lake has five basins and two permanent sources of surface inflow (Last, 2013). However, groundwater flow is the main contributor to the hydrologic budget of both lakes (Last, 2013). Physical and chemical properties of the two lakes are compared in Table 6.1. Manito Lake has a higher surface area and greater depth than West Reflex Lake. Because West Reflex Lake is a smaller, shallower lake, it will react more extremely to changes in the hydrologic balance.

Despite its proximity to West Reflex Lake, the reservoir effect in Manito Lake is negligible (Last *et al.*, 2010). Manito Lake also has water chemistry more similar to that of shallow groundwater than deep groundwater. Greater contribution of deep groundwater to West Reflex Lake than Manito Lake could account for the differences in chemistry and reservoir effect. Radiocarbon dating determined that the oldest microbialites in Manito Lake are 2300 cal yr BP (Last *et al.*, 2010). The maximum ages of the West Reflex Lake shoreline carbonates are not known. Microbialites are forming in both lakes at the present day.

The shoreline carbonate structures identified by Last *et al.* (2010) are isolated microbialite pinnacles, coalesced bioherms, laminated coatings, and cemented siliciclastic sediments. The same types of shoreline carbonates are present in West Reflex Lake. Several carbonate bioherms in Manito Lake are tens of meters in length. None of the West Reflex Lake microbialites formed coalesced structures of this scale. However, patches of individual bioherms ten of metres long are present in West Reflex Lake. They may represent an early stage in the formation of these carbonate “reefs”.

The mineralogy of Manito Lake and West Reflex Lake shoreline carbonates are similar: predominantly aragonite with calcite, high-Mg calcite and dolomite. However, Manito Lake contains calcite after ikaite and monohydrocalcite, which were not observed in West Reflex Lake. It is possible that the West Reflex Lake microbialites were not forming at a time when

temperatures were cool enough for ikaite to develop, or calcite pseudomorphs after ikaite may not have been preserved.

Shoreline carbonate morphology in lakes in this region does not appear to be determined by size of the lake or anion or cation dominance. Both lakes have low concentrations of Ca^{2+} compared to the inflowing groundwater, high alkalinity, and high Mg/Ca. To determine the effect of microorganisms on shoreline carbonate development in the two lakes, it would be informative to determine if the microbial communities of the lakes are similar.

7 Conclusions

West Reflex Lake is a hypersaline (94.9 g/L TDS) and alkaline (pH 9.5) lake in the Canadian Great Plains. The lake has decreased in size since the 1940s and has a present surface area of 4.0 km^2. Since the 1960s, the salinity of the lake has increased tenfold. West Reflex Lake is topographically closed. The lake loses water to evaporation and receives most of its water from springs that discharge into the lake. Shoreline carbonates structures have formed on the shore of the lake near the springs.

West Reflex Lake has high Cl^- and SO_4^{2-} concentrations relative to other lakes in the region (Hammer, 1978). The chemistry of the lake is similar to the chemistry of the deep groundwater in the region. This similarity, combined with the anomalously old radiocarbon age of the carbonate, suggests that the chemistry of West Reflex Lake is strongly influenced by deep groundwater. Nearby lakes have chemistries very different to that of West Reflex Lake. Possible reasons for West Reflex Lake's unusual chemistry include its location in a buried bedrock valley that channels deep groundwater flow, a base of impermeable till preventing the loss of water carrying solutes, and a local fracture system that carries saline water from the Prairie Evaporite.

The chemistry of West Reflex Lake affects the mineralogy and chemistry of the lacustrine carbonates precipitated in the basin. West Reflex Lake has a high Mg/Ca ratio (48), which favours the precipitation of aragonite over calcite. Calcium carbonate in the form of aragonite, and to a lesser extent, calcite, precipitated on microorganisms near the springs. Carbonate precipitation is controlled by the availability of Ca^{2+} ions, which are supplied to the lake by saline springs.

The four types of shoreline carbonate structures observed in West Reflex Lake are isolated pinnacles, bioherms, beachrock, and laminated coatings. The isolated pinnacles are 15-

30 cm high, columnar or dome-shaped structures. Bioherms are 30-80 cm high aggregates of pinnacles on a base of carbonate-cemented sand. Both have a thrombolitic internal fabric composed of branching filaments. Beachrock underlies the isolated pinnacles and bioherms. Laminated coatings of micrite and microspar, 1-5 mm thick, are present on bioherms, beachrock, cobbles and boulders.

The West Reflex Lake thrombolites (bioherms and isolated pinnacles) have 20-40% porosity. They are composed of aragonite in the form of clotted micrite and micrite coated coarse filaments. The thrombolites also contain <4% dolomite and protodolomite. Plant molds and evaporite pseudomorphs are present in places. A micritic crust coats the exterior of many of the thrombolites. The isolated pinnacles likely formed in the last 50 years. Thrombolites develop in locations where light and nutrient availability are sufficient for microorganisms to grow, and Ca^{2+} availability is sufficient for carbonate precipitation. Large pores in the thrombolites channel groundwater flow that supplies Ca^{2+} for abiotic precipitation of carbonate in the pores.

The beachrock in West Reflex Lake is a lithic arenite composed of sub-rounded to rounded, well-sorted, medium sand size grains. The sand grains are 40-60% quartz, 20-40% lithic fragments, and 10-20% feldspar, cemented by microcrystalline aragonite and high-Mg calcite. Fenestral porosity in the beachrock is lined by coarsely laminated botryoidal aragonite cements. Beachrock formation in West Reflex Lake is affected by microbial activity. Microorganisms in the sediment stabilize the sediment and allow the development of microcrystalline aragonite cement. Abiotic precipitation of finely laminated botryoidal cement and isopachous radial fibrous aragonite cement in the pores occurs when conditions such as temperature or salinity are not favourable for the growth of microorganisms.

Laminated coatings are composed of alternating layers of micritic aragonite and microsparitic aragonite and calcite. Porosity is fenestral. In places, the micrite contains fine sand grains or molds of brine shrimp eggs. Laminated coatings form from microbial mats that drape over the surface of substrates such as bioherms and cobbles. Seasonal variation in lake water chemistry appears to influence the deposition of micrite vs. microspar. The microspar laminae likely formed in the summer.

The stable oxygen and carbon isotope ratios of the shoreline carbonates of West Reflex Lake covary, suggesting that the lake was closed during the time the carbonates were forming. The $\delta^{18}O$ values of the thrombolites increase from interior to exterior. This result implies that lake level decreased as the thrombolites were deposited. Radiocarbon dating of plant material and carbonate from an isolated pinnacle suggests that the lake has a 5000 year reservoir effect.

The dominant process of carbonate precipitation that formed the microbialites in West Reflex Lake is biologically-influenced calcification. The microcrystalline aragonite that makes up the bulk of the microbialite is a typical microbial precipitate (cf. Neumeier, 1999; Della Porta, 2015). The micrite also fluoresces strongly, an indication of the presence of diffuse organic matter (Dravis and Yurewicz, 1985). Extracellular polymeric substances (EPS) that are produced by microorganisms chelate Ca^{2+} ions supplied to the lake by saline springs. When EPS is broken down by heterotrophic bacteria, Ca^{2+} is released and calcium carbonate minerals precipitate.

Cementation occurs on the primary microbial carbonate substrate. Many of the cements are colourless and have large, well-formed crystals that do not fluoresce. In these cements, no evidence exists for biological influence. These cements precipitated at a time when the microenvironment was supersaturated with respect to aragonite or calcite but the pores did not

contain significant amounts of microbial EPS. Microcrystalline aragonite cements are interlaminated with abiotic cements, suggesting that biotic and abiotic precipitation alternated.

West Reflex Lake is 22 km west of Manito Lake, the first lake in the Canadian Great Plains whose microbialites have been studied in detail. Unlike West Reflex Lake, Manito Lake's chemistry is more similar to that of shallow groundwater than deep groundwater. Both lakes have the same types of shoreline carbonates: isolated pinnacles, bioherms, laminated coatings, and cemented siliciclastics. However, many of the Manito Lake microbialites are much larger: up to tens of metres in length. The West Reflex Lake microbialites have not coalesced into structures this large, and may represent an earlier stage in the development of lacustrine carbonate reefs.

West Reflex Lake is a worthwhile study site because of its easy access, unusual chemistry, and importance for shorebirds. Many future projects on the lake and its surrounding are possible. The following are suggestions for future studies:

1. Investigation of the chemistry and presence or absence of shoreline carbonates in East Reflex Lake and Gordon Lake.
2. Core studies to examine the changes in mineralogy, texture, and stable isotope characteristics of West Reflex Lake over time.
3. Improved geochronology of the shoreline carbonates to refine our understanding of the timing of shoreline carbonate development in West Reflex Lake relative to other lakes in the region.
4. Detailed study of the hydrogeology of the area to determine the source of solutes.
5. Microbiological studies that enable the correlation of different mineralogies, textures, or structures to different microbial communities.

References

Alberta Environment and Parks. 2016. Groundwater observation well network [online]. Available from http://esrd.alberta.ca/water/programs-and-services/groundwater/groundwater-observation-well-network/default.aspx [cited 6 May 2016].

Arp, G. 1995. Lacustrine bioherms, spring mounds, and marginal carbonates of the Ries-impact-crater (Miocene, Southern Germany). Facies, **33**:35-90.

Arp, G., Hofmann, J., and Reitner, J. 1998. Microbial fabric formation in spring mounds ("microbialites") of alkaline salt lakes in the Badain Jaran sand sea, PR China. PALAIOS, **13**:581-592.

Arp, G., Reimer, A., and Reitner, J. 1999a. Calcification in cyanobacterial biofilms of alkaline salt lakes. European Journal of Phycology, **34**:393-403.

Arp, G., Thiel, V., Reimer, A., Michaelis, W., and Reitner, J. 1999b. Biofilm exopolymers control microbialite formation at thermal springs discharging into the alkaline Pyramid Lake, Nevada, USA. Sedimentary Geology, **126**:159-176.

Arp, G., Reimer, A., and Reitner, J. 2001. Photosynthesis-induced biofilm calcification and calcium concentrations in Phanerozoic oceans. Science, **292**:1701-1704.

Benson, L., White, L.D., and Rye, R. 1996. Carbonate deposition, Pyramid Lake subbasin, Nevada: 4. Comparison of the stable isotope values of carbonate deposits (tufas) and the Lahontan lake-level record. Palaeogeography, Palaeoclimatology, Palaeoecology, **122**:45-76.

Beyersbergen, G.W. 2009. Shorebird migration surveys of Alberta-Saskatchewan border lakes and the north-central lakes of Saskatchewan: 1995-1998. Available from Canadian Wildlife Service, Edmonton, AB. Technical Report Series Number 505.

Birks, S.J., and Remenda, V.N. 1999. Hydrogeological investigation of Chappice Lake, southeastern Alberta: groundwater inputs to a saline basin. Journal of Paleolimnology, **21:**235-255.

Blinn, D.W. 1993. Diatom community structure along physicochemical gradients in saline lakes. Ecology, **74**:1246-1263.

Braissant, O., Decho, A.W., Dupraz, C., Glunk, C., Przekop, K.M., and Visscher, P.T. 2007. Exopolymeric substances of sulfate-reducing bacteria: interactions with calcium at alkaline pH and implication for formation of carbonate minerals. Geobiology, **5**:401-411.

Braithwaite, C.J.R., Casanova, J., Frevert, T., and Whitton, B.A. 1989. Recent stromatolites in landlocked pools on Aldabra, western Indian Ocean. Palaeogeography, Palaeoclimatology, Palaeoecology, **69:**145-165.

Buick, R., Dunlop, J.S.R., and Groves, D.I. 1981. Stromatolite recognition in ancient rocks: an appraisal of irregularly laminated structures in an Early Archean chert-barite unit from North Pole, Western Australia. Alcheringa: An Australasian Journal of Paleontology, **5**:161-181.

Burne, R.V., and Moore, L.S. 1987. Microbialites: organosedimentary deposits of benthic microbial communities. PALAIOS, **2**:241-254.

Canfield, D.E., Buchmann, R.W., and Hoyer, M.V. 1983. Freeze-out of salts in hard-water lakes. Limnology and Oceanography, **28**:970-977.

Carlson, V.A., and Topp, L.M. 1971. Bedrock topography of the Wainwright map area, NTS 73D, Alberta. Research Council of Alberta, Edmonton, AB. Scale 1:250 000.

Cumings, E.R. 1932. Reefs or bioherms?. Geological Society of America Bulletin, **43**:337-352.

Della Porta, G. 2015. Carbonate build-ups in lacustrine, hydrothermal and fluvial settings: comparing depositional geometry, fabric types and geochemical signature. *In* Microbial carbonates in space and time: implications for global exploration and production. *Edited by* D.W.J. Bosence, K.A. Gibbons, D.P. Le Heron, W.A. Morgan, T. Pritchard, and B.A. Vining. Geological Society, London. pp. 17-68.

Deocampo, D. 2010. The geochemistry of continental carbonates. *In* Developments in Sedimentology, Volume 62. *Edited by* A.M. Alonso-Zarza and L.H. Tanner. Elsevier, Amsterdam. pp. 1-45.

Donovan, J.J. 1994. On the measurement of reactive mass fluxes in evaporative groundwater-source lakes. *In* Sedimentology and Geochemistry of Modern and Ancient Saline Lakes, SEPM Special Publication No. 50. *Edited by* R.W. Renaut and W.M. Last. SEPM, Tulsa, OK. pp. 33-50.

Donovan, J.J., and Rose, A.W. 1994. Geochemical evolution of lacustrine brines from variable-scale groundwater circulation. Journal of Hydrology, **154**:35-62.

Douglas, S., Abbey, W., Mielke, R., Conrad, P., and Kanik, I. 2008. Textural and mineralogical biosignatures in an unusual microbialite from Death Valley, California. Icarus, **193**:620-636.

Dove, P., de Yoreo, J., and Weiner, S. 2003. Biomineralization. Mineralogical Society of America, Washington, DC.

Dravis, J.J., and Yurewicz, D.A. 1985. Enhanced carbonate petrography using fluorescence microscopy. Journal of Sedimentary Petrology, **55:**795-804.

Dunham, R.J. 1962. Classification of carbonate rocks according to depositional texture. *In* Classification of Carbonate Rocks. *Edited by* W.E. Ham. American Association of Petroleum Geologists Memoir 1, Tulsa, OK. pp. 102-121.

Dupraz, C., and Strasser, A. 1999. Microbialites and micro-encrusters in shallow coral bioherms (Middle to Late Oxfordian, Swiss Jura mountains). Facies, **40**:101-130.

Dupraz, C., Reid, R.P., Braissant, O., Decho, A.W., Norman, R.S., and Visscher, P.T. 2009. Processes of carbonate precipitation in modern microbial mats. Earth-Science Reviews, **96**:141-162.

Environment and Climate Change Canada. 2015. Temperature and precipitation chart for 1981 to 2010 Canadian climate normals: Artland [online]. Available from http://climate.weather.gc.ca/climate_ normals/results_1981_2010_e.html?stnID=3207 [cited 2 May 2016].

Fang, X., and Pomeroy, J.W. 2008. Drought impacts on Canadian prairie watershed snow hydrology. Hydrological Processes, doi:10.1002/hyp.7074.

Ferris, F.G., Thompson, J.B., and Beveridge, T.J. 1997. Modern freshwater microbialites from Kelly Lake, British Columbia, Canada. PALAIOS, **12**:213-219.

Fisheries and Environment Canada. 1978. Mean annual lake evaporation. Hydrological Atlas of Canada. Ministry of Supply and Services, Ottawa, ON.

Friedman, G.M. 1972. Significance of Red Sea in problem of evaporites and basinal limestones. AAPG Bulletin, **56**:1072-1086.

Fritz, S.C., Juggins, S., and Battarbee, R.W. 1993. Diatom assemblages and ionic characterization of lakes of the northern Great Plains, North America: a tool for reconstructing past salinity and climate fluctuations. Canadian Journal of Fisheries and Aquatic Sciences, **50**:1844-1856.

Fritz, S.C., Engstrom, D.R., and Haskell, B.J. 1994. 'Little Ice Age' aridity in the North American Great Plains: a high-resolution reconstruction of salinity fluctuations from Devils Lake, North Dakota, USA. The Holocene, **4**:69-73.

Flügel, E. 2010. Microfacies of carbonate rocks: analysis, interpretation and application, 2nd edition. Springer-Verlag, Berlin.

Gischler, E. Gibson, M.A., and Oschmann, W. 2008. Giant Holocene freshwater microbialites, Laguna Bacalar, Quintana Roo, Mexico. Sedimentology, **55**:1293-1309.

Google Earth. 2016. [Reflex Lakes]. Available from https://goo.gl/maps/jr33LDteba42 [accessed 21 November 2016].

Götte, T., and Richter, D.K. 2009. Quantitative aspects of Mn-activated cathodoluminescence of natural and synthetic aragonite. Sedimentology, **56**:483-492.

Grasby, S.E. 2000. Saline spring geochemistry, west-central Manitoba. Available from Manitoba Geological Survey, Winnipeg, MB. Report of Activities 2000.

Grosjean, M., Geyh, M.A., Messerli, B., and Schotterer, U. 1995. Late-glacial and early Holocene lake sediments, groundwater formation and climate in the Atacama Altiplano 22-24°S. Journal of Paleolimnology, **14**:241-252.

Grossman, I.G. 1968. Origin of the sodium sulfate deposits of the northern Great Plains of Canada and the United States. United States Geological Survey Professional Paper 600-B: B104-B109.

Guo, L., and Riding, R. 1992. Aragonite laminae in hot water travertine crusts, Rapolano Terme, Italy. Sedimentology, **39**:1067-1079.

Gustaffsson, J.P. 2010. Visual MINTEQ version 3.1 [online]: Available from https://vminteq.lwr.kth.se/download/ [cited 23 Aug 2016].

Hackbarth, D.A. 1975. Hydrogeology of the Wainwright area, Alberta. Available from Alberta Research Council, Edmonton, AB. Report 75-1.

Hammer, U.T. 1978. The saline lakes of Saskatchewan: III. Chemical characterization. Internationale Revue der gesamten Hydrobiologie und Hydrographie, **63**:311-335.

Hammer, U.T. 1986. Saline lakes: their distribution and characteristics. *In* Evaluating Saline Waters in a Plains Environment. *Edited by* D.T. Waite. Canadian Plains Research Center, Regina, Sask. pp. 1-22.

Hammer, U.T., and Haynes, R.C. 1978. The saline lakes of Saskatchewan: II. Locale, hydrography and other physical aspects. Internationale Revue der gesamten Hydrobiologie und Hydrographie, **63**:179-203.

Hammer, U.T., and Heseltine, J.M. 1988. Aquatic macrophytes in saline lakes of the Canadian prairies. Hydrobiologia, **158**:101-116.

Hammer, U.T., Sheard, J.S., and Kranabetter, J. 1990. Distribution and abundance of littoral benthic fauna in Canadian prairie saline lakes. Hydrobiologia, **197**:173-192.

Hay, R.L. 1968. Chert and its sodium-silicare precursors in sodium-carbonate lakes of East Africa. Contributions to Mineralogy and Petrology, **17**:255-274.

Hendry, M.J., Cherry, J.A., and Wallick, E.I. 1986. Origin and distribution of sulfate in a fractured till in southern Alberta, Canada. Water Resources Research, **22**:45-61.

Hillgärtner, H., Dupraz, C., and Hug, W. 2001. Microbially induced cementation of carbonate sands: are micritic meniscus cements good indicators of vadose diagenesis? Sedimentology, **48**:117-131.

Horath, T., Neu, T.R., and Bachofen, R. 2006. An endolithic microbial community in dolomite rock in central Switzerland: characterization by reflection spectroscopy, pigment analyses, scanning electron microscopy, and laser scanning microscopy. Microbial Ecology, **51**:353-364.

Horton, T.W., Defliese, W.F., Tripati, A.K., and Oze, C. 2015. Evaporation induced ^{18}O and ^{13}C enrichment in lake systems: a global perspective on hydrologic balance effects. Quaternary Science Reviews, **131B**:365-379.

IBA Canada. 2010. Manito Lake area (includes Reflex, Freshwater, Wells, Colette and Cipher Lakes) [online]: Available from http://www.ibacanada.com/site.jsp?siteID=SK089 [cited 7 November 2016].

Kelley, L.I., Smith, J.J., and Holmden, C. 1998. Stable isotope and chemical composition of groundwater associated with sodium sulfate deposits, southern Saskatchewan. Available from Saskatchewan Geological Survey, Regina, SK. Miscellaneous Report 98-4.

Kempe, S. Kazmierczak, J., Landmann, G., Konuk, T., Reimer, A., and Lipp, A. 1991. Largest known microbialites discovered in Lake Van, Turkey. Nature, **349**:605-608.

Kennard, J.M., and James, N.P. 1986. Thrombolites and stromatolites: two distinct types of microbial structures. PALAIOS, **1**:492-503.

Last, F.M. 2013. Carbonate microbialite formation in a prairie saline lake in Saskatchewan, Canada: paleohydrologic and paleoenvironmental implications. Ph.D. thesis, Department of Geological Sciences, University of Manitoba, Winnipeg, MB.

Last, F.M., Last, W.M., and Halden, N.M. 2010. Carbonate microbialites and hardgrounds from Manito Lake, an alkaline, hypersaline lake in the northern Great Plains of Canada. Sedimentary Geology, **225**:34-49.

Last, W.M. 1984. Sedimentology of playa lakes of the northern Great Plains. Canadian Journal of Earth Sciences, **21**:107-125.

Last, W.M. 1989. Continental brines and evaporites of the northern Great Plains of Canada. Sedimentary Geology, **64**:207-221.

Last, W.M. 1992. Chemical composition of saline and subsaline lakes of the northern Great Plains, western Canada. International Journal of Salt Lake Research, **1**:47-76.

Last, W.M. 2001. Mineralogical analysis of lake sediments. *In* Tracking Environmental Change Using Lake Sediments Volume 2: Physical and Geochemical Methods. *Edited by* W.M. Last and J.P. Smol. Kluwer Academic Publishers, Dordrecht, The Netherlands. pp. 143-187.

Last, W.M., and Ginn, F.M. 2005. Saline systems of the Great Plains of western Canada: an overview of the limnogeology and paleolimnology. Saline Systems, doi:10.1186/1746-1448-1-10.

Last, W.M., and Last, F.M. 2012. Lacustrine carbonates of the northern Great Plains of Canada. Sedimentary Geology, **277-278**:1-31.

Last, W.M. and Schweyen, T.H. 1983. Sedimentology and geochemistry of saline lakes of the Great Plains. Hydrobiologia, **105**:245-263.

Last, W.M., Teller, J.T., and Forester, R.M. 1994. Paleohydrology and paleochemistry of Lake Manitoba, Canada: the isotope and ostracode records. Journal of Paleolimnology, **12**:269-282.

Leng, M.J., and Marshall, J.D. 2004. Palaeoclimate interpretation of stable isotope data from lake sediment archives. Quaternary Science Reviews, **23**:811-831.

Li, H.-C., and Ku, T.-L. 1997. $\delta^{13}C$- $\delta^{18}O$ covariance as a paleohydrological indicator for closed-basin lakes. Paleogeography, Palaeoclimatolgy, Palaeoecology, **133**:69-80.

Luzón, A., Mayayo, M.J., and Pérez, A. 2009. Stable isotope characterisation of co-existing carbonates from the Holocene Gallocanta lake (NE Spain): palaeolimnological implications. International Journal of Earth Science, **98**:1129-1150.

Macdonald, D.E. 1982. Marl resources of Alberta. Available from Alberta Research Council, Edmonton, AB. Earth Sciences Report 82-1.

MacDonald, G.M., Beukens, R.P., and Kieser, W.E. 1991. Radiocarbon dating of limnic sediments: a comparative analysis and discussion. Ecology, **72**:1150-1155.

Millard, M.J. 1990. Geology and groundwater resources of the Battleford area (73C), Saskatchewan. Available from Saskatchewan Research Council, Saskatoon, SK. Report R-1210-5-E-90.

National Air Photo Library. 1946. [Reflex Lake]. Air photo. 1:20000. A10888, Photo 209. Natural Resources Canada, Ottawa, ON.

Natural Resources Canada. 2016. Reflex Lakes [online]: Available from http://geogratis.gc.ca/site/eng/extraction [cited 22 December 2016].

Nelson, S.T., Wood, M.J., Mayo, A.L., Tingey, D.G., and Eggett, D. 2005. Shoreline tufa and tufaglomerate from Pleistocene Lake Bonneville, Utah, USA: stable isotopic and mineralogical records of lake conditions, processes, and climate. Journal of Quaternary Science, **20**:3-19.

Neumeier, U. 1999. Experimental modelling of beachrock cementation under microbial influence. Sedimentary Geology, **126**:35-46.

Petrash, D.A., Lalonde, S.V., Pecoits, E., Gingras, M., and Konhauser, K.O. 2010. Microbially catalyzed cementation of modern gypsum-dominated microbialites [online]: Available from http://www.geoconvention.com/archives/2010/0826_GC2010_Microbially_Catalyzed_Cementation.pdf [accessed 15 September 2016].

Pham, S.V., Leavitt, P.R., McGowan, S., Wissel, B., and Wassenaar, L.I. 2009. Spatial and temporal variability of prairie lake hydrology as revealed using stable isotopes of hydrogen and oxygen. Limnology and Oceanography, **54:**101-118.

Planavsky, N., and Grey, K. 2007. Stromatolite branching in the Neoproterozoic of the Centralian Superbasin, Australia: an investigation into sedimentary and microbial control of stromatolite morphology. Geobiology, **6**:33-45.

Power, I.M., Wilson, S.A., Dipple, G.M., and Southam, G. 2011. Modern carbonate microbialites from an asbestos open pit pond, Yukon, Canada. Geobiology, **9**:180-195.

Prescott, D.R.C., Engley, L.C., Sturgess, D. 2010. Implementation of the Alberta piping plover recovery plan, 2005-2010: final program report. Government of Alberta Fish and Wildlife Division, Alberta Species at Risk Report No. 129.

Reimer, P.J. Bard, E., Bayliss, A., Beck, J.W., Blackwell, P.G., Ramsey, C.B, Buck, C.E., Cheng, H., Edwards, R.L., Friedrich, M., Grootes, P.M., Guilderson, T.P., Haflidason, H., Hajdas, I., Hatté, C., Heaton, T.J., Hoffmann, D.L., Hogg, A.G., Hughen, K.A., Kaiser, K.F., Kromer, B., Manning, S.W., Niu, M., Reimer, R.W., Richards, D.A., Scott, E.M., Southon, J.R., Staff, R.A., Turney, C.S.M., van der Plicht, J. 2013. IntCal13 and Marine13 radiocarbon age calibration curves 0–50,000 years cal BP. Radiocarbon, **55**:1869–1887.

Reitner, J., Neuweiler, F., Flajs, G., Vigener, M., Keupp, H., Meischner, D., Paul, J., Warnke, K., Weller, H., Dingle, P., Hensen, C., Schäfer, P., Gautret, P., Leinfelder, R.R., Hussner, H., and Kaufmann, B. 1995. Mud mounds: a polygenetic spectrum of fine-grained carbonate buildups. Facies, **32**:1-69.

Riding, R. 2000. Microbial carbonates: the geological record of calcified bacterial-algal mats and biofilms. Sedimentology, **47**:179-214.

Riding, R. 2008. Abiogenic, microbial and hybrid authigenic carbonate crusts: components of Precambrian stromatolites. Geologia Croatica, **61**:73-103.

Rosen, M.R., Arehart, G.B., and Lico, M.S. 2004. Exceptionally fast growth rate of <100-yr-old tufa, Big Soda Lake, Nevada: implications for using tufa as a paleoclimate proxy. Geology, **32**:409-412.

Rozanski, K., Araguas-Araguas, L., and Gonfiantini, R. 1993. Isotopic patterns in modern global precipitation. *In* Climate Change in Continental Isotopic Records. *Edited by* P.K. Swart, L.C. Lohmann, J. McKenzie, and S. Savin. American Geophysical Union, Geophysical Monograph 78, Washington, D.C. pp.1-36.

Russo, F., Gautret, P., Mastandrea, A., Perri, E. 2006. Syndepositional cements associated with nannofossils in the Marmolada Massif: evidences of microbially mediated primary marine cements? (Middle Triassic, Dolomites, Italy). Sedimentary Geology, **185**:267-275.

Rutherford, A.A. 1970. Water quality survey of Saskatchewan surface waters. Chemistry Division, Saskatchewan Research Council C-70-1, Saskatoon, SK.

Ryves, D.B. 1994. Diatom dissolution in saline lake sediments: an experimental study in the Great Plains of North America. Ph.D. thesis, Department of Geography, University College London, London, UK.

Sami, T.T., and James, N.P. 1994. Peritidal carbon platform growth and cyclicity in an early Proterozoic foreland basin, upper Pethei Group, northwest Canada. Journal of Sedimentary Research, **B64**:111-131.

Scholl, D.W., and Taft, W.H. 1964. Algae, contributors to the formation of calcareous tufa, Mono Lake, California. Journal of Sedimentary Petrology, **34**:309-319.

Spadafora, A., Perri, E., McKenzie, J.A., and Vasconcelos, C. 2010. Microbial biomineralization processes forming modern Ca:Mg carbonate stromatolites. Sedimentology, **57**:27-40.

Talbot, M.R. 1990. A review of the palaeohydrological interpretation of carbon and oxygen isotopic ratios in primary lacustrine carbonates. Chemical Geology (Isotope Geoscience Section), **80**:261-279.

Talbot, M.R., and Kelts, K. 1990. Paleolimnological signatures from carbon and oxygen isotopic ratios in carbonates from organic carbon-rich lacustrine sediments. *In* Lacustrine Basin Exploration – Case studies and modern analogs. *Edited by* B.J. Katz. American Association of Petroleum Geology Memoir 50, Tulsa, Oklahoma. pp. 99-112.

Timms, B.V., Hammer, U.T., and Sheard, J.W. 1986. A study of benthic communities in some saline lakes in Saskatchewan and Alberta, Canada. Internationale Revue der gesamten Hydrobiologie und Hydrographie, **71**:759-777.

Tranter, M. 2011. Isotopic fractionation of freezing water. *In* Encyclopedia of Snow, Ice and Glaciers. *Edited by* V.P. Singh, P. Singh, and U.K. Haritashya. Springer, Dordrect, Netherlands. pp. 668-669.

Valero-Garcés, B.L., Laird, K.R., Fritz, S.C., Kelts, K., Ito, E., and Grimm, E.C. 1997. Holocene climate in the northern Great Plains inferred from sediment stratigraphy, stable isotopes, carbonate geochemistry, diatoms, and pollen at Moon Lake, North Dakota. Quaternary Research, **48**:359-369.

Von der Borch, C.C., Bolton, B., and Warren, J.K. 1977. Environmental setting and microstructure of subfossil lithified stromatolites associated with evaporites, Marion Lake, South Australia. Sedimentology, **24:** 693-708.

Wallick, E.I. 1981. Chemical evolution of groundwater in a drainage basin of Holocene age, east-central Alberta, Canada. Journal of Hydrology, **54**:245-283.

Wallis, C. 1991. Reconnaissance survey of saline wetlands and springs in the grassland-parkland region of eastern Alberta. Prairie for Tomorrow, World Wildlife Fund Canada, Edmonton, Alberta.

Wassenaar, L., Aravena, R., Hendry, J., and Fritz, P. 1991. Radiocarbon in dissolved organic carbon, a possible groundwater dating method: case studies from Western Canada. Water Resources Research, **27**:1975-1986.

Webb, G.E., Jell, J.S., and Baker, J.C. 1999. Cryptic intertidal microbialites in beachrock, Heron Island, Great Barrier Reef: implications for the origin of microcrystalline beachrock cement. Sedimentary Geology, **126**:317-334.

Wells, R.E., and Cornish, B.J. 1999. Piping plover habitat classification and inventory of selected parkland region lakes. Available from the Alberta Environment Land and Forest Service. Edmonton, Alberta.

Williams, W.D. 2002. Environmental threats to salt lakes and the likely status of inland saline ecosystems in 2025. Environmental Conservation, **29**:154-167.

Witkind, I.J. 1952. The localization of sodium-sulfate deposits in northeastern Montana and northwestern North Dakota. American Journal of Science, **250**:667-676.

Wright, D.T., and Kirkham, A. 2011. The role of bacterial sulphate reduction in carbonate replacement of vanished evaporites: examples from the Holocene, Jurassic and Neoarchaean. International Association of Sedimentologists Special Publication, **43**:299-314.

Wright, G.N., McMechan, M.E., and Potter, D.E.G. 1994. Structure and architecture of the Western Canada Sedimentary Basin. *In* Geological Atlas of the Western Canada Sedimentary Basin. *Edited by* G.D. Mossop and I. Shetsen. Canadian Society of Petroleum Geologists and Alberta Research Council, Edmonton, Alberta. pp. 25-40.

Yuan, F., Linsley, B.K., and Howe, S.S. 2006. Evaluating sedimentary geochemical lake-level tracers in Walker Lake, Nevada, over the last 200 years. Journal of Paleolimnology, **36**:37-54.

Appendix A: Water chemistry data from ALS Laboratories.

Sample Details/Parameters	Result	Qualifier*	D.L.	Units	Extracted	Analyzed	Batch
L1616805-1 WEST REFLEX LAKE							
Sampled By: CLIENT on 21-MAY-15 @ 11:30							
Matrix:							
Miscellaneous Parameters							
Bicarbonate (HCO3)	5000		1.2	mg/L		21-JUL-15	
Carbonate (CO3)	5460		0.60	mg/L		21-JUL-15	
Hydroxide (OH)	<0.34		0.34	mg/L		21-JUL-15	
Oxygen, Dissolved	0.10	RWHS	0.10	mg/L		27-MAY-15	R3197218
Phosphorus (P)-Total	0.432	DLA	0.020	mg/L		01-JUN-15	R3199346
Sulfate (SO4)	8120		150	mg/L		27-MAY-15	R3197146
Alkalinity, Total (as CaCO3)	13200		10	mg/L		02-JUN-15	R3200815
Dissolved Metals by ICP-MS							
Aluminum (Al)-Dissolved	<0.020		0.020	mg/L	28-MAY-15	28-MAY-15	R3197673
Antimony (Sb)-Dissolved	0.0041		0.0010	mg/L	28-MAY-15	28-MAY-15	R3197673
Arsenic (As)-Dissolved	0.182		0.0010	mg/L	28-MAY-15	28-MAY-15	R3197673
Barium (Ba)-Dissolved	0.0556		0.00050	mg/L	28-MAY-15	28-MAY-15	R3197673
Beryllium (Be)-Dissolved	<0.0010		0.0010	mg/L	28-MAY-15	28-MAY-15	R3197673
Bismuth (Bi)-Dissolved	<0.00050		0.00050	mg/L	28-MAY-15	28-MAY-15	R3197673
Boron (B)-Dissolved	23.0	DLA	0.30	mg/L	28-MAY-15	29-MAY-15	R3198762
Cadmium (Cd)-Dissolved	<0.00020		0.00020	mg/L	28-MAY-15	28-MAY-15	R3197673
Calcium (Ca)-Dissolved	4.09		0.20	mg/L	28-MAY-15	28-MAY-15	R3197673
Cesium (Cs)-Dissolved	0.00116		0.00050	mg/L	28-MAY-15	28-MAY-15	R3197673
Chromium (Cr)-Dissolved	<0.0020		0.0020	mg/L	28-MAY-15	28-MAY-15	R3197673
Cobalt (Co)-Dissolved	<0.00050		0.00050	mg/L	28-MAY-15	28-MAY-15	R3197673
Copper (Cu)-Dissolved	<0.0020		0.0020	mg/L	28-MAY-15	28-MAY-15	R3197673
Iron (Fe)-Dissolved	0.22		0.10	mg/L	28-MAY-15	28-MAY-15	R3197673
Lead (Pb)-Dissolved	<0.0010		0.0010	mg/L	28-MAY-15	28-MAY-15	R3197673
Lithium (Li)-Dissolved	2.20		0.010	mg/L	28-MAY-15	28-MAY-15	R3197673
Magnesium (Mg)-Dissolved	120		0.050	mg/L	28-MAY-15	28-MAY-15	R3197673
Manganese (Mn)-Dissolved	0.0071		0.0010	mg/L	28-MAY-15	28-MAY-15	R3197673
Molybdenum (Mo)-Dissolved	0.0105		0.00050	mg/L	28-MAY-15	28-MAY-15	R3197673
Nickel (Ni)-Dissolved	<0.0020		0.0020	mg/L	28-MAY-15	28-MAY-15	R3197673
Phosphorus (P)-Dissolved	0.74		0.50	mg/L	28-MAY-15	28-MAY-15	R3197673
Potassium (K)-Dissolved	976		0.10	mg/L	28-MAY-15	28-MAY-15	R3197673
Rubidium (Rb)-Dissolved	0.0470		0.00050	mg/L	28-MAY-15	28-MAY-15	R3197673
Selenium (Se)-Dissolved	<0.0050		0.0050	mg/L	28-MAY-15	28-MAY-15	R3197673
Silicon (Si)-Dissolved	1.29		0.30	mg/L	28-MAY-15	28-MAY-15	R3197673
Silver (Ag)-Dissolved	<0.0010		0.0010	mg/L	28-MAY-15	28-MAY-15	R3197673
Sodium (Na)-Dissolved	35200	DLA	0.50	mg/L	28-MAY-15	29-MAY-15	R3198762
Strontium (Sr)-Dissolved	0.0296		0.00050	mg/L	28-MAY-15	28-MAY-15	R3197673
Tellurium (Te)-Dissolved	<0.0010		0.0010	mg/L	28-MAY-15	28-MAY-15	R3197673
Thallium (Tl)-Dissolved	<0.0050		0.0050	mg/L	28-MAY-15	28-MAY-15	R3197673
Thorium (Th)-Dissolved	0.0017		0.0010	mg/L	28-MAY-15	28-MAY-15	R3197673
Tin (Sn)-Dissolved	<0.00060		0.00060	mg/L	28-MAY-15	28-MAY-15	R3197673
Titanium (Ti)-Dissolved	0.0048		0.0010	mg/L	28-MAY-15	28-MAY-15	R3197673
Tungsten (W)-Dissolved	<0.0020		0.0020	mg/L	28-MAY-15	28-MAY-15	R3197673
Uranium (U)-Dissolved	0.0450		0.00050	mg/L	28-MAY-15	28-MAY-15	R3197673
Vanadium (V)-Dissolved	0.0055		0.0020	mg/L	28-MAY-15	28-MAY-15	R3197673
Zinc (Zn)-Dissolved	<0.020		0.020	mg/L	28-MAY-15	28-MAY-15	R3197673
Zirconium (Zr)-Dissolved	0.0428		0.0010	mg/L	28-MAY-15	28-MAY-15	R3197673
Nitrogen Total							
Nitrate in Water by IC							
Nitrate (as N)	43		10	mg/L		27-MAY-15	R3197146
Nitrate+Nitrite							
Nitrate and Nitrite as N	49		11	mg/L		28-MAY-15	

Sample Details/Parameters	Result	Qualifier*	D.L.	Units	Extracted	Analyzed	Batch
L1616805-1 WEST REFLEX LAKE Sampled By: CLIENT on 21-MAY-15 @ 11:30 Matrix:							
Nitrite in Water by IC							
Nitrite (as N)	5.6		5.0	mg/L		27-MAY-15	R3197146
Total Kjeldahl Nitrogen							
Total Kjeldahl Nitrogen	8.14	DLA	0.40	mg/L	28-MAY-15	02-JUN-15	R3200087
Total Nitrogen Calculated							
Total Nitrogen	57		11	mg/L		02-JUN-15	

Appendix B: Location and brief descriptions of samples collected from West Reflex Lake. Sample IDs correspond to numbers on Fig. 4.1.

Sample ID	Sample type	Latitude and longitude	Description of location	Dimensions (cm)	Morphology	Colour	Structures	Internal texture
WR-01	Isolated pinnacle	52.6558 N, 110.0139 W	Beside groundwater-fed inflow channel	18x13x14	Dome-shaped, symmetrical through horizontal plane	Pinkish grey (5YR 8/1), light olive grey (5Y 6/1), medium dark grey (N4)	Concentric, cm-scale layers apparent looking at bottom of sample. Layering cannot be seen from top of sample. Porosity is high between layers	Disorganized, filamentous Casts of plant material Variable porosity (higher on inside, lower on outside)
WR-03	Isolated pinnacle	52.6548 N, 110.0115 W	On sediment surface	13x16x6	Flat, tabular	Pinkish grey (5YR 8/1), greyish orange (10 YR 7/4), dark grey (N3)	Top surface contains casts of plant stems 3-4 mm diameter, encrusted with nodular carbonate Nodular carbonate coated with cream coloured carbonate	Porous, disorganized filamentous texture Filaments are hollow

Sample ID	Sample type	Latitude and longitude	Description of location	Dimensions (cm)	Morphology	Colour	Structures	Internal texture
WR-04	Laminated coating	52.6554 N, 110.0113 W	Near lake shoreline	13x8x6	Thin (<2 mm) crust on intrusive igneous cobble	Yellowish grey (5 Y 8/1)	1 or two laminations in carbonate (distinguished by colour), with nodular surface	Laminated
WR-05	Efflorescent crust on sediment	52.6568 N, 110.0156 W	On beach near campground	1X0.5x0.5	Thin, white halite and mirabilite crust on beach sand	White (N9)	Nodular	-
WR-06	Beach sand	52.6568 N, 110.0156 W	On beach near campground	-	Beach sand	Dark grey when wet	Laminated to thin bedded	Medium sand, subrounded, well sorted
WR-07	Beachrock	52.6548 N, 110.0115 W	On sediment surface	12x20x5	Flat, tabular	Very pale orange (10 YR 8/2), olive grey (5 Y 4/1), dark grey (N3)	Weak, discontinuous laminations, 1-2 mm thick, porosity in between	Dense, dark coloured, nodular carbonate coats surface and forms layers Porosity between layers only

Sample ID	Sample type	Latitude and longitude	Description of location	Dimensions (cm)	Morphology	Colour	Structures	Internal texture
WR-08	Bioherm	52.6541 N, 109.9994 W	Embedded in sediment in growth position	25x20x20	Shallow, upside down cone “root”, with 5 cm diameter columns protruding from top	Very pale orange (10 YR 8/2) to yellowish grey (5 Y 8/1)	Pinnacles growing out of wide, flat base Faint, discontinuous, mm-scale laminations Base made up of a number of planar cemented surfaces separated by porosity	Variable from nodular to filamentous Centre of pinnacles rubbly and structureless
WR-09	Bioherm	52.6700 N, 109.9899 W	On sediment surface	6x4x8	Segment of single pinnacle	White (N9) to very pale orange (10 YR 8/2)	Single pinnacle Concentric, 2-4 mm laminations Porosity highest in centre of pinnacle	Branching filamentous Coating on filaments from 0.1 to 1 mm diameter
WR-10	Bioherm	52.6730 N, 109.996 W	On sediment surface	10x8x6	Massive	Yellowish grey (5 Y 8/1), medium grey (N5), patches of dark yellowish orange (10 YR 6/6)	Massive	Branching filamentous, some planar, irregular sheets of carbonate (appears to have been underneath something, looks like inside of nodules)

Sample ID	Sample type	Latitude and longitude	Description of location	Dimensions (cm)	Morphology	Colour	Structures	Internal texture
WR-11	Bioherm	52.6729 N, 109.9972 W	Found on its side, not in situ	9x6x20	Segment of pinnacle	Pinkish grey (5 YR 8/1), light brown (5YR 5/6)	Possible very weak laminations, sub cm scale	Branching filamentous
WR-12	Bioherm	52.6719 N, 110.0022 W	On sediment surface	16x12x12	Very irregular, some horizontal clusters of tube-like features 3 mm diameter and ~7 cm long	Dark grey (N3), very pale orange (10 YR 8/2), greyish orange (10 YR 7/4)	Isolated column coated with laminated carbonate, several planar layers of carbonate at different angles	Nodular, branching filamentous, and coated plant material Very irregular
WR-13	Beachrock	52.6719 N, 110.0022 W	Sandstone underlying tufa	12x7x8	Fragment of sandstone broken from under tufa, irregular layering, contains tufa	Dusky yellow (5 Y 6/4), light olive grey (5 Y 5/2), yellowish grey (5 Y 8/1)	Nascent pinnacle growing from bottom layer of sandstone, other sandstone laminae terminate at pinnacle edge Layers 2 mm to 2 cm thick, irregular, discontinuous.	Nodular carbonate between layers Pinnacle has branching filamentous internal texture and possible 1-2 mm thick dense coating Exterior of sandstone coated in creamy, dense carbonate with nodular texture

Sample ID	Sample type	Latitude and longitude	Description of location	Dimensions (cm)	Morphology	Colour	Structures	Internal texture
WR-14	Bioherm	52.6728 N, 110.0031 W	On sediment surface	6x3x5	Dense carbonate coating on tufa	Coating: Pale yellowish brown (10 YR 6/2) Tufa: Greyish orange (10 YR 7/4)	Nodular surface	4-6 laminations in outer coating Tufa is branching filamentous
WR-15	Bioherm	52.6728 N, 110.0031 W	On sediment surface	8x6x4	Dense carbonate coating on tufa pinnacle	Pale yellowish brown (10 YR 6/2), dark yellowish orange (10 YR 6/6)	Pinnacles, faint laminations, sub cm scale	Porous, irregular coatings on filaments Dark, less porous, convex laminations look like previous tops of pinnacles

Sample ID	Sample type	Latitude and longitude	Description of location	Dimensions (cm)	Morphology	Colour	Structures	Internal texture
WR-16	Bioherm	52.6715 N, 110.0169 W	Cluster of pinnacles	9x7x5	Segment of pinnacle: top is broken and weathered, bottom is broken and fresh Cream coloured, dense nodular crust, covered by thin white coating	Pale yellowish brown (outer crust – 10 YR 6/2), white (thin coating -N9), grayish orange (interior – 10 YR 7/4)	Weak, irregular concentric laminations,	Dominantly shrubby, some filamentous, possible bladed crystals (ikaite pseudomorphs?) in centre, external coating is finely laminated
WR-17	Isolated pinnacle	52.6713 N, 110.0174 W	In place, upright pinnacle	13x8x5	Rubbly, irregular texture, does not really look like pinnacle	Pale yellowish brown (10 YR 6/2) to very pale orange (10 YR 8/2)	Structureless	Porous, rubbly , some branching filamentous

Sample ID	Sample type	Latitude and longitude	Description of location	Dimensions (cm)	Morphology	Colour	Structures	Internal texture
WR-18	Bioherm	52.6708 N, 110.0224 W	Pinnacle from cluster	8x4x4	Dense, translucent orange nodular carbonate, white nodular carbonate	Greyish orange (10 YR 7/4), very pale orange (10 YR 8/2), pale yellowish brown (10 YR 6/2)	Laminations ~1 cm thick	Laminations have white, friable, less porous 2-3 mm thick base and darker, nodular coated filamentous layer 1 cm thick
WR-19	Bioherm	52.6712 N, 110.0228 W	Two pieces from near base of large pinnacle cluster	11x7x2 and 6x4x2	Flat pieces	Yellowish grey (5 Y 8/1)	1st piece: Piece appears to be one contorted layer 2nd piece: two layers, each topped by dense, nodular crust	1st piece: translucent, nodular crust and coated filaments (one 3 cm long and 1.5 mm diam) Filaments arranged in network-like structure 2nd piece: translucent, nodular coated filaments, casts of bubbles

Sample ID	Sample type	Latitude and longitude	Description of location	Dimensions (cm)	Morphology	Colour	Structures	Internal texture
WR-20	Bioherm	52.6719 N, 109.9928 W	Piece from top of large pinnacle cluster	11x9x6	Segment of pinnacle	Moderate yellowish brown (10 YR 5/4), very pale orange (10 YR 8/2), yellowish grey (5 Y 8/1)	Possible, very weak, irregular laminations	Friable, branching filamentous Nodular coating has laminations
WR-21	Isolated pinnacle	52.6606 N, 110.0254 W	Upright pinnacle coated with salt, wet when collected	17x12x5	Domed	Dark yellowish orange (10 YR 6/6), pale yellowish brown (10 YR 6/2), white (N9)	Irregular layering defined by porosity	Branching filamentous

Appendix C: Appearance, distribution, and relationships of microscale components in West Reflex Lake shoreline carbonates.

Component	Description	Distribution within shoreline carbonates	Intergrading components
Irregular micrite	Dark grey, irregularly distributed micrite. Arranged into >100 μm patches with interparticle porosity between.	Occurs within pore spaces. Often has lower porosity near large fenestral pores.	Clotted micrite, sand grains
Clotted micrite	Dark grey micrite, concentrated in clots 50-80 μm diameter. Clots are elongate, with no lamination or zonation. Clots are often clustered together. Occasionally contains molds of coarse filaments.	Surface and interior; makes up a large proportion of the microbialite. Occurs in plant molds as geopetal fill.	Irregular micrite, coarse filaments, pellets, sand grains
Pellets	Dark grey micrite, with no internal structure. Peloids are ~300 μm long. Brine shrimp fecal pellets.	Interior of thrombolites; uncommon.	Clotted micrite, coarse filaments
Micrite crust	Dense, micritic crust with few pores. Forms a smooth coating over irregular, porous material beneath. Coarsens outward to microspar. Fills in porosity in underlying material.	Surface, rarely occurs as within microbialites, assumed to be former exposure surface.	Evaporite pseudomorphs, clotted micrite
Fine filaments	Composed of organic matter. Filaments are 0.5 to 8.0 μm in diameter and are round and smooth or flat.	Draped over exterior of carbonate cements and other microscale components.	All
Coarse filaments	Central pores of molds are 20-40 μm diameter. In place, organic matter is preserved. Filaments up to 3 mm long. Commonly micrite coated. Micrite coating is even and up to 20 μm thick. Filaments are sometimes branching.	Surface and interior of thrombolites; makes up a large proportion of the interior where present.	Clotted micrite, pellets, irregular micrite

Component	Description	Distribution within shoreline carbonates	Intergrading components
Non-filamentous microbial components	Cell molds, preserved cells, and desiccated biofilm are observed in pore space using scanning electron microscopy.	Fenestral and interparticle porosity in beachrock and thrombolites.	Clotted micrite, sand grains
Plant molds	200-400 μm diameter round or oval structures, often coated by micrite and then with cement. Form large pores.	Surface and interior; scattered through thrombolites and on surface of laminated coatings.	Evaporite pseudomorphs, clotted micrite, coarse filaments
Evaporite pseudomorphs	Elongate, with lozenge-shaped cross section. Often oriented in parallel clusters. Hollow and filled with clear carbonate crystals or are solid and composed of micrite to microspar.	Interior of thrombolites; in limited areas which tend to be composed almost entirely of evaporite pseudomorphs.	Irregular micrite, clotted micrite, plant molds
Carbonate rods	Bladed carbonate crystals arranged with parallel c-axes into rods widest at the midsection. Length 7-29 μm, width 4-15 μm.	Interior of thrombolites, forms ledges.	Evaporite pseudomorphs
Sand grains	Fine to medium sand, subrounded to rounded, well sorted. 40-60% quartz, 20-40% lithic fragments, 10-20% feldspar.	Beachrock, thrombolites, and rarely in laminated coatings	Irregular micrite, pellets, clotted micrite
Chert	Replaces evaporite pseudomorphs or irregular micrite. Beige in plain polarized light and contains scattered, dark brown inclusions.	Interior just underneath crust; occur in thrombolites, typically near the exterior.	Coarse filaments, irregular micrite, evaporite pseudomorphs

Appendix D: Description of layers in laminated crust on WR-15.

	Layer	Thickness (mm)	Texture	Porosity	Contact with overlying layer	Notes
1	Porous	20	Porous framework of clotted micrite and evaporite pseudomorphs	30%	Grey-brown micrite draped over surface of clotted micrite and evaporite pseudomorphs	
2	Grey-brown micrite	0.175-0.350	Weakly laminated	<5%	Separated from overlying micritic layer by porosity or porous, clotted micrite	Absent in places
3	Porous, clotted micrite	8	Porous framework of plant molds and clotted micrite	20-40%	Micrite draped over porous surface	Occurs only on one side of the pinnacle
4	Micrite	0.450-0.900	Weakly laminated, develops micro-columnar structure around filaments or other detritus	<5%	In places, separated from overlying layer by fenestral porosity	
5	Microspar	0.04-3.00	Laminated, defined by increase in proportion of micrite	20-40%, fenestral, large pores crossing lamination at tops of columns	Overlying layer adheres well to microspar	Thinnest between columns, thickest at apex of column
6	Micrite	0.01-0.425	Grey brown micrite with darker lamination at top	<5%	Bumpy/irregular upper surface, adheres well to microspar	Not present on the inward-facing side of the pinnacle
7	Microspar	0-	Weakly laminated	20-40%, large pores	Overlying layer adheres well	Not present on

	Layer	Thickness (mm)	Texture	Porosity	Contact with overlying layer	Notes
		1.875		cross cutting lamination at tops of columns	The top of this layer is weathered away in places, along with overlying material	the inward-facing side of the pinnacle; Thinnest between columns, thickest at apex of column
8	Finely laminated micrite	0-0.320	Thin, homogeneous, bumpy later of micrite, with red-brown and grey-brown laminated micrite above	<5%	Top of layer is weathered away over most of the pinnacle, only remains in depressions on surface, next layer is deposited on truncated ends	Not present on the inward-facing side of the pinnacle
9	Micrite	0-2.0	Contains round molds (possible brine shrimp eggs) and sand grains, overlain by finely laminated layer	5-10% interparticle, up to 20% moldic (eggs)	Coated with finely laminated micrite	
9b	Finely laminated microspar		Finely laminated microspar layer at top of layer 9	<5 %	Coated by massive micrite	
10	Massive micrite	0.2	Meniscus coating, grey micrite, smooth, thickest between columns	<5%	-	Not present on inward-facing side of pinnacle

Appendix E: Semi-quantitative estimates of mineral proportions based on X-ray refraction data. All components have been normalized to 100%.

Sample ID	Comments	Quartz (%)	Plagioclase (%)	Calcite (%)	HMC (%)	Proto-dolomite (%)	Dolomite (%)	Thenardite (%)	Aragonite (%)	Trona (%)	Halite (%)	Mol% Mg in Calcite	Mol% Mg in HMC	Mol% Ca in Proto-dolomite	Mol% Ca in Dolomite
WR-01-04	Exterior crust of microbialite and some filamentous material	1.35	0.00	6.14	0.00	0.00	0.00	0.00	92.50	0.00	0.00	3.26	-	-	-
WR-03-01	Nodular exterior crust on microbialite estimated dol/protodol peak	22.27	0.00	0.00	0.00	9.15	0.00	0.00	68.57	0.00	0.00	-	-	55.52	-
WR-03-02	Friable carbonate material at base of microbialite	8.47	0.00	0.00	23.48	3.61	4.26	0.00	60.18	0.00	0.00		8.45	61.01	51.85
WR-04-01	Bulk crust on cobble	3.38	0.00	0.00	0.00	3.11	0.00	0.00	93.51	0.00	0.00	-	-	55.27	-
WR-05-01	Efflorescent crust on beach sand Tentative Trona (sodium carbonate)	7.31	0.00	0.00	0.00	0.00	0.00	15.47	0.00	15.36	61.86	-	-	-	-
WR-06-01	Beach sand	91.10	7.69	1.22	0.00	0.00	0.00	0.00	0.00	0.00	0.00	2.39	-	-	-
WR-07-01	Nodular exterior crust on beachrock	9.62	0.00	2.87	0.00	19.49	0.00	0.00	68.02	0.00	0.00	0.28	-	56.50	-
WR-07-02	Friable, structureless material at base of beachrock	57.29	0.00	0.00	18.58	0.00	0.00	0.00	24.13	0.00	0.00	-	5.00	-	-
WR-08-01	Subhorizontal ledges at base of microbialite small dol/protodol (not quantified)	0.00	0.00	0.00	19.16	0.00	0.00	0.00	80.84	0.00	0.00	-	4.60	-	-
WR-08-02	Exterior crust from top of pinnacle in microbialite estimated dol/protodol peak	2.45	0.00	0.84	0.00	6.35	0.00	0.00	88.23	0.00	0.00	2.53	-	55.52	-
WR-09-01	Bulk sample of microbialite	0.00	0.00	19.21	0.00	0.00	0.00	0.00	80.79	0.00	0.00	1.86	-	-	-

Sample ID	Comments	Quartz (%)	Plagioclase (%)	Calcite (%)	HMC (%)	Proto-dolomite (%)	Dolomite (%)	Thenardite (%)	Aragonite (%)	Trona (%)	Halite (%)	Mol% Mg in Calcite	Mol% Mg in HMC	Mol% Ca in Proto-dolomite	Mol% Ca in Dolomite
	small dol/protodol (not quantified)														
WR-09-04	Questionable small dol/protodol	4.49	0.00	10.34	0.00	0.00	0.00	0.00	85.17	0.00	0.00	1.82	-	-	-
WR-10-01	Bulk of friable microbialite small dol/protodol (not quantified)	5.27	0.00	15.71	0.00	0.00	0.00	0.00	79.02	0.00	0.00	1.99	-	-	-
WR-10-03	Questionable k-feldspar	34.01	5.23	53.13	0.00	0.00	0.00	0.00	7.62	0.00	0.00	3.33	-	-	-
WR-11-01	Exterior of pinnacle	3.02	0.00	52.92	0.00	0.00	0.00	0.00	44.06	0.00	0.00	1.92	-	-	-
WR-12-01	Black, rubbly exterior of microbialite	3.34	0.00	0.00	10.17	0.00	0.00	0.00	86.49	0.00	0.00	-	4.67	-	-
WR-12-02	Bulk of beachrock small dol/protodol (not quantified)	9.51	0.00	29.90	0.00	0.00	0.00	0.00	60.59	0.00	0.00	1.82	-	-	-
WR-13-01	small dol/protodol (not quantified)	75.67	0.00	0.00	9.43	0.00	5.00	0.00	9.90	0.00	0.00	-	3.63	-	51.12
WR-14-01	Bulk of pinnacle poor calcite peak	1.00	0.00	2.24	0.00	7.50	0.00	0.00	89.26	0.00	0.00	0.14	-	56.71	-
WR-14-05	Exterior crust of pinnacle Good protodol	3.02	0.00	0.00	0.00	20.66	0.00	0.00	76.33	0.00	0.00	-	-	64.03	-
WR-15-03	Laminated crust on exterior of pinnacle	9.82	0.00	0.00	0.00	3.28	0.00	0.00	86.90	0.00	0.00	-	-	65.47	-
WR-15-04	Friable, white external crust on pinnacle	6.27	0.00	0.00	2.34	6.78	0.00	0.00	84.62	0.00	0.00	-	4.43	64.03	-
WR-15-05	estimated dol/protodol peak	0.00	0.00	0.00	0.00	3.42	0.00	0.00	96.58	0.00	0.00	-	-	55.52	-
WR-18-07	Bulk sample of microbialite	2.13	0.00	0.00	5.93	0.00	0.00	0.00	65.90	0.00	26.03	-	3.77	-	-
WR-19-01	Bulk sample of microbialite Questionable small dol/protodol	0.00	0.00	0.00	23.45	0.00	0.00	0.00	76.55	0.00	0.00	-	3.93	-	-
WR-20-02	Orange, opaque nodular crust on pinnacle	29.09	0.00	0.00	0.65	0.00	1.07	0.00	65.21	0.00	3.98	-	3.66	-	51.85
WR-20-04	Bulk sample of microbialite Questionable small	2.11	0.00	0.00	3.27	0.00	0.00	0.00	94.62	0.00	0.00	-	3.50	-	-

Sample ID	Comments	Quartz (%)	Plagioclase (%)	Calcite (%)	HMC (%)	Proto-dolomite (%)	Dolomite (%)	Thenardite (%)	Aragonite (%)	Trona (%)	Halite (%)	Mol% Mg in Calcite	Mol% Mg in HMC	Mol% Ca in Proto-dolomite	Mol% Ca in Dolomite
	dol/protodol; poor Calcite peak														
WR-21-03	Fresh, orange carbonate estimated small dol/protodol	0.00	0.00	0.00	1.37	0.00	0.64	0.00	98.00	0.00	0.00	-	3.63	-	51.85

Appendix F: Weight percentages of Ca, Mg, Sr, Mn, and Fe from microprobe analysis of shoreline carbonates from West Reflex Lake.

Spot ID	Mineralogy	Comment	Mg (wt%)	Ca (wt%)	Mn (wt%)	Fe (wt%)	Sr (wt%)
WR-01-Spot1-01	Aragonite	Micrite in an isolated pinnacle	0.17	39.89	<0.04	0	0.13
WR-01-Spot1-02	Aragonite	Exterior crust on an isolated pinnacle. Spot1-02 to Spot1-05 are from the interior to exterior of the crust.	0.36	39.52	<0.04	0.05	0.27
WR-01-Spot1-03	Aragonite	Exterior crust on an isolated pinnacle. Spot1-02 to Spot1-05 are from the interior to exterior of the crust.	0.13	41.62	<0.04	0.01	0.27
WR-01-Spot1-04	Aragonite	Exterior crust on an isolated pinnacle. Spot1-02 to Spot1-05 are from the interior to exterior of the crust.	0.12	42.79	<0.04	0	0.27
WR-01-Spot1-05	High-Mg calcite	Exterior crust on an isolated pinnacle. Spot1-02 to Spot1-05 are from the interior to exterior of the crust.	10.23	26.58	0.22	0.1	0.09
WR-01-Spot2-01	Calcite	Colourless botryoidal calcite cement in an isolated pinnacle	0.18	41.28	<0.04	0	0.09
WR-01-Spot2-02	Aragonite	Isopachous aragonite cement in an isolated pinnacle. Spot2-02 to Spot1-09 are from the interior to exterior of the cement.	0.14	40.08	<0.04	0.01	0.35
WR-01-Spot2-03	Aragonite	Isopachous aragonite cement in an isolated pinnacle. Spot2-02 to Spot1-09 are from the interior to exterior of the cement.	1.16	40.05	0.18	0.09	0.18

Spot ID	Mineralogy	Comment	Mg (wt%)	Ca (wt%)	Mn (wt%)	Fe (wt%)	Sr (wt%)
WR-01-Spot2-04	Aragonite	Isopachous aragonite cement in an isolated pinnacle. Spot2-02 to Spot1-09 are from the interior to exterior of the cement.	2.08	36.73	0.26	<0.05	0.08
WR-01-Spot2-05	Aragonite	Isopachous aragonite cement in an isolated pinnacle. Spot2-02 to Spot1-09 are from the interior to exterior of the cement.	0.04	41.3	<0.04	<0.05	0.2
WR-01-Spot2-06	Aragonite	Isopachous aragonite cement in an isolated pinnacle. Spot2-02 to Spot1-09 are from the interior to exterior of the cement.	0.04	39.06	<0.04	<0.05	0.27
WR-01-Spot2-07	Aragonite	Isopachous aragonite cement in an isolated pinnacle. Spot2-02 to Spot1-09 are from the interior to exterior of the cement.	1.92	35.39	0.24	0.06	0.11
WR-01-Spot2-08	Aragonite	Isopachous aragonite cement in an isolated pinnacle. Spot2-02 to Spot1-09 are from the interior to exterior of the cement.	0.08	39.9	<0.04	<0.05	0.26
WR-01-Spot2-09	Aragonite	Isopachous aragonite cement in an isolated pinnacle. Spot2-02 to Spot1-09 are from the interior to exterior of the cement.	0.05	36.98	<0.04	<0.05	0.27
WR-01-Spot2-010	Aragonite	Microcrystalline aragonite cement in isolated pinnacle	1.02	37.48	<0.04	<0.05	0.3
WR-01-Spot3-01	Aragonite	Coarsely laminated botryoidal aragonite cement in isolated pinnacle	0.16	39	0.07	<0.05	0.26
WR-01-Spot3-02	Aragonite	Coarsely laminated botryoidal aragonite cement in isolated pinnacle	0.08	37.98	0.06	<0.05	0.34
WR-01-Spot3-03	Aragonite	Coarsely laminated botryoidal aragonite cement in isolated pinnacle	0.15	40.64	<0.04	<0.05	0.32

Spot ID	Mineralogy	Comment	Mg (wt%)	Ca (wt%)	Mn (wt%)	Fe (wt%)	Sr (wt%)
WR-01-Spot3-04	Aragonite	Coarsely laminated botryoidal aragonite cement in isolated pinnacle	0.13	38.7	<0.04	<0.05	0.3
WR-01-Spot3-05	Aragonite	Coarsely laminated botryoidal aragonite cement in isolated pinnacle	0.08	38.34	0.06	<0.05	0.24
WR-01-Spot3-06	Aragonite	Coarsely laminated botryoidal aragonite cement in isolated pinnacle	0.04	38.27	0.05	<0.05	0.34
WR-01-Spot3-07	Calcite	Colourless botryoidal cement in an isolated pinnacle	0.55	36.38	0.64	0.21	0.09
WR-01-Spot4-01	Aragonite	Microcrystalline aragonite cement in isolated pinnacle	1.21	36.85	<0.04	0.07	0.34
WR-01-Spot4-02	Calcite	Finely laminated botryoidal calcite in isolated pinnacle	0.13	37.97	<0.04	<0.05	0.26
WR-01-Spot4-03	Calcite	Finely laminated botryoidal calcite in isolated pinnacle	0.09	34.53	<0.04	<0.05	0.26
WR-01-Spot4-04	Calcite	Finely laminated botryoidal calcite in isolated pinnacle	0.04	37.22	0.06	<0.05	0.28
WR-01-Spot4-05	Calcite	Finely laminated botryoidal calcite in isolated pinnacle	0.03	30.78	<0.04	<0.05	0.27
WR-01-Spot4-06	Calcite	Finely laminated botryoidal calcite in isolated pinnacle	0.14	28.77	<0.04	<0.05	0.33
WR-01-Spot4-07	Calcite	Finely laminated botryoidal calcite in isolated pinnacle	0.07	31.33	<0.04	<0.05	0.23
WR-03-Spot1-01	Aragonite	Clotted micrite in isolated pinnacle	1.3	39.98	0.59	0.42	0.08
WR-03-Spot1-02	Aragonite	Clotted micrite in isolated pinnacle	0.29	38.01	0.17	0.11	0.32

Spot ID	Mineralogy	Comment	Mg (wt%)	Ca (wt%)	Mn (wt%)	Fe (wt%)	Sr (wt%)
WR-03-Spot2-01	Aragonite	Microcrystalline aragonite cement in isolated pinnacle	1.15	39.27	0.38	0.26	<0.06
WR-03-Spot2-02	Calcite	Dogtooth cement in isolated pinnacle	1.24	33.39	<0.04	0.25	0.08
WR-03-Spot2-04	Calcite	Dogtooth cement in isolated pinnacle	1.97	38.26	0.18	0.84	<0.06
WR-03-Spot2-03	Aragonite	Microcrystalline aragonite cement in isolated pinnacle	1.72	36.59	<0.04	0.09	0.24
WR-03-Spot3-01	Aragonite	Red-brown botryoidal aragonite in isolated pinnacle	0.15	37.96	<0.04	<0.05	0.41
WR-03-Spot3-02	Aragonite	Red-brown botryoidal aragonite in isolated pinnacle	0.1	39.25	<0.04	<0.05	0.39
WR-03-Spot3-03	Aragonite	Red-brown botryoidal aragonite in isolated pinnacle	0.14	39.78	<0.04	<0.05	0.38
WR-03-Spot3-04	Aragonite	Red-brown botryoidal aragonite in isolated pinnacle	0.18	38.29	0.05	<0.05	0.37
WR-03-Spot3-05	Aragonite	Red-brown botryoidal aragonite in isolated pinnacle	0.2	38.53	<0.04	<0.05	0.34
WR-03-Spot3-06	Aragonite	Red-brown botryoidal aragonite in isolated pinnacle	0.18	39.91	<0.04	<0.05	0.32
WR-03-Spot4-01	Aragonite	Exterior crust on an isolated pinnacle. Spot4-01 to Spot4-04 are from the interior to exterior of the crust.	0.19	38.54	<0.04	<0.05	0.35
WR-03-Spot4-03	Aragonite	Exterior crust on an isolated pinnacle. Spot4-01 to Spot4-04 are from the interior to exterior of the crust.	0.17	40.78	<0.04	0.79	0.11

Spot ID	Mineralogy	Comment	Mg (wt%)	Ca (wt%)	Mn (wt%)	Fe (wt%)	Sr (wt%)
WR-03-Spot4-04	Aragonite	Exterior crust on an isolated pinnacle. Spot4-01 to Spot4-04 are from the interior to exterior of the crust.	0.11	40.34	<0.04	0.36	0.26
WR-08-Spot1-01	Calcite	Colourless botryoidal cement in a bioherm	0.15	39.12	<0.04	<0.05	0.45
WR-08-Spot1-02	Aragonite	Microcrystalline aragonite cement in bioherm	0.17	39.33	<0.04	<0.05	0.43
WR-08-Spot1-03	Aragonite	Micrite in bioherm	0.06	37.79	<0.04	<0.05	0.38
WR-08-Spot1-04	Aragonite	Microcrystalline aragonite cement in bioherm	0.06	37.72	<0.04	<0.05	0.32
WR-08-Spot1-05	Aragonite	Micrite in bioherm	0.13	38.37	<0.04	<0.05	0.46
WR-08-Spot1-06	Aragonite	Microcrystalline aragonite cement in bioherm	0.15	40.32	<0.04	<0.05	0.4
WR-08-Spot1-07	Calcite	Colourless botryoidal cement in a bioherm	0.16	38.83	<0.04	<0.05	0.44
WR-08-Spot1-08	Aragonite	Microcrystalline aragonite cement in bioherm	0.13	40.96	<0.04	0.09	0.31
WR-08-Spot2-01	Aragonite	Microcrystalline aragonite cement in bioherm	0.05	34.6	<0.04	<0.05	0.32
WR-08-Spot2-02	Aragonite	Microcrystalline aragonite cement in bioherm	0.12	41.22	<0.04	<0.05	0.34
WR-08-Spot2-03	Aragonite	Microcrystalline aragonite cement in bioherm	0.14	38.84	<0.04	0.06	0.38
WR-08-Spot2-04	Aragonite	Microcrystalline aragonite cement in bioherm	0.94	40.3	<0.04	0.06	0.11
WR-08-Spot2-05	Aragonite	Microcrystalline aragonite cement in bioherm	0.22	39.2	<0.04	<0.05	0.37
WR-08-Spot2-06	Calcite	Colourless botryoidal cement in a bioherm	0.12	39.57	<0.04	<0.05	0.36
WR-08-Spot2-07	Calcite	Colourless botryoidal cement in a bioherm	1.4	37.25	<0.04	0.11	0.07
WR-08-Spot2-08	Calcite	Colourless botryoidal cement in a bioherm	1.14	37.82	<0.04	0.08	0.11
WR-15-01	Aragonite	Spots across laminated crust shown in Figure 5.1	0.04	43.17	<0.04	0.07	0.36
WR-15-02	Aragonite	Spots across laminated crust shown in Figure 5.1	0.21	40.39	<0.04	<0.05	0.43
WR-15-03	Aragonite	Spots across laminated crust shown in Figure 5.1	<0.01	28.82	<0.04	<0.05	0.12

Spot ID	Mineralogy	Comment	Mg (wt%)	Ca (wt%)	Mn (wt%)	Fe (wt%)	Sr (wt%)
WR-15-04	Aragonite	Spots across laminated crust shown in Figure 5.1	0.15	5.01	<0.04	<0.05	<0.06
WR-15-05	Aragonite	Spots across laminated crust shown in Figure 5.1	0.16	42.77	<0.04	0.26	0.23
WR-15-06	Aragonite	Spots across laminated crust shown in Figure 5.1	0.18	42.62	<0.04	0.07	0.21
WR-15-07	Aragonite	Spots across laminated crust shown in Figure 5.1	0.11	40.6	<0.04	<0.05	0.39
WR-15-08	Aragonite	Spots across laminated crust shown in Figure 5.1	0.47	38.65	<0.04	2.51	0.22
WR-15-09	Aragonite	Spots across laminated crust shown in Figure 5.1	0.18	41.7	<0.04	0.15	0.25
WR-15-010	Aragonite	Spots across laminated crust shown in Figure 5.1	0.19	42.49	<0.04	0.09	0.25
WR-15-011	Aragonite	Spots across laminated crust shown in Figure 5.1	0.21	42.5	<0.04	0.08	0.37
WR-15-012	Aragonite	Spots across laminated crust shown in Figure 5.1	0.21	42.4	<0.04	<0.05	0.34
WR-15-013	Aragonite	Spots across laminated crust shown in Figure 5.1	0.1	43.07	<0.04	<0.05	0.31
WR-15-014	Aragonite	Spots across laminated crust shown in Figure 5.1	9.53	29.9	<0.04	0.06	<0.06
WR-15-015	Aragonite	Spots across laminated crust shown in Figure 5.1	0.1	44.23	<0.04	0.16	0.19
WR-15-016	Aragonite	Spots across laminated crust shown in Figure 5.1	9.86	28.24	0.05	0.21	<0.06
WR-15-017	Aragonite	Spots across laminated crust shown in Figure 5.1	0.09	43.58	<0.04	<0.05	<0.06
WR-15-018	Aragonite	Spots across laminated crust shown in Figure 5.1	9.91	29.02	<0.04	<0.05	<0.06
WR-15-019	Aragonite	Spots across laminated crust shown in Figure 5.1	0.14	43.73	<0.04	0.06	0.17
WR-15-020	Aragonite	Spots across laminated crust shown in Figure 5.1	0.07	43.98	<0.04	0.01	<0.06
WR-15-021	Aragonite	Spots across laminated crust shown in Figure 5.1	9.82	28.28	<0.04	0.15	<0.06
WR-15-022	Aragonite	Spots across laminated crust shown in Figure 5.1	0.09	42.63	<0.04	0.12	0.12
WR-15-023	Aragonite	Spots across laminated crust shown in Figure 5.1	0.09	43.7	<0.04	<0.05	0.12
WR-15-024	Aragonite	Spots across laminated crust shown in Figure 5.1	0.09	43.95	<0.04	<0.05	0.11
WR-15-025	Aragonite	Spots across laminated crust shown in Figure 5.1	0.08	43.37	<0.04	<0.05	0.07

Spot ID	Mineralogy	Comment	Mg (wt%)	Ca (wt%)	Mn (wt%)	Fe (wt%)	Sr (wt%)
WR-15-026	Aragonite	Spots across laminated crust shown in Figure 5.1	0.08	43.28	<0.04	<0.05	0.19
WR-15-027	Aragonite	Spots across laminated crust shown in Figure 5.1	0.11	43	<0.04	<0.05	0.34
WR-15-028	Aragonite	Spots across laminated crust shown in Figure 5.1	0.16	40.59	<0.04	0.07	0.28
WR-15-029	Aragonite	Spots across laminated crust shown in Figure 5.1	0.15	42.67	<0.04	<0.05	<0.06
WR-15-030	Aragonite	Spots across laminated crust shown in Figure 5.1	0.13	43.77	<0.04	<0.05	<0.06
WR-15-031	Aragonite	Spots across laminated crust shown in Figure 5.1	0.12	43.52	<0.04	<0.05	<0.06
WR-15-032	Aragonite	Spots across laminated crust shown in Figure 5.1	0.12	37.05	<0.04	<0.05	<0.06
WR-15-033	Aragonite	Spots across laminated crust shown in Figure 5.1	0.11	43.18	<0.04	<0.05	<0.06
WR-15-034	Aragonite	Spots across laminated crust shown in Figure 5.1	0.11	42.62	<0.04	<0.05	<0.06
WR-15-035	Aragonite	Spots across laminated crust shown in Figure 5.1	0.11	42.94	<0.04	<0.05	0.16
WR-15-036	Aragonite	Spots across laminated crust shown in Figure 5.1	0.23	41.96	<0.04	0.34	0.78
WR-15-037	Aragonite	Spots across laminated crust shown in Figure 5.1	0.76	41.74	<0.04	0.62	0.73
WR-15-038	Aragonite	Spots across laminated crust shown in Figure 5.1	0.06	41.23	0.09	0.11	<0.06
WR-15-039	Aragonite	Spots across laminated crust shown in Figure 5.1	10.89	23.34	0.37	0.19	<0.06
WR-15-040	Aragonite	Spots across laminated crust shown in Figure 5.1	0.09	41.26	0.26	0.25	<0.06
WR-15-041	Aragonite	Spots across laminated crust shown in Figure 5.1	0.19	42.83	<0.04	<0.05	0.37
WR-15-042	Aragonite	Spots across laminated crust shown in Figure 5.1	0.1	42.65	<0.04	<0.05	0.27
WR-15-043	Aragonite	Spots across laminated crust shown in Figure 5.1	0.1	42.35	<0.04	<0.05	0.3
WR-15-044	Aragonite	Spots across laminated crust shown in Figure 5.1	0.82	40.59	<0.04	0.06	0.39
WR-15-045	Aragonite	Spots across laminated crust shown in Figure 5.1	1.18	35.78	<0.04	2.77	0.69
WR-15-046	Aragonite	Spots across laminated crust shown in Figure 5.1	0.12	43.13	<0.04	<0.05	0.19
WR-15-047	Aragonite	Spots across laminated crust shown in Figure 5.1	0.12	43	<0.04	0.06	0.23

Spot ID	Mineralogy	Comment	Mg (wt%)	Ca (wt%)	Mn (wt%)	Fe (wt%)	Sr (wt%)
WR-15-048	Aragonite	Spots across laminated crust shown in Figure 5.1	0.22	43.04	<0.04	<0.05	0.29
WR-15-049	Aragonite	Spots across laminated crust shown in Figure 5.1	0.23	42.76	<0.04	0.17	0.36
WR-15-050	Aragonite	Spots across laminated crust shown in Figure 5.1	0.19	42.57	<0.04	<0.05	0.45
WR-15-051	Aragonite	Spots across laminated crust shown in Figure 5.1	0.1	44.3	<0.04	<0.05	0.21
WR-15-052	Aragonite	Spots across laminated crust shown in Figure 5.1	0.17	42.91	<0.04	0.02	0.28
WR-15-053	Aragonite	Spots across laminated crust shown in Figure 5.1	0.13	42.39	<0.04	<0.05	0.36
WR-15-054	Aragonite	Spots across laminated crust shown in Figure 5.1	10.39	28.54	0.09	0.09	0.14
WR-15-055	Aragonite	Spots across laminated crust shown in Figure 5.1	0.26	43.68	<0.04	0.07	0.51
WR-15-056	Aragonite	Spots across laminated crust shown in Figure 5.1	0.21	43.52	<0.04	<0.05	0.35
WR-15-057	Aragonite	Spots across laminated crust shown in Figure 5.1	0.21	43.07	<0.04	<0.05	0.34
WR-20-Spot1-01	Aragonite	Clotted micrite in bioherm	0.13	39.14	<0.04	<0.05	0.44
WR-20-Spot1-02	Aragonite	Clotted micrite in bioherm	0.12	41.37	<0.04	<0.05	0.26
WR-20-Spot1-03	Aragonite	Exterior crust on a bioherm. Spot1-03 to Spot1-08 are from the interior to exterior of the crust.	0.14	40.57	<0.04	<0.05	0.34
WR-20-Spot1-04	Aragonite	Exterior crust on a bioherm. Spot1-03 to Spot1-08 are from the interior to exterior of the crust.	0.15	39.66	<0.04	<0.05	0.38
WR-20-Spot1-05	Aragonite	Exterior crust on a bioherm. Spot1-03 to Spot1-08 are from the interior to exterior of the crust.	0.11	39.46	<0.04	<0.05	0.45
WR-20-Spot1-06	Aragonite	Exterior crust on a bioherm. Spot1-03 to Spot1-08 are from the interior to exterior of the crust.	0.1	39.44	<0.04	<0.05	0.34
WR-20-Spot1-07	Aragonite	Exterior crust on a bioherm. Spot1-03 to Spot1-08 are from the interior to exterior of the crust.	0.15	38.93	<0.04	<0.05	0.33

Spot ID	Mineralogy	Comment	Mg (wt%)	Ca (wt%)	Mn (wt%)	Fe (wt%)	Sr (wt%)
WR-20-Spot1-08	Aragonite	Exterior crust on a bioherm. Spot1-03 to Spot1-08 are from the interior to exterior of the crust.	0.17	40.94	<0.04	0.15	0.36

Appendix G: Stable carbon and oxygen isotope values from shoreline carbonates of West Reflex Lake.

Client ID	Description	$\delta^{13}C$ (‰, VPDB)	$\delta^{18}O$ (‰, VPDB)
WR-01-01	Black, nodular carbonate inside pores in isolated pinnacle	3.9	-6.2
WR-01-02	Creamy, filamentous carbonate in isolated pinnacle	4.5	-5.8
WR-01-03	Exterior crust on isolated pinnacle	4.1	-6.7
WR-03-01	Creamy nodular coating on isolated pinnacle	3.9	-6.7
WR-03-02	Beige, slightly filamentous carbonate from isolated pinnacle	2.5	-6.6
WR-07-03	Separated layer of black, nodular carbonate	0.1	-11.6
WR-08-01	Sample from bulk of pinnacle from bioherm	0.3	-8.3
WR-09-02	Interior of pinnacle from bioherm, creamy, filamentous	2.9	-8.2
WR-09-03	Next outermost layer of bioherm	3.1	-7.7
WR-10-02	Friable crust on bioherm	4.5	-6.3
WR-10-03	Thrombolitic material from bioherm	2.3	-8.3
WR-11-02	Interior of pinnacle from bioherm, orange, filamentous	2.3	-9.1
WR-11-03	Near exterior of pinnacle from bioherm, orange, filamentous	2.3	-7.7
WR-13-02	Outer crust on beachrock sample	4.3	-6.4
WR-13-03	Isolated pinnacle in beachrock sample	1.6	-7.7
WR-14-02	Innermost layer of dense, nodular crust in bioherm	4.5	-6.7
WR-14-02 dup	Duplicate of WR-14-02	4.6	-6.6
WR-14-03	Middle layer of dense, nodular crust in bioherm	3.4	-6.8
WR-14-03 dup	Duplicate of WR-14-03	3.7	-6.6
WR-14-04	Outermost layer of dense, nodular crust in bioherm	4.0	-6.8
WR-14-04 dup	Duplicate of WR-14-04	4.1	-6.7

Client ID	Description	$\delta^{13}C$ (‰, VPDB)	$\delta^{18}O$ (‰, VPDB)
WR-15-01	Dark orange filamentous interior of bioherm	3.1	-6.6
WR-15-02	Beige, filamentous part of bioherm	2.9	-6.8
WR-15-02 dup	Duplicate of WR-15-02	2.9	-7.0
WR-15-03	Laminated coating	4.8	-6.6
WR-15-03 dup	Duplicate of WR-15-03	4.6	-6.7
WR-15-04	White external crust from bioherm	4.3	-6.6
WR-15-04 dup	Duplicate of WR-15-04	4.1	-6.6
WR-16-01	Beige, inner filamentous pinnacle from bioherm	0.4	-9.4
WR-16-02	Middle filamentous pinnacle from bioherms	1.1	-8.1
WR-16-02 dup	Duplicate of WR-16-02	1.1	-8.2
WR-16-03	Outer, knobby crust on pinnacle from bioherm	1.1	-7.1
WR-16-03 dup	Duplicate of WR-16-03	1.4	-7.0
WR-16-04	Laminated crust on pinnacle from bioherm	3.4	-6.4
WR-16-04 dup	Duplicate of WR-16-04	3.3	-6.4
WR-17-01	Dense, friable carbonate in bioherm	0.9	-8.5
WR-17-01 dup	Duplicate of WR-17-01	0.9	-8.5
WR-17-02	Translucent, filamentous carbonate in bioherm	0.3	-8.8
WR-17-02 dup	Duplicate of WR-17-02	0.0	-9.0
WR-18-01	Bottom chalky layer of bioherm	3.7	-6.7
WR-18-02	Bottom filamentous layer on bioherm	1.7	-6.6
WR-18-03	Top chalky layer on bioherm	1.6	-6.4
WR-18-04	Top filamentous layer on bioherm	2.2	-6.4
WR-18-05	Top opaque, creamy nodular crust on bioherm	4.0	-6.7
WR-18-06	Top translucent, orange nodular crust on bioherm	-2.2	-8.6
WR-19-01	Nodular grey-beige flat piece of bioherm	-0.1	-7.7
WR-20-01	Pinnacle interior from bioherm	-0.1	-8.4
WR-20-02	Orange, opaque nodular crust on bioherm	2.4	-6.9
WR-20-03	White chalky, flaky crust on bioherm	4.1	-6.0

Client ID	Description	$\delta^{13}C$ (‰, VPDB)	$\delta^{18}O$ (‰, VPDB)
WR-21-01	Branching, filamentous material from isolated pinnacle	3.3	-6.7
WR-21-02	Black nodular material from inside pores in isolated pinnacle	2.1	-8.1